E.3.5 Debris Mixing

The debris constituents used in testing were first weighed in a dry state. The test debris was thoroughly wetted with warm water and mixed with a power mixer prior to introduction into the test flume. Fibrous debris was soaked in warm water prior to test apparatus introduction to prevent agglomeration.

E.3.6 Debris Introduction

For the Phase 1 Debris Transport Test, debris was manually introduced into the flume above the retaining basket.

For Phase 2 testing, the debris was primarily introduced through a debris injection nozzle above the retaining basket using a trash pump and debris injection hopper (see Figure E.3-7 and Figure E.3-8). The first step for hopper operation was opening a small bypass flow from the recirculation piping downstream of the strainer. Opening the bypass flow limits the addition of water from outside of the test environment and maintains a conservative dilution level to prevent agglomeration. The debris insertion trough was filled from below with the bypass flow, which then overflowed into the area where the debris-laden water was pumped into the test apparatus through the trash pump. The hopper was filled using approximately 40 gallons of water prior to debris insertion into the trough. This provided a dilution ratio for fiber entering the retaining basket of approximately 40 parts water to one part fiber by volume for the typical fiber batch size of 0.35 pounds to prevent agglomeration (0.35 pounds of fiber is approximately one gallon). After each debris constituent was added to the test apparatus, the debris injection hopper was flushed with clean water. After the non-chemical debris introduction, the trash pump was disassembled to verify debris was not trapped inside the pump. Any debris that was found in the trash pump after disassembly was mixed with water and placed in the test apparatus downstream of the retaining basket.

Figure E.3-7 Debris Introduction Nozzle

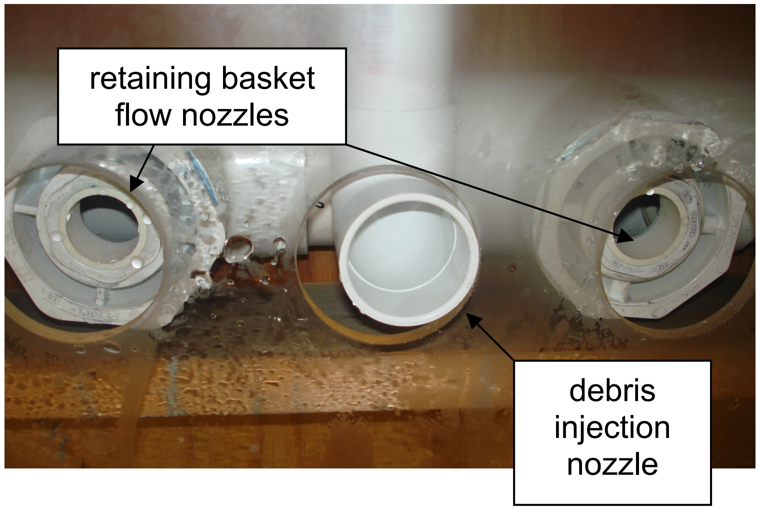

Figure E.3-8 Debris Injection Hopper

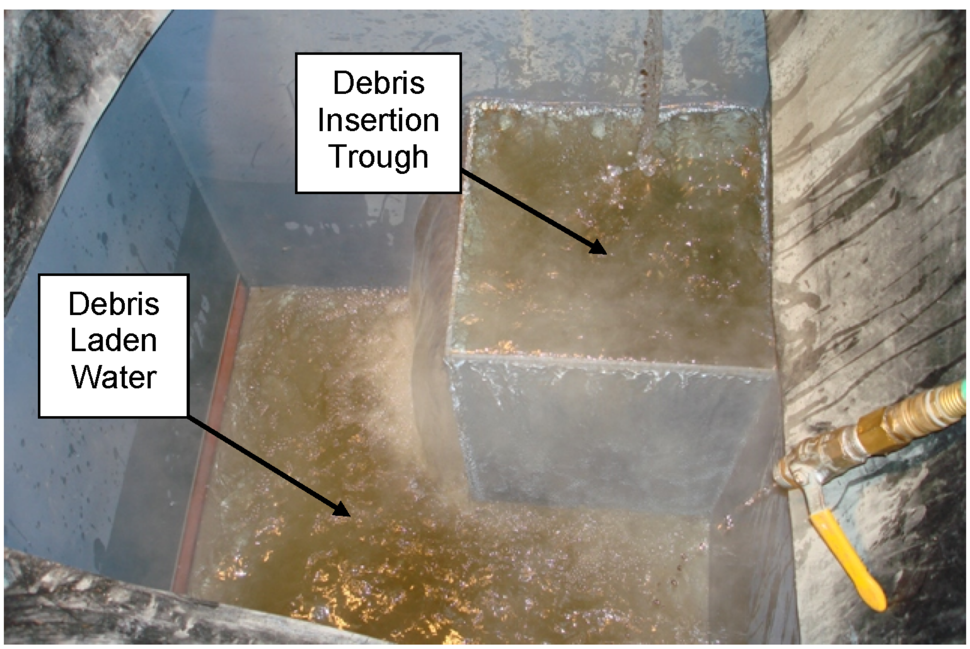

Phase 1 testing demonstrated that the "dirt and dust" debris damaged the trash pump seal. The dirt and dust was introduced through the retaining basket observation window (see Figure E.3-9) in accordance with the test plan.

Figure E.3-9 Dirt and Dust Introduction

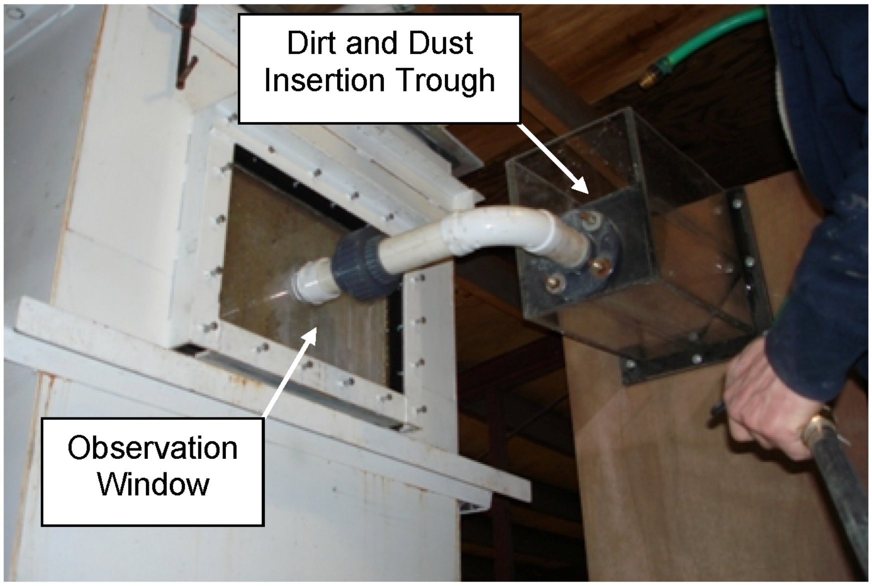

E.3.7 Downstream Debris Sampling

Three sampling ports are installed in the flume recirculation flow loop downstream of the pressure taps used to measure strainer head loss. Each port is connected to a valve in a three-valve array. Two pumps (main sampling pump and a back-up pump) are calibrated to a desired flow such that the flow velocity in the three ports is representative of the velocity in the recirculation flow loop. Samples are drawn during debris testing as required by procedure. Samples are collected at a location downstream of the test strainer and miniflow line tap and upstream of the main recirculation pump. Therefore, the debris load collected in the bypass samples is representative of the test fluid that would bypass the strainer and enter the ECCS. Prior to drawing a sample, the sampling lines are flushed to remove any residual debris from the previous sample. Water not collected by the sampling bottles (flush water) was captured in a bucket and reintroduced into the test flume downstream of the retaining basket.

E.3.8 Filter Housing Units

The fiber-only bypass tests collected fibrous debris downstream of the strainer using two filter housing units (see Figure E.3-10). Each filter housing unit contained locations for six filter bags. The one micron filter bags used during the test were weighed before and after the bypass test to determine the net mass of fiber bypass. These procedures were followed to weigh the bags pre- and post-test to verify that the mass increase resulted from debris content and not moisture. The test plan specified the procedures for weighing the filter bags. To switch filter housing units during the test, the upstream valve of the unit with clean filter bags was opened to fill the unit. Next, the downstream valve of the new unit was opened, allowing recirculated water to freely flow through both units. Immediately after, the downstream valve of the old unit was closed, followed by closing the upstream valve of the old unit to secure flow. The water inside of the old tank was then drained beneath the filter bags and discarded to a waste tank.

Figure E.3-10 Filter Housing Units

E.3.9 Water Management

The water management system consists of two parts, water removal and water addition. The test apparatus water volume increased as the wetted debris was added to the test apparatus. To maintain the prototypical strainer submergence, an overflow weir conduit was cut into the back wall of the test flume (see Figure E.3-11). The conduit captured the debris-laden water mix and filtered out the debris with one micron filter bags located behind the rear wall of the flume (see Figure E.3-12). The debris captured by the filter bags was flushed periodically to return the captured debris back into the test apparatus downstream of the retaining basket.

Figure E.3-11 Aft End of Flume Tank

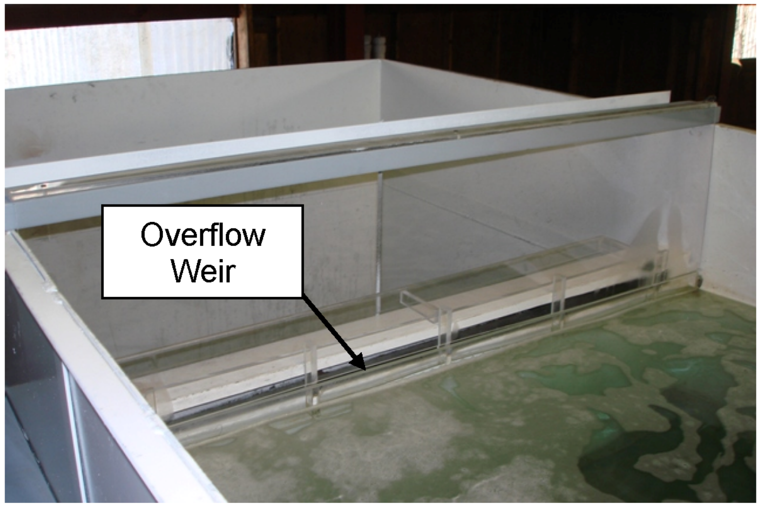

Figure E.3-12 Overflow Weir Filter bags

As the debris bed clogged the retaining basket, the water level in the basket area increased above the water level surrounding the strainer. The water volume increase in the retaining basket decreased the available volume of water surrounding the strainer. As the volume in the strainer area decreased below prototypical level, town water was added downstream of the retaining basket through the water addition piping (see Figure E.3-13). The town water was directed against acrylic plates, trickling the flow down directly in front of the basket, which does not disturb any potential debris bed that formed on the strainer.

Figure E.3-13 Water Addition

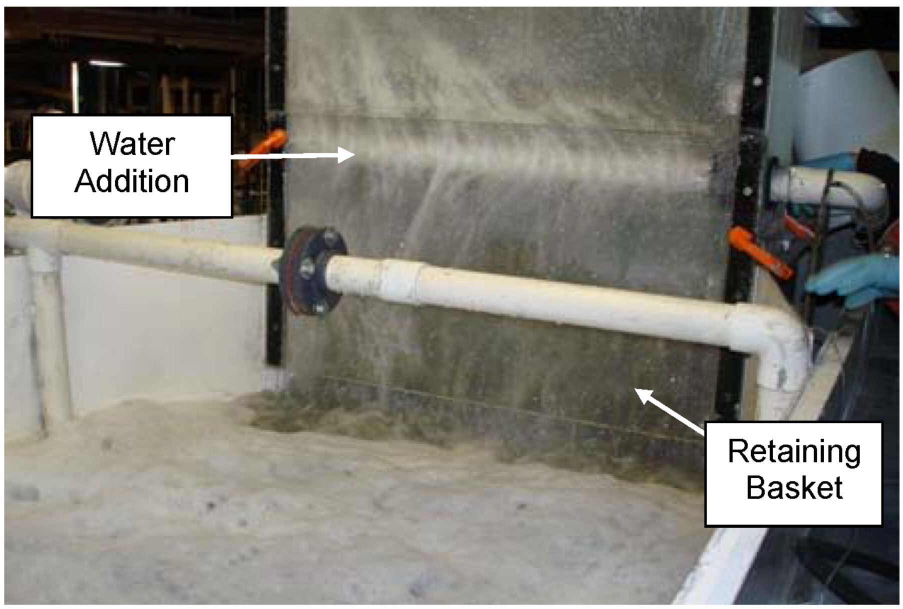

E.3.10 Test Strainer

The test strainer is prototypical of the U.S. EPR design. The strainer configuration used for Phase 1 and Phase 2 testing is the same. Table E.3-1 and Table E.3-2 provide the strainer scaling summary for Phase 1 and Phase 2 testing, respectively.

The basic geometry of the ECCS strainer is preserved for testing. Figure E.3-14 shows the strainer drawing with the outline of the modeled portion. Dimensions B and C are unchanged from the plant configuration. A small 0.75 ft portion on the bottom of the strainer is comprised of skirt and support feet. This portion is not considered an active screen area and is not included in the test strainer design. To maintain proper water submergence above the strainer, the modeled IRWST water level in the test flume is reduced from 10 ft to 9.25 ft. Dimension A is based on conservatively modeling the sump exit location with respect to the strainer faces.

Figure E.3-14 Modeled Portion of Strainer

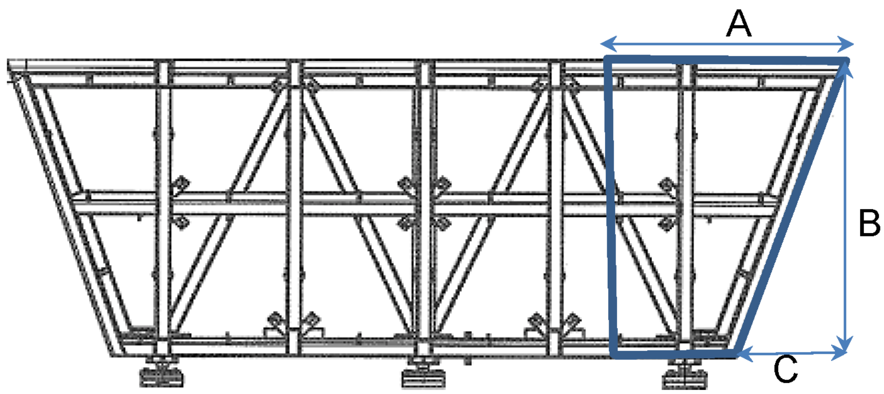

Figure E.3-15 shows the layout of the strainer supports with respect to the strainer sump cover. To conservatively represent the flow within the strainer, the test facility represents the strainer face with the minimum clearance from the sump to the face of the strainer. Dimension A is therefore determined by matching the distance from the strainer face directly to the leading edge of the sump cover. The sump cover size is scaled by flow area to the flow rate of the test flume.

Figure E.3-15 Strainer Support and Sump Cover (overhead view)

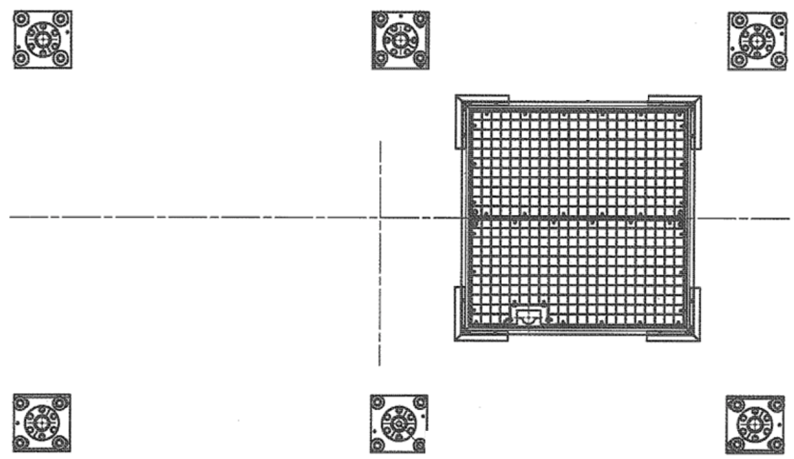

The test strainer had a surface area of approximately 70.6 ft^2 when fully submerged. The sump suction in the strainer contains a vortex suppressor prototypical to plant design. The pressure downstream of the strainer was measured approximately ten inches below the vortex suppressor. The filtering surface varied in the series of tests performed in January and February 2011. Table E.3-3 shows the filter media used on the strainer's surface during testing and the approximate specifications of the filter media.

Table E.3-3 Strainer Filter Media

Test #	Filter Media	Opening Size (in)	Opening Shape	Thickness (in)	Pattern	Hole Spacing (in)
Test 1	Perforated Plate	0.045	Circle	0.016	Staggered	0.066
Test 1A	Perforated Plate	0.045	Circle	0.016	Staggered	0.066
Test 1B	Wire Mesh	0.06	Square	0.020	N/A	N/A
Test 1C	Wire Mesh	0.06	Square	0.020	N/A	N/A
Test 1D	Wire Mesh	0.08	Square	0.028	N/A	N/A
Test 1E	Wire Mesh	0.08	Square	0.028	N/A	N/A
Test 2A	Wire Mesh	0.06	Square	0.020	N/A	N/A
Test 2D	Wire Mesh	0.08	Square	0.028	N/A	N/A
Test 2E	Wire Mesh	0.08	Square	0.028	N/A	N/A
Test 2F	Wire Mesh	0.08	Square	0.028	N/A	N/A

E.3.11 Test Retaining Basket

Two different retaining basket models were used for ECCS strainer performance testing. Phase 1 testing uses a retaining basket modeled in accordance with the scaling summary of Table E.3-1. Phase 2 testing uses a retaining basket modeled in accordance with the scaling summary of Table E.3-2.

Retaining Basket Scaling Methodology - Phase 1 Testing

The U.S. EPR design utilizes four retaining baskets consisting of two single compartment retaining baskets and two double compartment retaining baskets. A scaled single compartment basket was used for Phase 1 testing. For the retaining basket, a reference flow per unit area of wetted screen was determined. The flow per unit area of screen is determined using the minimum wetted surface area of the single compartment retention basket. The flow rate scale factor of approximately 9.37% was applied to the postulated conservative flow scenario of 100% of the break flow entering a single retaining basket. The flow rate together with the flow per unit wetted screen area determines the retaining basket modeled screen area. Conservatively, the retaining basket is modeled to only be open on the side of the facility that is facing the strainer. Arranging the test facility in this manner allows debris to travel freely from the retention basket to the strainer. The test basket frontal area mesh consists of 0.083” (2.1mm) openings, which is consistent with the U.S. EPR single and double compartment basket design. Both the retaining basket and the strainer are elevated in the plant. In the test flume these heights are not considered. This results in a conservative scenario of debris transport to the active strainer and retaining basket filtering surfaces. For the retaining basket, a low velocity area under the basket floor is not represented resulting in less debris settling. For the strainer, lowering the strainer face to the floor exposes the strainer to more floor transported tumbling debris.

The test facility retaining basket volume scaled by approximately 9.4%, matching the conservative plant flow per unit volume described above. Dividing the scaled retaining basket volume by the screened retaining basket area yields the test flume retaining basket depth.

Retaining Basket Scaling Methodology – Phase 2 Testing

The U.S. EPR utilizes two retaining basket designs in the IRWST. These designs consist of the single and double compartment retaining basket arrangements. The scaled large compartment of the double compartment retaining basket was used for Phase 2 testing. The double compartment retaining basket is separated into a large and small compartment. The small compartment basket is designed to capture any debris laden water that may enter the IRWST from the annular area of containment. The large compartment basket receives flow from the heavy floor opening. The portions of screened area that are scaled for the test apparatus include the large compartment’s left, right, front, and bottom surfaces. For conservatism, the area between the large and small compartment of the double compartment basket is not modeled. The retaining basket area modeled was reduced by the 100 ft^2 margin identified by miscellaneous debris.

Table E.3-4, Retaining Basket (RB) Scaling Summary and Modeled Parameters provides the retaining basket scaling summary and modeled parameters for the large compartment of the double compartment retaining basket. The scaled volume ensures that the retaining basket receives a prototypical flow per unit volume. The double compartment retaining basket is positioned on pedestals 0.66 feet above the IRWST floor. The bottom surface area of the basket is covered with a meshed screen of the same perforation size as the remainder of the basket. Consistent with the retaining basket design, the test basket is raised above the test floor with the bottom area screened and scaled approximately 9.37%. Subtracting the scaled bottom portion of the retaining basket from the scaled total surface area of the retaining basket provides the scaled vertical portion of the test basket. Based on the test apparatus maintaining 1:1 vertical scale, the test basket is designed and constructed to reach 16.57 feet above the test apparatus floor which is consistent with the plant design. The test basket width is determined by dividing the ‘scaled vertical surface area’ by the ‘RB screened vertical height’ in the test apparatus (excluding the pedestal height). The test apparatus retaining basket length (screened basket front face to back wall) is determined by dividing the ‘scaled RB volume’ by the ‘RB screened height’ and the ‘test apparatus RB width’.

Table E.3-5 shows the filter media used on the retaining basket surface during testing and the specifications of the filter media.

Table E.3-4 Retaining Basket (RB) Scaling Summary and Modeled Parameters

Description	Value[2]	Unit
Scale	9.37	%
Total RB Surface Area	642.00	ft^2
Scaled Total RB Surface Area	60.17	ft^2
RB Floor Surface Area	120.38	ft^2
Scaled RB Floor Surface Area	11.28	ft^2
Plant Vertical RB Surface Area	521.62	ft^2
Test Apparatus Vertical Surface Area	48.89	ft^2
RB Vertical Height	16.57	ft
RB Pedestal Height	0.66	ft
RB Screened Vertical Height	15.91	ft
Test Apparatus RB Width	3.07	ft
Plant RB Volume	2024.00	ft^3
Scaled RB Volume	189.71	ft^3
Test Apparatus RB Length[1]	3.88	ft

Note[1]: A retaining basket length of 3.7 feet is used instead of 3.88 feet. This length creates the correct scaling for the surface area of the retaining basket bottom.

Note[2]: Only surface areas and volumes are scaled.

Table E.3-5 Retaining Basket Filter Media

Test #	Retaining Basket Filtering Media	Opening Size (in)	Opening Shape	Thickness (in)	Pattern	Hole Spacing (in)
Test 1	Perforated Plate	0.045	Circle	0.016	Staggered	0.066
Test 1A	Wire Mesh	0.045	Square	0.018	N/A	N/A
Test 1B	Wire Mesh	0.06	Square	0.020	N/A	N/A
Test 1C	Wire Mesh	0.06	Square	0.020	N/A	N/A
Test 1D	Wire Mesh	0.08	Square	0.028	N/A	N/A
Test 1E	Wire Mesh	0.08	Square	0.028	N/A	N/A
Test 2A	Wire Mesh	0.06	Square	0.020	N/A	N/A
Test 2D	Wire Mesh	0.08	Square	0.028	N/A	N/A
Test 2E	Wire Mesh	0.08	Square	0.028	N/A	N/A
Test 2F	Wire Mesh	0.08	Square	0.028	N/A	N/A

E.3.12 Flume Vertical Flow Water Management

The majority of the water flow downstream of the strainer was re-introduced to the test flume with a nozzle delivery system. This was accomplished to represent the LOCA return flow onto the heavy floor and into one of four retaining baskets through the heavy floor openings. The plant design provides approximately 15.3 feet of water free-fall before the water reaches the surface of the IRWST pool. The test flume represents an adjusted 1:1 vertical scale of the U.S. EPR IRWST design. To conserve the vertical scale in the test facility, the momentum produced by the water free-fall must be preserved. The test facility ceiling limits the free-fall of water to approximately 8 feet. Therefore, the velocity of the water exiting the nozzles above the flume pool is increased to represent the plant's actual water free-fall conditions.

E.4 Debris Description

Debris types for strainer performance testing consist of non-chemical and chemical debris. The non-chemical debris types and amounts are based on the Debris Generation Evaluation for the U.S. EPR (Appendix C). The chemical debris types and amounts are based on the Chemical Effects Evaluation for the U.S EPR (Appendix D).

The following sections discuss the debris types used for testing. Specific debris types, quantities, and surrogate materials used in testing are documented in the debris allocation tables in Section E.5.

E.4.1 Reflective Metallic Insulation (RMI)

During the Debris Transport Test conducted in December 2009, RMI debris pieces of 2 mil thickness and various sizes from 0.25 inch x 0.25 inch up to 4 inch x 4 inch were shown to sink and settle on the bottom of the retaining basket. Due to the non-transport characteristics of RMI under design flow conditions, RMI was not included in subsequent tests. Removing RMI from subsequent tests also prevents the possibility of RMI debris trapping fibrous debris in the retaining basket, thus resulting in less conservative test conditions. Figure E.4-1 depicts typical RMI test debris.

Figure E.4-1 RMI Test Debris

E.4.2 Particulate Debris

The particulate used in U.S. EPR strainer testing comprised of latent dirt and dust, microtherm and coatings.

The U.S. EPR coatings debris source term consists of epoxy and inorganic zinc. Surrogates used during strainer testing were acrylic for the epoxy and tin powder for the inorganic zinc. The acrylic powder has an average density of approximately 77.4 lbs/ft^3. The acrylic coatings have a similar density, size, and shape characteristics to plant containment coatings and are a suitable surrogate material. The tin powder has a particle density of 445.3 lbs/ft^3 (compared to 457 lbs/ft^3 for inorganic zinc). Because inorganic zinc is considered a hazardous material, tin powder was used as the surrogate material.

During a debris transport test accomplished in December 2009, a small amount of coating chips were introduced to the test flume retaining basket. The majority of chips, when viewed with an underwater camera, appeared to cover the top 12 inches of submerged retaining basket screen where a higher velocity flow towards the strainer appeared to exist. Chips that were not caught in the initial current near the surface sank to the floor of the retaining basket. These observations determined that the qualified epoxy coatings could conservatively be tested in fine particulate and chip form. This conservatively increased the total epoxy coating source term by 34 percent. The coating chips comprised of acrylic paint chips that were 5/8 inch or less in length and approximately 4 to 12 mils in thickness (see Figure E.4-2). The coatings were weighed in a dry state, and then wetted and mixed before insertion into the test apparatus.

Figure E.4-2 Coating Chips

E.4.3 Fiber

Latent fiber is the only source of fiber generated in the U.S. EPR plant during a LOCA (see Appendix C). The latent fiber surrogate form was heat treated NUKON® that was shredded into fiber fines. The latent fiber was soaked in warm water and diluted before test apparatus insertion.

E.4.4 Miscellaneous Debris

During the Debris Transport Test conducted in December 2009, miscellaneous debris materials were added to the flume to document how these items responded to the test flow conditions. The miscellaneous debris consists of various debris items expected to be found in containment. The specific miscellaneous debris used for testing is listed in Section E.5.

E.4.5 Chemical Debris

The predicted chemical precipitates generated after a postulated LOCA in the U.S. EPR containment are calcium phosphate ($Ca_3(PO_4)_2$), aluminum oxyhydroxide, and sodium aluminum silicate ($NaAlSi_3O_8$). Since $NaAlSi_3O_8$ is considered hazardous, aluminum oxyhydroxide (ALOOH) is used as a surrogate. Because the characteristics of $NaAlSi_3O_8$ are similar to AlOOH, ALOOH is used for testing in lieu of $NaAlSi_3O_8$.

E.5 Debris Quantities and Introduction Sequence

E.5.1 Phase 1 Testing - Debris Transport Test No. 1

For the Debris Transport Test, debris was manually added to the fume flow above the retaining basket. Table E.5-1 provides the debris allocation and flume flow rate for the Debris Transport Test. The following is the list of debris and approximate sizes introduced into the flume during the Debris Transport Test.

- leather work glove
- plastic glove
- caution tag (6 inch x 3 inch plastic material)
- caution label (yellow ribbon 2.5 feet in length)
- white cloth (1 foot x 1.5 feet)
- 2 plastic tie wraps (1 foot and 2 feet long)
- ¾ inch nylon rope (2 feet long)
- plastic chain link (1.5 feet long)
- plastic bag (1 foot x 2 feet)
- ear plugs (1 set connected with an elastic string)
- ear plugs (1 set in a plastic bag)
- ¼ inch x ¼ inch RMI
- ½ inch x ½ inch RMI
- 4 inch x 4 inch RMI
- coating chips (5/8 inches and smaller)

Table E.5-1 Debris Allocation and Flume Flow Rate for the Debris Transport Test

Scaling Factor 9.37%			Wt Conversions	Debris Scaled		
Debris Type	U/M	Quantity	(lbs / ft^3 or ft^2)	(lbm)	Units	Debris Form / (Surrogate)
Fibers (Design Basis)						
NUKON (Small Fines)	ft^3	n/a	2.4	n/a	lbm	Shredded Fiber (Binder Burned Out)
Latent Fibers	lbm	n/a	n/a	n/a	lbm	Shredded Fiber
			Total Fibrous Debris	**0.0**		
RMI						
Total RMI	ft^2	2098.87				
RMI (1/4" x 1/4")	ft^2	111.24	0.0813	0.85	lbm	
RMI (1/2" x 1/2")	ft^2	444.96	0.0813	3.39	lbm	
RMI (1" & 2")	ft^2	1017.95	0.0813	7.76	lbm	
RMI Larges (4" and 6") (Limited to 25% RMI total)	ft^2	524.72	0.0813	4.00	lbm	
			Total RMI Debris	**15.99**		
Particulates						
Latent Particulate; Dirt & Dust	lbm	n/a	n/a	n/a	lbm	PCI PWR Dirt Mix (85% of Latent Debris)
Microtherm	ft^3	n/a	15.0	n/a	lbm	Microtherm® Free Flow
Coatings (lbs)						
Qualified Coatings	lbm	459.82	94	43.10	lbm	Acrylic Paint Chips (5/8" and smaller)
Qualified Coatings	lbm	n/a	457	n/a	lbm	IOZ Powder (Tin Powder)
Unqualified Coatings	lbm	n/a	94	n/a	lbm	Acrylic Powder or Walnut Shell Powder
			Total Particulate Debris	**43.10**		
Chemical Debris Concentrations						
Sodium Aluminum Silicate (Unknown)	lbm	n/a	n/a	n/a	lbm	Chemical Surrogate - AlOOH
Calcium Phosphate (Unknown)	lbm	n/a	n/a	n/a	lbm	Chemical Surrogate - $Ca_3(PO_4)_2$
Aluminum Oxyhydroxide (Unknown)	lbm	n/a	n/a	n/a	lbm	Chemical Surrogate - AlOOH
			Total Surrogate Debris	**0.0**	lbm	
Miscellaneous Debris						
Labels, Stickers, Tape, Placards, Tags	ft^2	100.00	n/a	note 1	ft^2	Miscellaneous Debris

Flume Water Level	ft	9.25	
Scaling Factor	%	9.37%	
Target Flume Flow	gpm	307.81	

note 1: scaled miscellaneous debris is provided as a combination of various debris items

E.5.2 Phase 2 Testing – Head Loss Tests

Head loss testing sequentially batched the debris into the test apparatus consistent with strainer testing guidance (Reference 3). The test loop recirculation pump was started and the design flow rate established before debris was introduced. The test plan detailed the timing of debris introduction and the data acquisition computer, and the log book recorded actual debris introduction times for the tests.

There was no time delay between the introductions of the various particulate debris constituents. There was a minimum of two flume turnovers, or 28 minutes, between fiber batch additions to observe any increase to the strainer or retaining basket differential pressure. One flume turnover is the time it takes for the debris laden water to circulate through the test flume one time. After the fiber was introduced, there was a minimum of five flume turnovers before coating chip introduction. After the coating, chips and a minimum of five flume turnovers the chemical debris addition began and continued until the chemical was inserted into the test apparatus.

The fine particulate debris was introduced into the test apparatus based on density, with the least dense (most transportable) debris inserted first. The order for debris introduction, along with the measured amounts, was as follows:

Fine Particulate Debris

Batch 1: Microtherm (1.55 lbm).

Batch 2: Acrylic powder particulate debris (35.60 lbm).

Batch 3: Dirt and dust (12.20 lbm).

Batch 4: Tin powder particulate debris (90.40 lbm).

Fine Fibrous Debris

Batch 5: Fine NUKON® fibers (0.21 lbm).

Batch 6: Fine NUKON® fibers (0.34 lbm).

Batch 8: Fine NUKON® fibers (0.34 lbm).

Batch 9: Fine NUKON® fibers (0.34 lbm).

Batch 10: Fine NUKON® fibers (0.34 lbm).

Batch 11: Fine NUKON® fibers (0.34 lbm).

Batch 12: Fine NUKON® fibers (0.29 lbm).

Note: Batch 5 was added to the test apparatus directly between the retaining basket and strainer a directed in the test plan.

Coating Chip Debris

Batch 13: Acrylic coating chips (12.00 lbm).

Chemical Precipitate Debris

Batch 14: Aluminum Oxyhydroxide (33 percent of plant concentration).

Batch 15: Calcium Phosphate (33 percent of plant concentration).

Batch 16: Aluminum Oxyhydroxide (33 percent of plant concentration).

Batch 17: Calcium Phosphate (33 percent of plant concentration).

Batch 18: Aluminum Oxyhydroxide (33 percent of plant concentration).

Batch 19: Calcium Phosphate (33 percent of plant concentration).

Batch 20 and after: Chemical addition per the test plan until the chemical is introduced.

The first three batches of ALOOH were added to the flume in approximately 5.8 gallon amounts. The first three batches of $Ca_3(PO_4)_2$ were added to the flume in approximately 13.4 gallon amounts. After the first three batches of each chemical precipitate were added to the flume, the flume reached the chemical concentration that is expected in the plant following LOCA. After the first three batches, the ALOOH and $Ca_3(PO_4)_2$ were added to the flume in approximately 4.4 and approximately 10.2 gallon amounts, respectively, until 100 percent of the scaled quantity by mass of chemical was introduced into the test flume. The chemical batching prevented the flume from becoming overly concentrated with chemical debris, possibly causing the chemical to settle more quickly to the flume floor.

Chemical addition comprised of approximately 40 total batches of each chemical precipitate until 100 percent of the chemical debris source term was introduced to the flume. The batching process comprised of one ALOOH batch introduction followed by one $Ca_3(PO_4)_2$ batch introduction, with a five minute interval between the two precipitates. One flume turnover (14 minutes) was allotted before the next batch of ALOOH was introduced to the test flume. The chemical was introduced to the test apparatus between the retaining basket and strainer. After chemical addition was completed, there was a minimum of 15 flume turnovers before test termination.

The chemical amounts used for testing, based on early calculations, bound the values identified in Appendix D. Since subsequent calculations yielded lower quantities, the as-tested amounts were not updated. The amount for ALOOH was combined with the value for sodium aluminum silicate. This is considered acceptable for testing as ALOOH is used as a surrogate for sodium aluminum silicate.

Table E.5-2 Debris Allocation and Flume Flow Rate for Head Loss Tests

Scaling Factor 9.37%			Wt Conversions	Debris Scaled		
Debris Type	**U/M**	**Quantity**	**(lbs / ft^3 or ft^2)**	**(lbm)**	**Units**	**Debris Form / (Surrogate)**
Fibers (Design Basis)						
Latent Fibers	lbm	22.50	n/a	2.11	lbm	Shredded Fiber (Binder Burned Out)
			Total Fibrous Debris	**2.11**		
RMI						
Total RMI	ft^2	2119.03				
RMI (1/4" x 1/4")	ft^2	112.31	0.0813	0.86	lbm	Size distribution based on NUREG CR/6808
RMI (1/2" x 1/2")	ft^2	449.23	0.0813	3.42	lbm	Size distribution based on NUREG CR/6808
RMI (1" & 2")	ft^2	1027.73	0.0813	7.83	lbm	Size distribution based on NUREG CR/6808
RMI Larges (4" and 6") (Limited to 25% RMI total)	ft^2	529.76	0.0813	4.04	lbm	Size distribution based on NUREG CR/6808
			Total RMI Debris	**16.15**		
Particulates						
Latent Particulate; Dirt & Dust	lbm	127.50	n/a	11.95	lbm	PCI PWR Dirt Mix (85% of Latent Debris)
Microtherm	ft^3	1.00	15.0	1.41	lbm	Microtherm® Free Flow
Coatings (lbs)						
Qualified Coatings	lbm	126.50	94	11.86	lbm	Acrylic Powder or Walnut Shell Powder
Qualified Coatings	lbm	958.70	457	89.86	lbm	IOZ Powder (Tin Powder)
Unqualified Coatings	lbm	250.00	94	23.43	lbm	Acrylic Powder or Walnut Shell Powder
			Total Particulate Debris	**138.50**		
Chemical Debris Concentrations						
Sodium Aluminum Silicate	kg	77.0	(2.2 lbs/kg)	15.91	lbm	Chemical Surrogate - AlOOH
Calcium Phosphate	kg	81.0	(2.2 lbs/kg)	16.74	lbm	Chemical Surrogate - $Ca_3(PO_4)_2$
Aluminum Oxyhydroxide	kg	0.00	(2.2 lbs/kg)	0.00	lbm	Chemical Surrogate - AlOOH
			Total Surrogate Debris	**32.65**	lbm	
Miscellaneous Debris						
Labels, Stickers, Tape, Placards, Tags	ft^2	100.00	n/a	n/a	ft^2	Miscellaneous Debris
Flume Water Level	ft	9.25				
Scaling Factor	%	9.37%				
Target Flume Flow	gpm	307.81	/323 for later tests			
Wetted Screened Basket Surface Area (Excluding Structure)	ft^2	27.50				
Un-Wetted Screened Basket Surface Area (Excluding Structure)	ft^2	17.90				
Strainer Surface Area	ft^2	70.60				
Thin Bed Size	ft	0.005	1/16 th inch fiber bed			
Required Fiber for 1/16" Bed on Wetted Retaining Basket	ft^3	0.14				
Required Fiber for 1/16" Bed on Wetted Retaining Basket	lbm	0.34	NUKON Density of 2.4 lbm/ft3			
Required Fiber for 1/16" Bed on Wetted Retaining Basket	ft^3	0.09				
Required Fiber for 1/16" Bed on Wetted Retaining Basket	lbm	0.22	NUKON Density of 2.4 lbm/ft3			
Required Fiber for 1/16" Bed on Strainer	ft^3	0.37				
Required Fiber for 1/16" Bed on Strainer	lbm	0.88	NUKON Density of 2.4 lbm/ft3			

Table E.5-3 Chemical Debris Additions and Flume Flow Rate for the Head Loss Tests

Pump Flow Rate During Chem. Batching	Pump Flow (gpm)	Pump Flow (ft^3 / sec)	Flume Depth (ft)	Flume Volume (cu ft @ 9.25')	Pipe Volume (cu ft)	Total Volume (cu ft)	Total Volume (gal)	Flume Flow (cfs)	One flume cycle (sec)	1 Flume Turn Over FTO (min)	2 Flume Turn Over FTO (min)
	307.81	**0.686**	**9.25**	**519.39**	**31.60**	**550.99**	**4,121.70**	0.686	803.44	**14.0**	**28.0**
	0r 323.0 for later tests										
Chemical Debris Concentrations	**U/M**	**Quantity**	**(lbs / ft^3 or ft^2)**	**Scaled Quantity**	**Qty w/ Bump Ups**	**U/M**					
Chemical Bump Up Added for Soluability	**%**	**1.0%**		9.37%							
Chemical Bump Up to Eliminate Bag Filters	**%**	**1.4%**									
Sodium Aluminum Silicate	**max lbm**	**169.75**		**15.91**	**16.30**	lbm					
Aluminum Oxyhydroxide	**max lbm**	**0.00**		**0.00**	**0.00**	lbm					
Calcium Phosphate	**max lbm**	**178.60**		**16.74**	**17.15**	lbm					
			Total Surrogate Debris	**32.65**	**33.45**	lbm					
	Plant Calculated lbm	**Scaled Test lbm**	**Chemicals**	**Plant Conc**	**Flume Conc**	**U/M**	**lbs to = Plant Conc**	**lbs / batch to start; 1 PTO in between**	**lbs / batch thereafter; 1 PTO in between**	**Est No. of PTO's Req'd**	**EST Minutes to Introduce Chemicals**
Aluminum Oxyhydroxide	**169.75**	**16.30**	**ALOOH**	0.000392	0.003955	lbs/gal	**1.61**	**0.5329**	**0.4037**	**39.40**	**552**
Calcium Phosphate	**178.60**	**17.15**	**Cal Phos**	0.000412	0.004161	lbs/gal	**1.70**	**0.5607**	**0.4248**	**39.40**	**197**
Totals	**348.35**	**33.45**	**Totals**	0.000804	0.008116	lbs/gal	**3.31**	**1.0936**	**0.8285**	**39.40**	**749**
				433,242	4,121.7	gal		**Batch Sizes**			
				57,916	**551.0**	ft^3		**33.00%**	**25.00%**		**12.48**
					Conversion of "grams / liter" to "lbs / gallon"	1	gram	=	0.0022	lbs	
						1	liter	=	0.26417	gallons	
						1	g / l	=	0.00835	lbs / gallon	
						11	g / l	=	0.0918	lbs / gallon	
						5	g / l	=	0.04173	lbs / gallon	
				Batch Volumes							
					33% Batches @	**0.53**	**lbm**	=	**5.81**	**gal of ALOOH mix**	
					25% Batches @	**0.40**	**lbm**	=	**4.40**	**gal of ALOOH mix**	
					33% Batches @	**0.56**	**lbm**	=	**13.44**	**gal of Cal Phosphate mix**	
					25% Batches @	**0.42**	**lbm**	=	**10.18**	**gal of Cal Phosphate mix**	

E.5.3 Phase 2 Testing - Fibrous Debris Only Bypass Tests (Incremental Addition)

Fibrous only bypass testing was performed in January and February 2011 using the revised debris source term as determined by the debris generation calculation. The fiber was introduced to the flume in small batches equal to the approximate amount of fiber that could form a 1/16 inch fiber bed on the wetted retaining basket. The test measured fiber bypass with 25 percent of the total fiber added to the test flume assuming that approximately 23 percent of the debris enters one of the four retaining baskets (approximately 2 percent will be inserted downstream of the retaining basket).

Fiber bypassing the strainer was captured by multiple filter bags in one of two filter housing units connected in parallel to the recirculation loop (see Section E.3.8).

Table E.5-4 shows the order for debris introduction and the measured amounts. After every three batches, the recirculation flow was changed to the clean set of filters. There was one flume turnover between fiber batch introductions. After every three batches, the debris injection trash pump was disassembled to recover and re-add any debris trapped within the pump housing. The flume recirculated for five flume turnovers after the debris was introduced to verify the bypassed debris was captured in the filter bags.

Table E.5-4 Fibrous Debris Only Test Batching

Fiber Batch #	Fiber Batch Size (lbm)	Area Inserted
1	0.06	Strainer Area
2	0.35	Retaining Basket
3	0.15	Retaining Basket
Change Filters		
4	0.05	Strainer Area
5	0.35	Retaining Basket
6	0.15	Retaining Basket
Change Filters		
7	0.05	Strainer Area
8	0.35	Retaining Basket
9	0.15	Retaining Basket
Change Filters		
10	0.05	Strainer Area
11	0.35	Retaining Basket
12	0.14	Retaining Basket
End of Test		

Table E.5-5 Debris Allocation and Flume Flow Rate for the Fibrous Debris Only Sample Bypass Test

Scaling Factor 9.37%			Wt Conversions	Debris Scaled		
Debris Type	**U/M**	**Quantity**	**(lbs / ft^3 or ft^2)**	**(lbm)**	**Units**	**Debris Form / (Surrogate)**
Fibers (Design Basis)						
Latent Fibers	lbm	22.50	n/a	2.11	lbm	Shredded Fiber (Binder Burned Out)
			Total Fibrous Debris	**2.11**		
RMI						
Total RMI	ft^2	2119.03				
RMI (1/4" x 1/4")	ft^2	112.31	0.0813	n/a	lbm	Size distribution based on NUREG CR/6808
RMI (1/2" x 1/2")	ft^2	449.23	0.0813	n/a	lbm	Size distribution based on NUREG CR/6808
RMI (1" & 2")	ft^2	1027.73	0.0813	n/a	lbm	Size distribution based on NUREG CR/6808
RMI Larges (4" and 6") (Limited to 25% RMI total)	ft^2	529.76	0.0813	n/a	lbm	Size distribution based on NUREG CR/6808
			Total RMI Debris	**0.0**		
Particulates						
Latent Particulate; Dirt & Dust	lbm	n/a	n/a	n/a	lbm	PCI PWR Dirt Mix (85% of Latent Debris)
Microtherm	ft^3	n/a	15.0	n/a	lbm	Microtherm® Free Flow
Coatings (lbs)						
Qualified Coatings	lbm	n/a	94	n/a	lbm	Acrylic Powder or Walnut Shell Powder
Qualified Coatings	lbm	n/a	457	n/a	lbm	IOZ Powder (Tin Powder)
Unqualified Coatings	lbm	n/a	94	n/a	lbm	Acrylic Powder or Walnut Shell Powder
			Total Particulate Debris	**0.0**		
Chemical Debris Concentrations						
Sodium Aluminum Silicate	lbm	n/a	n/a	n/a	lbm	Chemical Surrogate - AlOOH
Calcium Phosphate	lbm	n/a	n/a	n/a	lbm	Chemical Surrogate - $Ca_3(PO_4)_2$
Aluminum Oxyhydroxide	lbm	n/a	n/a	n/a	lbm	Chemical Surrogate - AlOOH
			Total Surrogate Debris	**0.0**	lbm	
Miscellaneous Debris						
Labels, Stickers, Tape, Placards, Tags	ft^2	100.00	n/a	n/a	ft^2	Miscellaneous Debris
Flume Water Level	ft	9.25				
Scaling Factor	%	9.37%				
Target Flume Flow	gpm	307.81	/323 for later tests			
Strainer and Basket Surface Area	ft^2	130.77				

E.6 Test Results

E.6.1 Phase 1 Tests

This section presents the results of the Phase 1 testing. The Phase 1 tests used a 0.08 inch wire mesh on the strainer and the retaining basket and were performed at a higher fiber debris source term.

E.6.1.1 *Clean Strainer Head Loss Test*

The Clean Strainer Head Loss Test determines the head loss of the clean strainer for five different flume flow rates. For this test, the measured flow rates, head losses, and water temperatures were averaged over the test duration once the desired flow rate was achieved. Table E.6-1 summarizes the clean strainer head loss results for the target flow rates.

Table E.6-1 Clean Strainer Head Loss Test Results

Target Flow (gpm)	Measured Basket Flow (gpm)	Measured Mini-Flow (gpm)	Measured Total Flow (gpm)	Temperature (°F)	Measured Strainer Head Loss (ft. H_2O)
230.9	204.8	28.9	233.7	116.2	0.246
269.3	247.6	28.9	276.5	118.1	0.313
307.8	286.9	28.8	315.7	119.3	0.385
346.3	326.5	28.8	355.3	120.7	0.464
384.8	363.4	28.4	391.8	119.9	0.539

E.6.1.2 *Design Basis Debris Loaded Strainer Head Loss Test*

The Design Basis Debris Loaded Strainer Head Loss Test determines the debris bed head loss for the U.S. EPR design basis accident. Table E.6-2 shows the maximum and average measured head losses recorded during the test period. During this test, the maximum head loss occurred prior to the completion of particulate addition and before fiber and chemicals were added to the test apparatus.

Table E.6-2 Maximum and Average Measured Head Loss for the Design Basis Debris Loaded Strainer Head Loss Test

	Hour	Total Flow (gpm)	Temp (°F)	Measured Basket Head Loss (ft. of water)	Strainer Head Loss (ft. of water)
Average	N/A	316.8	115.9	6.27	0.377
Maximum	00.13	328.0	118.2	0	0.414

Figure E.6-1 shows the strainer and retaining basket head loss data recorded during Test No. 4. As indicated in Figure E.6-1, the strainer head loss remains constant during the test. The retaining basket overflows after the addition of coating chips, and then remains constant until the final batch of chemical debris is added to the test flume. Following the final batch of chemical debris, an approximate 1.3 foot measured increase in retaining basket head loss occurs over 3.6 hours. Towards the end of the test, there was a slight increase in the recorded retaining basket head loss caused by evaporation of water in the test apparatus. Following the test, the flume was drained revealing an essentially clean strainer screen.

Figure E.6-1 Strainer and Retaining Basket Head loss Data for the Design Basis Debris Loaded Strainer Head Loss Test

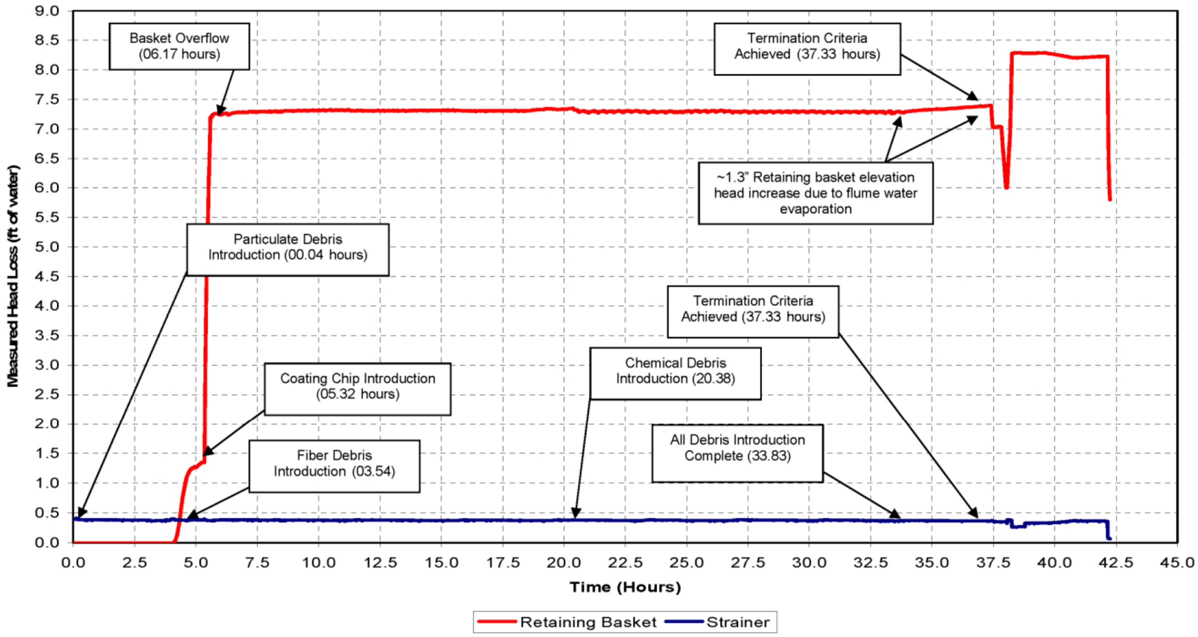

E.6.1.3 *Fibrous Debris Only Sample Bypass Test*

The Fibrous Debris Only Sample Bypass Test establishes the transport characteristics of fibers introduced incrementally up through the maximum design basis fiber load. This test evaluates how a fibrous debris bed forms on the retaining basket and strainer. Debris bypass testing was performed during this type test to provide debris bypass results for downstream analysis.

The Fibrous Debris Only Sample Bypass Test was originally performed as Test No. 2. After Test No. 2 was terminated, the debris introduction pump was dismantled and a small amount of fibrous debris was found in the pump's internals. As a result, Test No. 2 was invalidated and the test was repeated as Test No. 2A.

Test No. 2A used the same procedures used in Test No.2. Table E.6-3 shows the head loss data measured during the Fiber Debris Only Sample Bypass Test No. 2A. The debris loaded head loss for Test 2A is not used as a design basis head loss because only one debris constituent was introduced for the test and chemical effects were not present. After the fibrous debris was introduced to the test flume, the debris introduction pump was dismantled to verify that remnants of fiber did not remain in the pump internals. A small amount of debris was discovered and reintroduced to the test flume through the observation window after the pump was dismantled.

Table E.6-3 Head Loss Data for Fibrous Debris Only Sample Bypass Test No. 2A

Time	Procedure Action	Total Flow (gpm)	Temp (°F)	Measured Basket Head Loss (ft. of water)	Strainer Head Loss (ft. of water)
09:02:42	1st batch of fiber added	318	114	0.0	0.375
09:20:18	1st batch completed	317	113	0.0	0.376
09:48:21	2nd batch of fiber added	314	115	0.001	0.388
09:51:39	2nd batch completed	319	115	0.015	0.385
13:21:56	test termination	312	120	0.091	0.391

Fiber bypass sampling was conducted during Test 2A. These samples are analyzed for percent bypass and used for downstream effects analysis. Thirteen samples were drawn and analyzed. The results of the analysis quantify the amount of fibrous debris that penetrated the strainer during testing. Table E.6-4 summarizes the bypass test results. Results of testing and analysis conclude a total fibrous debris bypass percentage of 34.4 percent. The bypass was determined using a scanning electron microscope measurement technique.

Table E.6-4 Bypass Test Results

TEST 3A			LENGTH						Diameter			Flow Rate (gpm)	Smpl Size (mL)
Sample	Time (min)	Fibers (per smpl)	Long (%)	Med (%)	Short (%)	Long (μm)	Med (μm)	Short (μm)	Thick (μm)	Med (μm)	Thin (μm)		
B	N/A	94	8%	52%	40%	900	300	80	10	6	3	280.9	25
1	0	90	16%	66%	18%	1200	350	80	10	7	3	285.4	25
2	4	1501	8%	61%	31%	1100	300	90	12	7	4	290.4	25
4	14	11150	3%	53%	44%	1200	250	90	11	7	3	281.9	25
5	19	22360	2%	54%	44%	850	250	90	10	6	3	288.3	25
6	24	20707	2%	49%	49%	1100	250	90	10	7	3	287.6	25
9	39	10747	4%	48%	48%	950	300	80	12	7	3	288.1	25
10	44	10467	2%	47%	51%	850	250	90	10	6	4	285.0	25
11	49	9300	2%	46%	52%	1100	250	80	11	7	3	288.6	25
12	54	8080	2%	40%	58%	850	300	80	10	7	3	291.0	25
17	106	137	4%	52%	44%	1300	250	90	12	7	3	290.9	25
22	176	108	3%	65%	32%	950	250	80	11	7	3	287.0	25
27	246	163	8%	59%	33%	900	250	80	11	7	3	288.5	25

E.6.1.4 *Debris Loaded Strainer Head Loss Thin Bed Test*

The Debris Loaded Strainer Head Loss Thin Bed Test determines if a higher head loss is possible with a thin bed of fibers, particulate, and chemical debris present rather than with the design basis quantity of debris. Figure E.6-2 shows the strainer and retaining basket head loss for the debris loaded. Based on testing results, there was no formation of a thin bed on the strainer. When draining the flume after test termination, the strainer screen appeared nearly free of debris.

Figure E.6-2 Strainer and Retaining Basket Head Loss Data for the Thin Bed Test

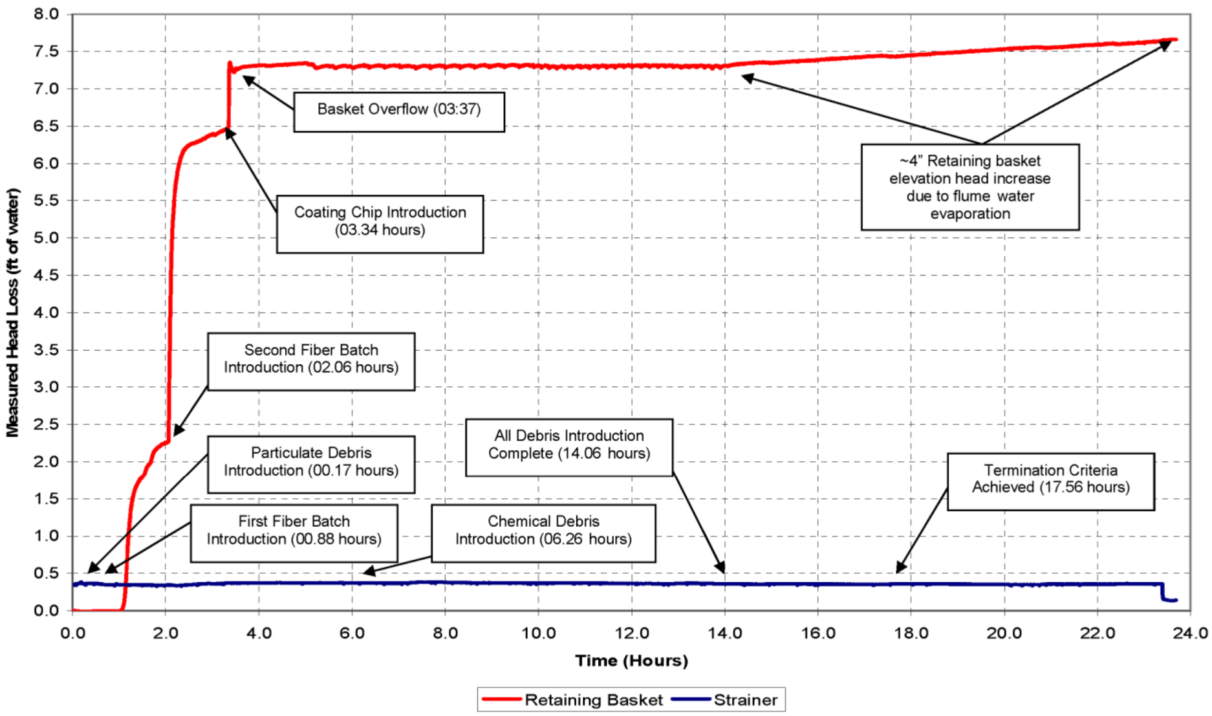

E.6.2 Debris Transport Test

The Debris Transport Test determines the transportability of reflective metallic insulation (RMI), coatings (in the form of paint chips), and miscellaneous debris including other miscellaneous debris. Section E.5.1 lists the debris types used for the Debris Transport Test. The test results conclude the debris was captured and contained within the retaining basket. Table E.6-5 details the Debris Transport Test results.

Table E.6-5 Debris Transport Test Results

Debris Type	Debris Transport Response
leather work glove	* floated on the surface of the water
plastic glove	* floated on the surface of the water
caution tag (6 inch x 3 inch plastic material)	settled on retaining basket floor
caution label (yellow ribbon 2.5 feet in length)	* floated on the surface of the water
white cloth (1 foot x 1.5 feet)	* floated on the surface of the water
2 plastic tie wraps (1 foot and 2 feet long)	settled on retaining basket floor
¾ inch nylon rope (2 feet long)	settled on retaining basket floor
plastic chain link (1.5 feet long)	* floated on the surface of the water
plastic bag (1 foot x 2 feet)	* floated on the surface of the water
ear plugs (1 set connected with an elastic string)	* floated on the surface of the water
ear plugs (1 set in a plastic bag)	* floated on the surface of the water
¼ inch x ¼ inch RMI	settled on retaining basket floor
½ inch x ½ inch RMI	settled on retaining basket floor
4 inch x 4 inch RMI	settled on retaining basket floor
coating chips (5/8 inches and smaller)	* most floated on the surface

* These debris items were observed to float on the surface of the water and lay against the retaining basket screen due to the direction of the test flume flow.

E.6.3 Clean Strainer Head Loss Test

Table E.6-6 presents the various clean strainer head losses recorded throughout the tests. This data represents the average raw data collected prior to debris introduction. The target flow rate was increased for Tests 1D, 1E, 2E, and 2F because of an input change to use the pump run out flow for the flow rate.

Table E.6-6 Clean Strainer Head Loss Test Results

Test #	Target Flow Rate (gpm)	Average Flow Rate (gpm)	Time Recorded (min)	Average Head Loss (ft of water)	Strainer Filter Media
Test 1	307.8	316.5	8.2	0.33	0.045" Perf
Test 1A	307.8	312.8	6.6	0.41	0.045" Mesh
Test 1B	307.8	313.1	6.1	0.38	0.06" Mesh
Test 1C	307.8	318.1	14.5	0.42	0.06" Mesh
Test 2A	307.8	311.7	5.1	0.32	0.06" Mesh
Test 1D	323.0	325.9	11.5	0.43	0.06" Mesh
Test 1E	323.0	329.9	5.1	0.43	0.08" Mesh
Test 2D	323.0	327.6	5.6	0.42	0.08” Mesh
Test 2E	323.0	327.4	16.0	0.42	0.08" Mesh
Test 2F	323.0	326.2	5.7	0.42	0.08" Mesh

E.6.4 Test 1: Thin Bed Head Loss Test

Test 1 was performed on January 4, 2011 using 0.045 inches perforated plate on the filtering surface of both the strainer and retaining basket. Figure E.6-3 shows the raw data collected throughout the test. The test duration was 4.9 hours. The particulate debris was added to the test flume, followed by the first batch of fiber (0.21 pounds). The first batch of fiber was inserted downstream of the retaining basket. The second batch of fiber (0.34 pounds) immediately followed the first batch and was introduced to the retaining basket. The strainer differential pressure increased within 15 minutes of adding the initial fiber. The next batch of fiber was not added until two hours and 30 minutes after the initial batch, when the strainer differential pressure stabilized at 1.6 feet of water. After the next batch of fiber (0.34 pounds), the strainer differential pressure rose to 6.3 feet of water at a flow rate of 307.1 gpm with 1.3 pounds of fiber remaining for addition. At this point, the test was terminated because of excessive differential pressure across the strainer. There was no change to the retaining basket observed or recorded throughout the test. Drain down of the test flume after termination revealed that the strainer had a thin bed (approximately 1/16th inch thick) form on the entire strainer. The retaining basket appeared free of debris.

Figure E.6-3 Test 1 Raw Data

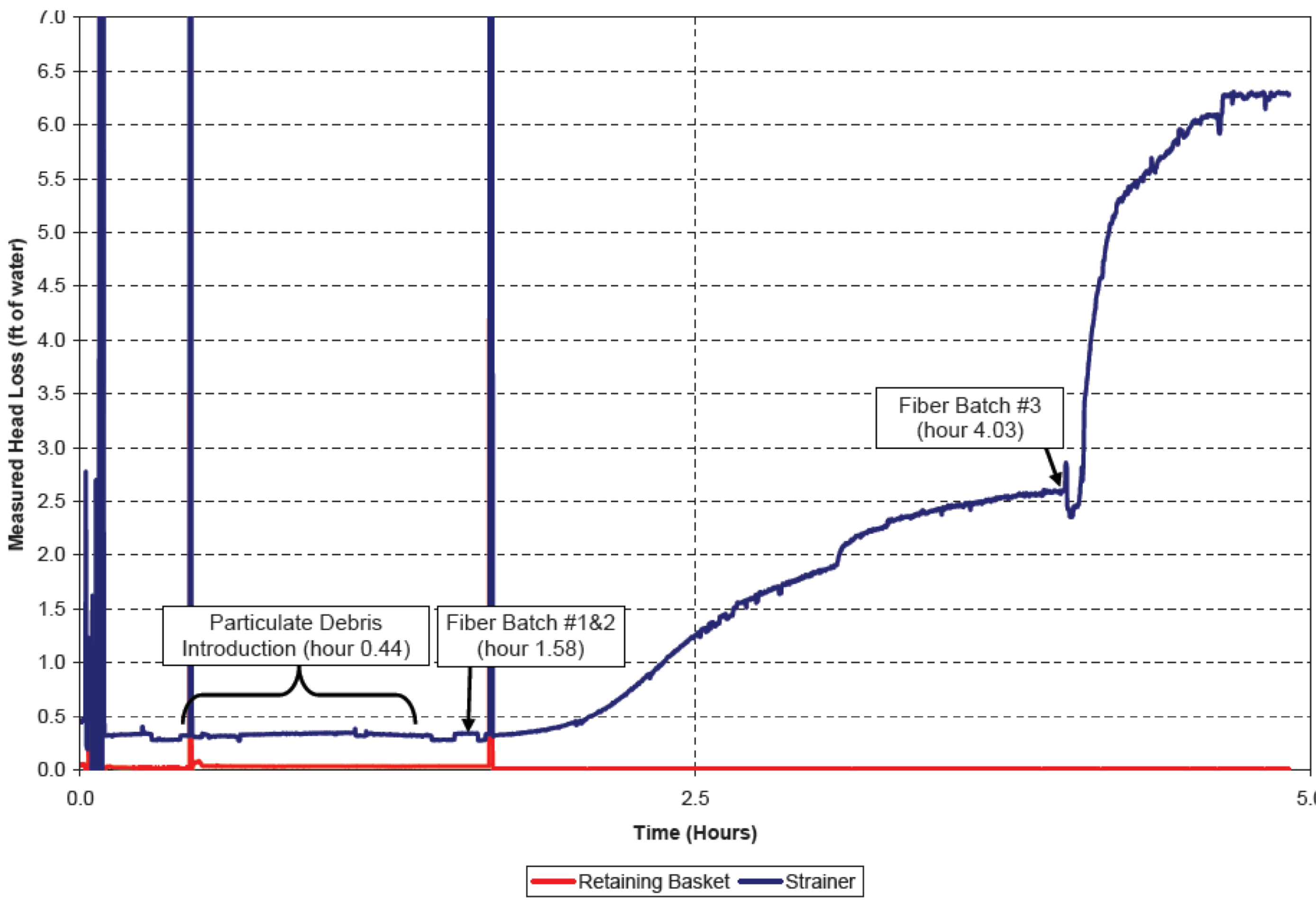

Note: The spikes in measured head loss occur at the instances where the differential pressure cells were bled

E.6.5 Test 1A

Test 1A was performed on January 6, 2011 using 0.045 inches of perforated plate on the retaining basket and 0.045 inches wire mesh on the strainer. Figure E.6-4 shows the raw data collected during the test. The test duration was 4.3 hours. The particulate debris was added to the test flume, followed by the first batch of fiber (0.21 pounds). The first batch of fiber was inserted downstream of the retaining basket. The second batch of fiber (0.34 pounds) immediately followed the first batch and was introduced to the retaining basket. After two flume turnovers and no change to strainer differential pressure, the third batch of fiber was introduced. The strainer differential pressure increased within 10 minutes of adding the third batch of fiber (0.89 pounds of total fiber in flume). The fourth batch of fiber was not added until one hour and 47 minutes after the third batch, when the strainer differential pressure stabilized at 2.9 feet of water. After the fourth batch of fiber, the strainer differential pressure rose to 5.8 feet of water at a flow rate of 311.8 gpm with 1.0 pound of fiber remaining for addition. At this point, the test was terminated because of excessive differential pressure across the strainer. There was no change to the retaining basket observed or recorded throughout the test. Similar to Test 1, drain down revealed a thin debris bed covering the strainer. The retaining basket appeared free of debris.

Figure E.6-4 Test 1A Raw Data

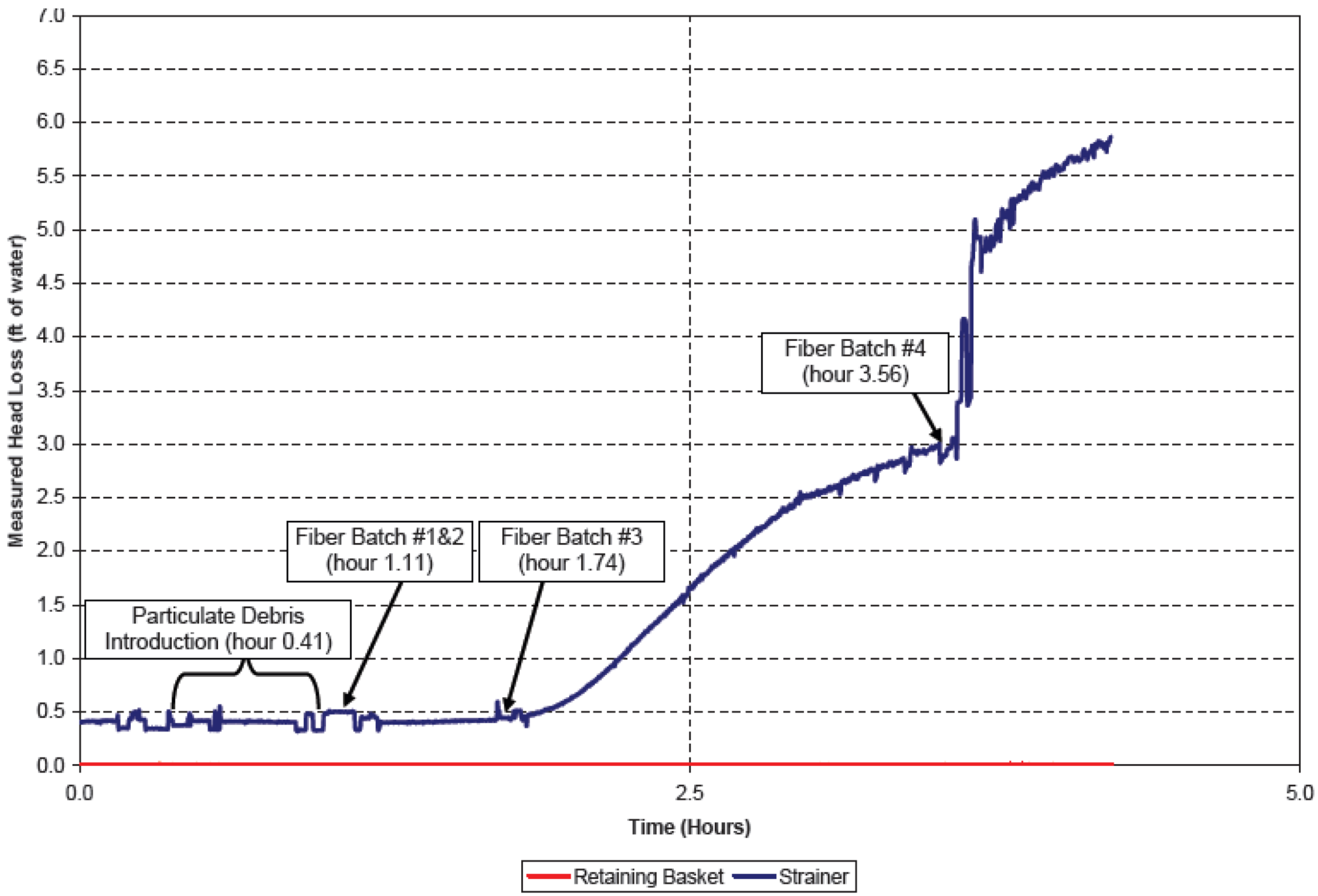

E.6.6 Test 1B

Test 1B was performed on January 13 through 14, 2011 using 0.06 inch wire mesh on the filtering surface of the strainer and retaining basket. Figure E.6-3 shows the raw data collected during the test. The test duration was 33.8 hours. The particulate debris was added to the test flume, followed by the batching of the fibrous debris. There was no change to strainer or retaining basket differential pressure after the fine particulate and fiber was added to the test apparatus. The retaining basket began to rise 30 minutes after the coating chips were introduced. The retaining basket continued to rise over the next four hours to approximately 6.5 feet above the strainer pool area, but it did not overflow. Prior to chemical addition, there was no measurable increase in the strainer differential pressure, and the retaining basket measured head loss decreased to 6.0 feet. After several chemical batch additions with no change to retaining basket or strainer head loss, the chemical batching rate was increased and documented in the test plan. Floating debris was removed, mixed with water, and re-added throughout the test to verify there was no debris floating. The maximum recorded strainer differential pressure during the last 15 flume turnovers was 0.394 feet of water at a flow rate of 321.6 gpm. The test terminated with the retaining basket head loss of 6.1 feet of water. The strainer and retaining basket headloss had stabilized to a rate of change less than one percent over the previous 30 minute time interval.

Figure E.6-5 Test 1B Raw Data

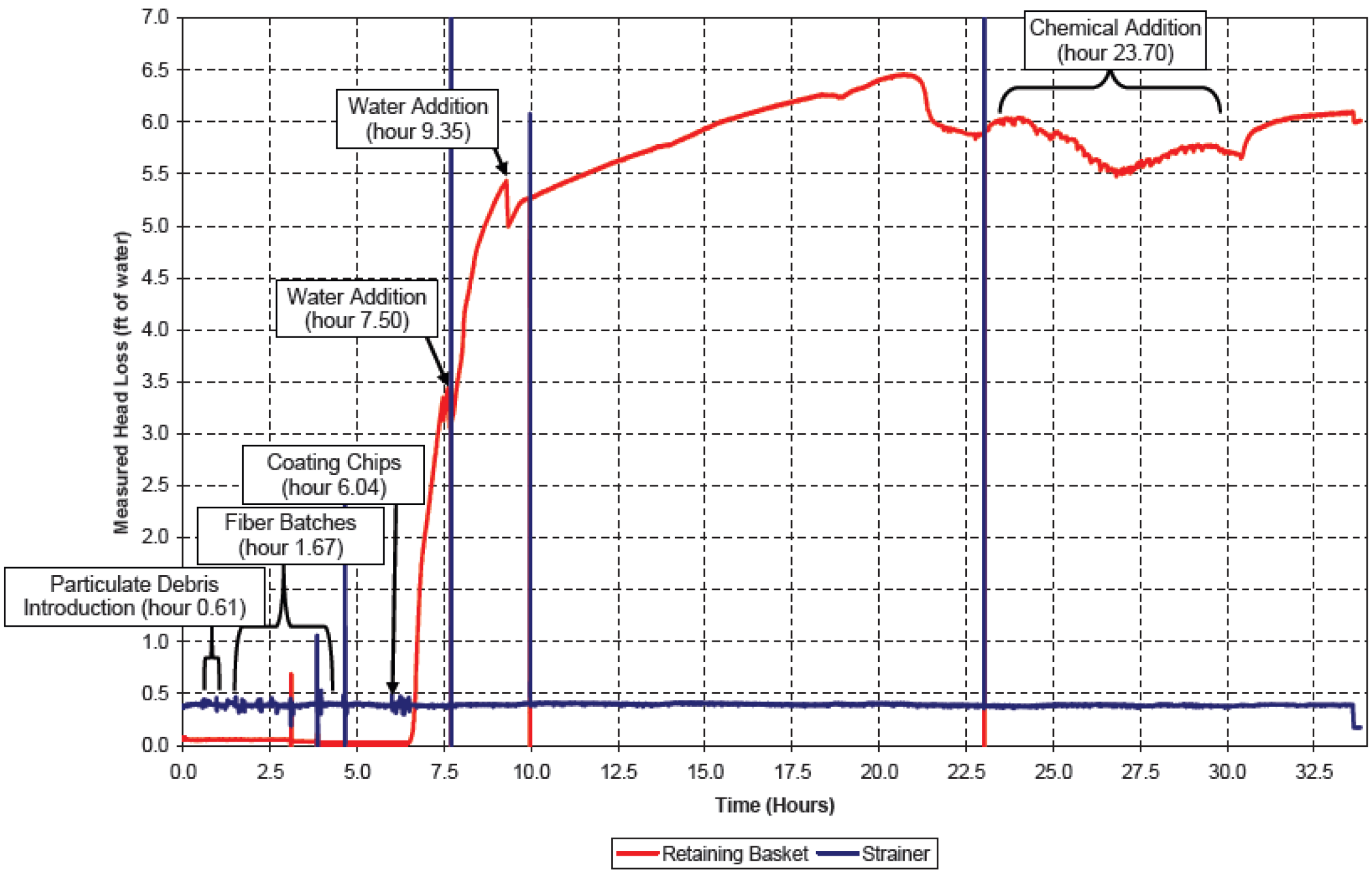

Note: The spikes in measured head loss occur at the instances where the differential pressure cells were bled

E.6.7 Test 1C

Test 1C was performed on January 19 through 20, 2011 using 0.06 inch wire mesh on the filtering surface of the strainer and retaining basket. Figure E.6-6 shows the raw data collected during the test. The test duration was 31.2 hours. The particulate debris was added to the test flume, followed by the batching of the fibrous debris. There was no change to strainer or retaining basket differential pressure after the fine particulate and fiber was added to the test apparatus. The retaining basket began to rise 30 minutes after the coating chips were introduced. The retaining basket continued to rise over the next five hours to approximately 6.3 feet above the strainer pool area, but it did not overflow. Prior to chemical addition, there was no measurable increase in the strainer differential pressure, and the retaining basket measured head loss had decreased to 6.1 feet. After several chemical batch additions with no change to retaining basket or strainer head loss, the chemical batching rate was increased and documented in the test plan. Floating debris was removed, mixed with water, and re-added throughout the test to verify there was no debris floating. The maximum recorded strainer differential pressure during the last 15 flume turnovers was 0.417 feet of water at a flow rate of 317.8 gpm. The test terminated with the retaining basket head loss of 6.2 feet of water. The strainer and retaining basket head loss had stabilized to a rate of change less than one percent over the previous 30 minute time interval.

Figure E.6-6 Test 1C Raw Data

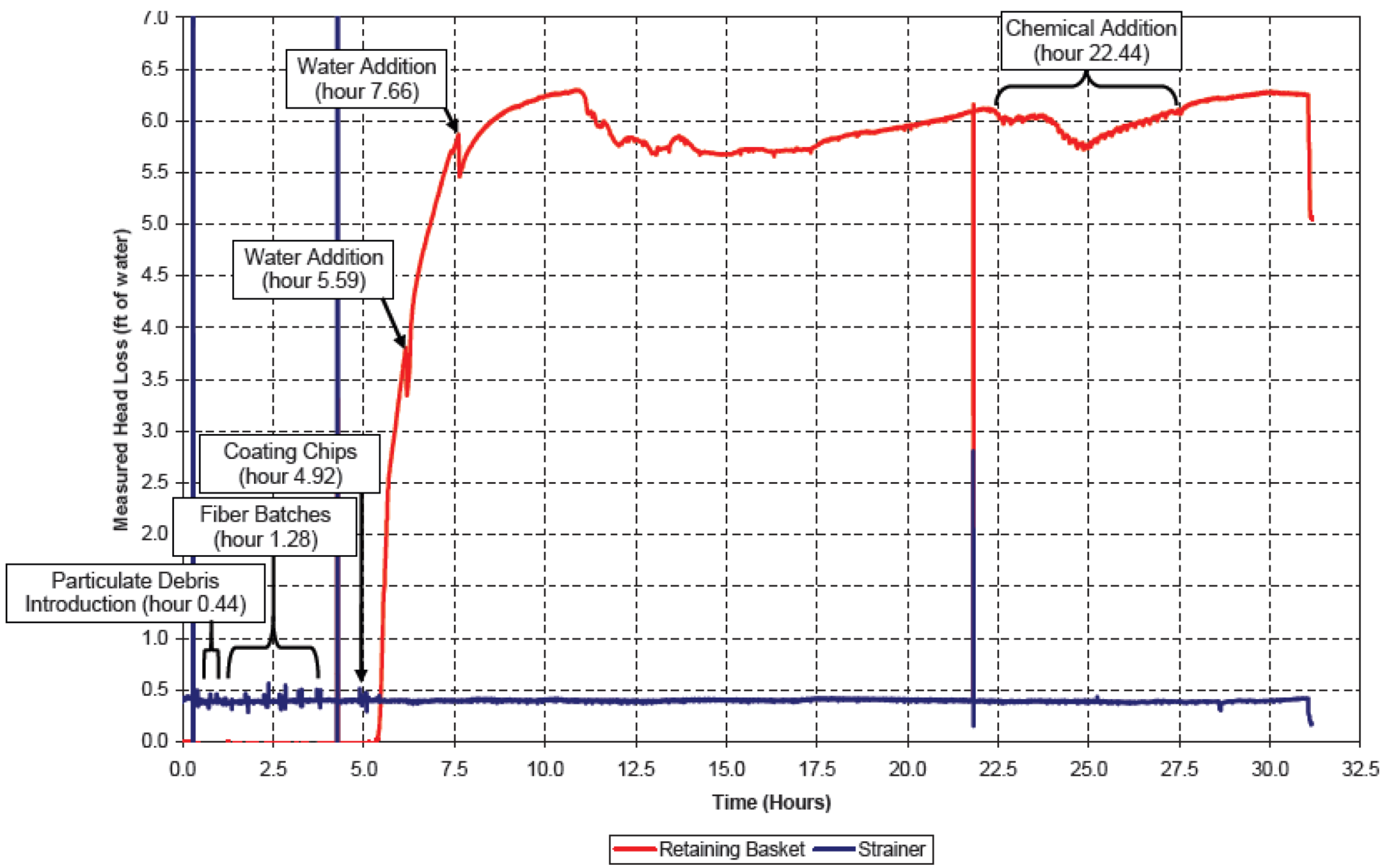

Note: The spikes in measured head loss occur at the instances where the differential pressure cells were bled

E.6.8 Test 1D

Test 1D was performed on January 26 through 27, 2011 using 0.08 inch wire mesh on the filtering surface of the strainer and retaining basket. Figure E.6-7 shows the raw data collected during the test. The test duration was 34.6 hours. The particulate debris was added to the test flume, followed by the batching of the fibrous debris. There was no change to strainer or retaining basket differential pressure after the fine particulate and fiber was added to the test apparatus. The retaining basket began to rise 35 minutes after the coating chips were introduced. The retaining basket continued to rise over the next four hours to approximately 2.4 feet above the strainer pool area. Prior to chemical addition, there was no measurable increase in the strainer differential pressure, and the retaining basket measured head loss had decreased to 2.1 feet. After several chemical batch additions with no change to retaining basket or strainer head loss, the chemical batching rate was increased and documented in the test plan. Floating debris was removed, mixed with water, and re-added throughout the test to verify there was no debris floating. The maximum recorded strainer differential pressure during the last 15 flume turnovers was 0.427 feet of water at a flow rate of 325.8 gpm. The test terminated with the retaining basket head loss of 2.1 feet of water. The strainer and retaining basket head loss had stabilized to a rate of change less than one percent over the previous 30 minute time interval. After termination, the test flume was drained and revealed that approximately 90 percent of the top of the strainer was covered with debris. The front face of the strainer was free of debris. The retaining basket had a thin debris bed up to the level where it was clogged. Hundreds of holes penetrated the retaining baskets debris bed when the water level was completely emptied in the area of the strainer.

Figure E.6-7 Test 1D Raw Data

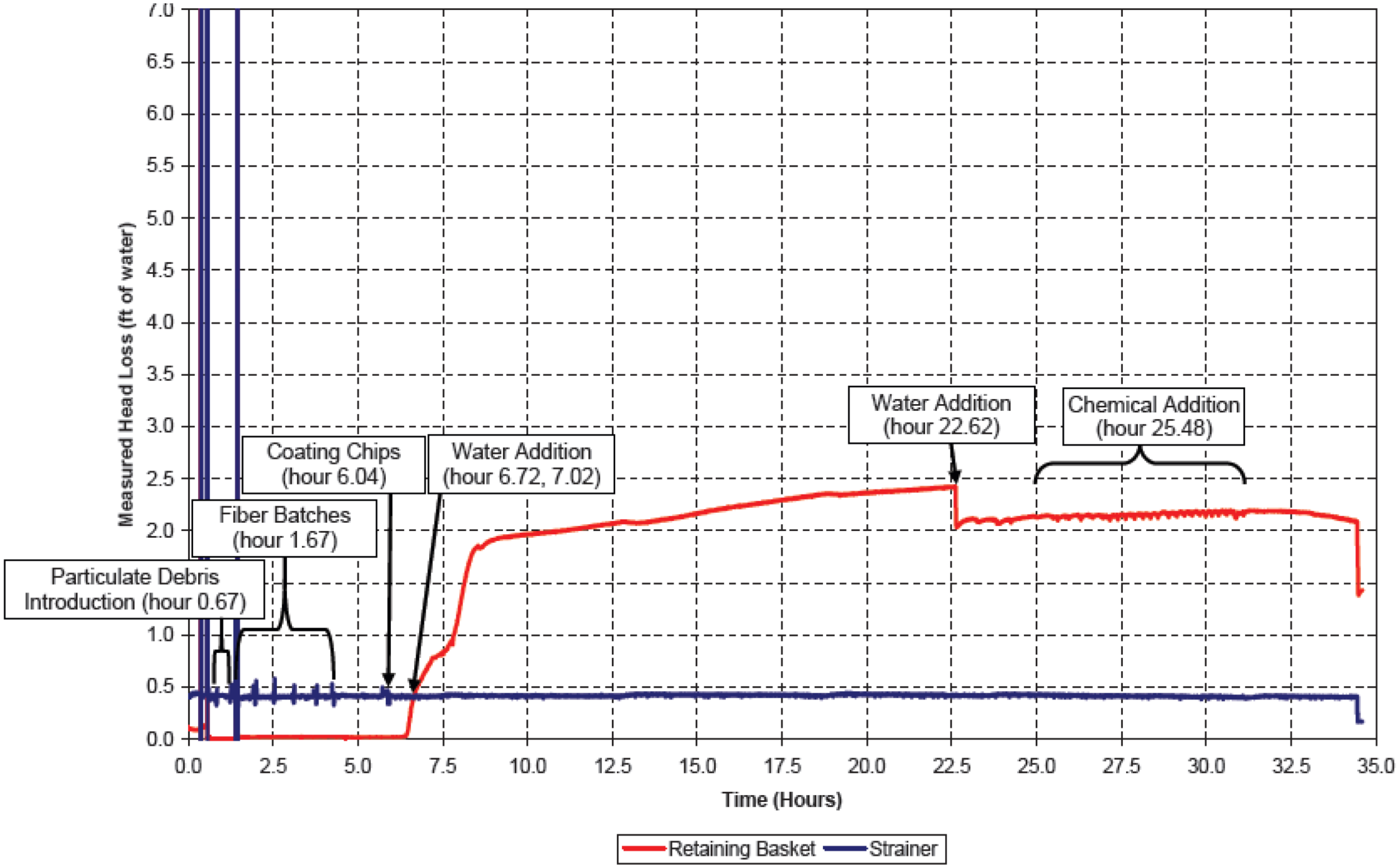

Note: The spikes in measured head loss occur at the instances where the differential pressure cells were bled

E.6.9 Test 1E

Test 1E was performed on February 1 through 2, 2011 using 0.08 inch wire mesh on the filtering surface of the strainer and retaining basket. Figure E.6-8 shows the raw data collected during the test. The test duration was 32.1 hours. The particulate debris was added to the test flume, followed by the batching of the fibrous debris. There was no change to strainer or retaining basket differential pressure after the fine particulate and fiber was added to the test apparatus. The retaining basket began to rise 33 minutes after the coating chips were introduced. The retaining basket continued to rise over the next five hours to approximately 2.2 feet above the strainer pool area. Prior to chemical addition, there was no measurable increase in the strainer differential pressure, and the retaining basket measured head loss had decreased to 2.1 feet. After several chemical batch additions with no change to retaining basket or strainer head loss, the chemical batching rate was increased and documented in the test plan. Floating debris was removed, mixed with water, and re-added throughout the test to verify there was no debris floating. The maximum recorded strainer differential pressure during the last 15 flume turnovers was 0.423 feet of water at a flow rate of 330.2 gpm. The test terminated with the retaining basket head loss of 2.4 feet of water. The strainer and retaining basket head loss had stabilized to a rate of change less than one percent over the previous 30 minute time interval. Drain down revealed the same observations as Test 1D.

Figure E.6-8 Test 1E Raw Data

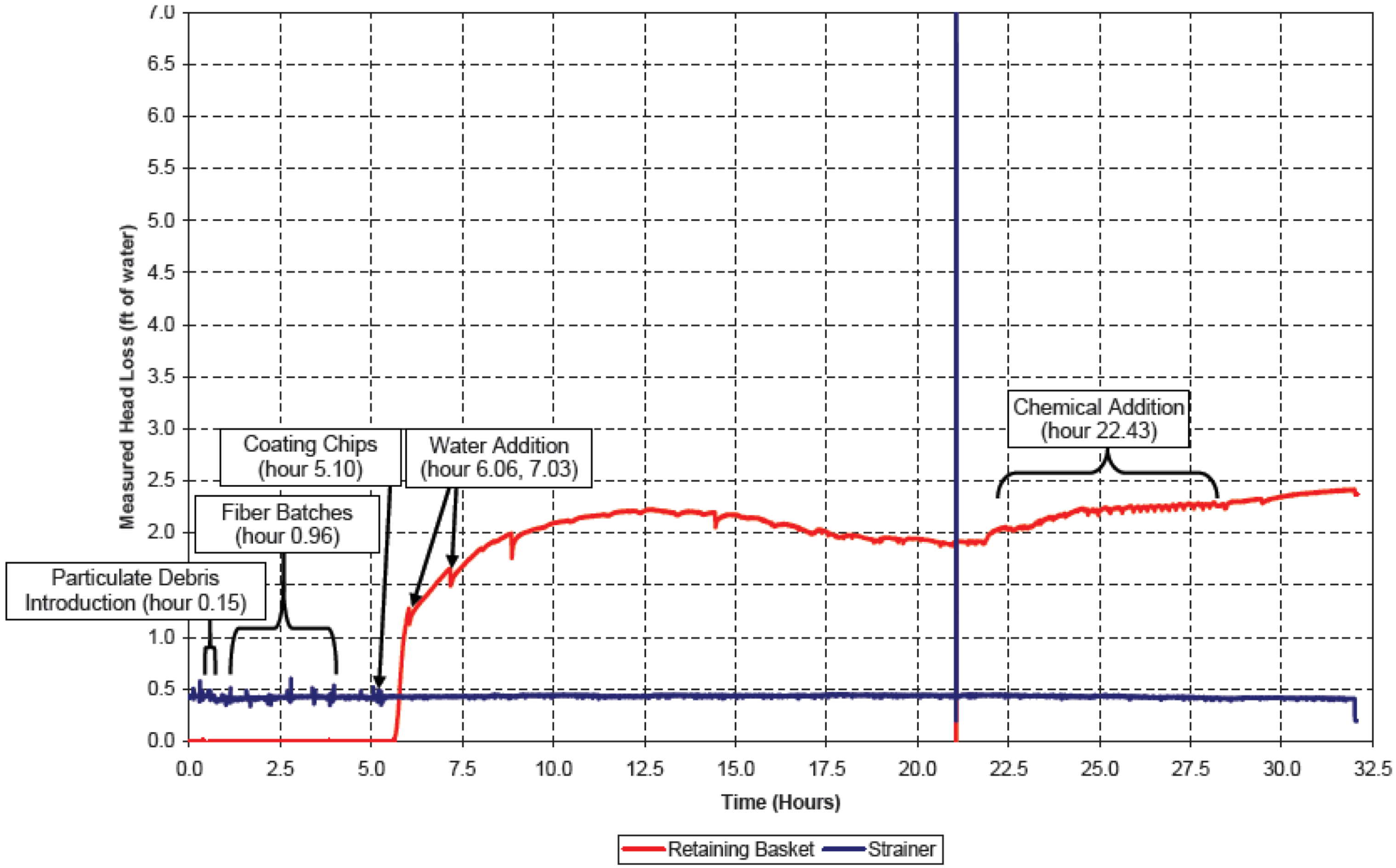

Note: The spike in measured head loss occur at the instances where the differential pressure cells were bled

E.6.10 Test 2A

Test 2A was completed on January 11, 2011 with 0.06 inch mesh on the retaining basket and strainer. This test used filter bags to capture any debris that bypassed the retaining basket and strainer. The differential pressure recorded across the retaining basket and strainer did not change during the test. This was an expected result because particulate debris was not included to induce a solid debris bed. Floating fiber was continually swept off the top of the test flume, mixed with water, and reintroduced to the test flume along the downstream face of the retaining basket. Table E.6-7 shows the filter bag weights before and after the test.

Table E.6-7 Test 2A Pre and Post Filter Bag Weights

Filter Bag #	Pre Test Weight (g)	Post Test Weight (g)	Net (g)
30	295.51	322.47	26.96
31	285.81	306.17	20.36
32	267.86	295.59	27.73
33	259.04	291.54	32.50
34	261.86	279.85	17.99
35	287.94	308.43	20.49
36	297.80	315.63	17.83
37	294.80	329.89	35.09
38	294.28	316.58	22.30
39	279.81	314.20	34.39
40	252.18	272.19	20.01
41	251.54	290.64	39.10
42	255.24	280.76	25.52
43	257.41	290.70	33.29
44	253.37	282.14	28.77
45	261.57	296.46	34.89
46	294.99	313.31	18.32
47	288.51	322.15	33.64
48	280.75	301.07	20.32
49	284.67	321.67	37.00
50	274.65	297.40	22.75
51	281.71	315.72	34.01
52	279.43	301.36	21.93
53	284.14	322.18	38.04

Table E.6-8 shows the bypass fraction calculated after 25 percent, 50 percent, 75 percent, and 100 percent of debris was added to the flume. After the fiber addition, the flume was recirculated for five additional turnovers to verify the filter bags captured the fiber.

Table E.6-8 Test 2A Fiber Bypass

Filter Bags	Test Order	Net Bypass (g)	Net Bypass (lbm)	Total Fiber in Flume (lbm)	Bypass Fraction (%)
30-35	First	146.03	0.3219	0.56	57.5%
36-41	Second	314.75	0.6939	1.11	62.5%
42-47	Third	489.18	1.0785	1.66	65.0%
48-53	Fourth	663.23	1.4622	2.20	66.5%

E.6.11 Test 2D

Test 2D was completed on January 24, 2011 with 0.08 inch wire mesh on the retaining basket and strainer. The Test 2D fiber only bypass test was terminated after the initial fiber introduction to the retaining basket because of water discoloration. The discoloration was caused by particulate debris trapped in the debris introduction system. The test was terminated because the particulate debris would have been captured by the filter bags, yielding inaccurate bypass results.

E.6.12 Test 2E

Test 2E was completed on January 25, 2011 with 0.08 inch wire mesh on the retaining basket and strainer. This test used filter bags to capture any debris that bypassed the retaining basket and strainer. The differential pressure recorded across the retaining basket and strainer did not change during the test. Floating fiber was continually swept off the top of the test flume, mixed with water, and reintroduced to the test flume along the downstream face of the retaining basket. Drain down of the test flume after the test revealed that approximately 50 percent of the strainer was covered with a thin layer of fiber. The top two to three inches of retaining basket screen was covered with fiber at the test water level. Additionally, there was one clump of fiber that was freed from below a support once the water level dropped to less than eight feet. The clump of fiber was approximately four inches by 10 inches by one inch.

Table E.6-9 Test 2E Pre and Post Filter Bag Weights

Filter Bag #	Pre Test Weight (g)	Post Test Weight (g)	Net (g)
150	262.95	280.10	17.15
151	251.81	297.53	45.72
152	261.76	279.50	17.74
153	259.07	278.13	19.06
154	264.41	281.88	17.47
155	261.80	302.49	40.69
156	254.49	297.81	43.32
157	264.86	286.86	22.00
158	249.29	288.80	39.51
159	259.98	281.07	21.09
160	256.17	298.14	41.97
161	256.97	275.37	18.40
162	260.54	292.15	31.61
163	251.43	272.31	20.88
164	258.23	294.29	36.06
165	258.42	281.54	23.12
166	262.13	296.62	34.49
167	250.98	263.68	12.70
168	255.30	300.76	45.46
169	261.57	285.29	23.72
170	247.45	292.04	44.59
171	255.87	282.99	27.12
172	253.54	278.75	25.21
173	250.17	275.55	25.38

Table E.6-10 shows the bypass fraction calculated after 25 percent, 50 percent, 75 percent, and 100 percent of debris was added to the flume. After the fiber addition, the flume was recirculated for five additional turnovers to verify that the filter bags captured the fiber.

Table E.6-10 Test 2E Fiber Bypass

Filter Bags	Test Order	Net Bypass (g)	Net Bypass (lbm)	Total Fiber in Flume (lbm)	Bypass Fraction (%)
150-155	First	157.83	0.3480	0.56	62.1%
156-161	Second	344.12	0.7587	1.11	68.3%
162-167	Third	502.98	1.1089	1.66	66.8%
168-173	Fourth	694.46	1.5310	2.20	69.6%

E.6.13 Test 2F

Test 2F was completed on January 31, 2011 with 0.08 inch wire mesh on the retaining basket and strainer. This test used filter bags to capture any debris that bypassed the retaining basket and strainer. The differential pressure recorded across the retaining basket and strainer did not change during the test. Floating fiber was continually swept off the top of the test flume, mixed with water, and reintroduced to the test flume. Table E.6-11 shows the filter bag weights before and after the test. Drain down of the test flume after the test revealed that approximately 50 percent of the strainer was covered with a thin layer of fiber. The top two to three inches of retaining basket screen was covered with fiber at the test water level. Additionally, there was one clump of fiber that was freed from below a support once the water level dropped to less than eight feet. The clump of fiber was approximately six inches by 4 inches by one inch.

Table E.6-11 Test 2F Pre and Post Filter Bag Weights

Filter Bag #	Pre Test Weight (g)	Post Test Weight (g)	Net (g)
223	249.47	267.48	18.01
222	248.47	287.64	39.17
221	256.07	278.51	22.44
220	250.47	286.26	35.79
219	250.73	268.89	18.16
218	254.53	291.22	36.69
217	265.28	280.99	15.71
216	254.55	273.11	18.56
215	256.23	279.55	23.32
214	257.47	293.11	35.64
213	255.76	289.46	33.70
212	263.39	299.87	36.48
211	259.02	293.85	34.83
210	254.71	273.14	18.43
209	257.49	282.32	24.83
208	256.79	292.74	35.95
207	257.26	279.93	22.67
206	265.81	301.76	35.95
205	252.38	273.17	20.79
204	253.68	294.00	40.32
203	253.89	277.73	23.84
202	254.51	271.07	16.56
201	249.15	287.43	38.28
200	254.84	293.90	39.06

Table E.6-12 shows the bypass fraction calculated after 25 percent, 50 percent, 75 percent, and 100 percent of debris was added to the flume. After the fiber addition, the flume was recirculated for five additional turnovers to verify that the filter bags captured the fiber.

Table E.6-12 Test 2F Fiber Bypass

Filter Bags	Test Order	Net Bypass (g)	Net Bypass (lbm)	Total Fiber in Flume (lbm)	Bypass Fraction (%)
218-223	First	170.26	0.3754	0.56	67.0%
212-217	Second	333.67	0.7356	1.11	66.3%
206-211	Third	506.33	1.1163	1.66	67.2%
200-205	Fourth	685.18	1.5106	2.20	68.7%

E.7 Conclusions

E.7.1 Debris Transport Test

The results of the Debris Transport Test are provided in Section E.6.2. The test results demonstrate that the test debris was entirely captured and contained within the retaining basket. Therefore, it is concluded that there are no adverse effects to the ECCS strainer operation.

E.7.2 Head Loss Testing

Table E.7-1 summarizes the head loss testing performed in January and February 2011. Test 1 and 1A demonstrated that small hole size openings on the strainer created excessive head losses across the strainer with only small amounts of fiber introduced to the test flume. Test 1 and 1A also demonstrate the conservative method of challenging the strainer with incremental fiber addition. Test 1B, 1C, 1D, and 1E did not show an increase in strainer differential pressure and only recorded a retaining basket rise after the addition of paint chips. Though the top of the strainer was significantly covered with debris during the last four tests, the front face remained mostly free of debris as observed during drain downs. Tests 1B through 1E were performed using the entirety of the design basis debris source term. As a result, Test 4 (design basis debris loading strainer head loss test) was not required. Test 1C and 1E were performed to confirm repeatability.

Table E.7-1 Head Loss Testing Summary

Test #	Retaining Basket	Strainer	Strainer Head Loss (ft of water)	Basket Rise (ft)
Test 1	0.045" Perf	0.045" Perf	6.3	0
Test 1A	0.045" Perf	0.045" Mesh	5.8	0
Test 1B	0.06" Mesh	0.06" Mesh	0.394	6.1
Test 1C	0.06" Mesh	0.06" Mesh	0.417	6.2
Test 1D	0.08" Mesh	0.08" Mesh	0.427	2.1
Test 1E	0.08" Mesh	0.08" Mesh	0.423	2.4

E.7.3 Bypass Testing

Table E.7-2 summarizes the bypass testing performed in January and February 2011. The summary shows that using 0.06 inch wire mesh does not significantly reduce the amount of bypass compared to the 0.08 inch wire mesh. The bounding bypass fraction from testing was 69.6 percent bypass. The fiber bypass test with full fiber addition (Test 3) was not required because the basket did not overflow because of thin bed testing.

Table E.7-2 Bypass Testing Summary

Test #	Retaining Basket	Strainer	First 25% Bypass	Total Bypass
Test 2A	0.06" Mesh	0.06" Mesh	57.5%	66.5%
Test 2E	0.08" Mesh	0.08" Mesh	62.1%	69.6%
Test 2F	0.08" Mesh	0.08" Mesh	67.0%	68.7%

Figure E.7-1 shows the repeatability of the bypass test results. It also shows that the bypass fraction observed increased linearly after each addition. In other words, each incremental addition had a similar bypass fraction. The difference between the two mesh sizes was not significant with respect to bypass fraction. The final configuration selected was 0.08 inch wire mesh on the strainer and retaining basket.

Figure E.7-1 Bypass Fraction per Fuel Assembly

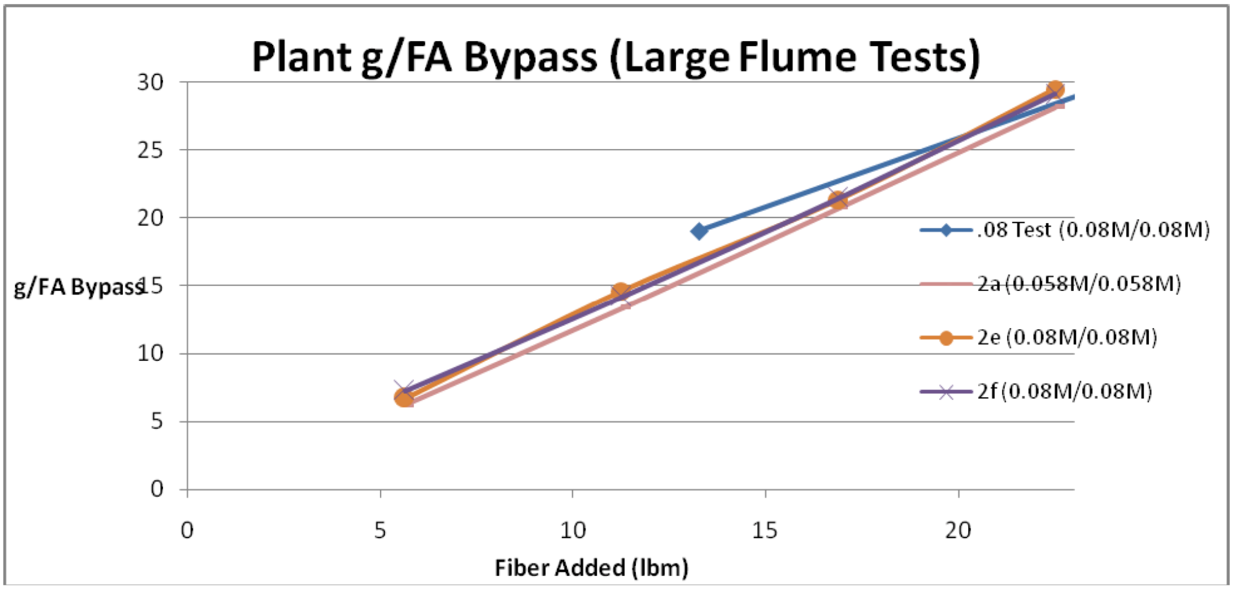

E.7.4 Filter Media Results

Ten tests were conducted over a five week period to test the various filter media for the retaining basket and strainer. Testing concluded that both 0.06 inch wire mesh and 0.08 inch wire mesh on the strainer and retaining basket provide sufficient margin with regards to strainer differential pressure. Tests 1D, 1E, 2E and 2F comprise the design basis testing for this configuration

E.8 References

1. NEI 04-07 Vol. 1 (Methodology), “Pressurized Water Reactor Sump Performance Evaluation Methodology,” December 2004.

2. NEI 04-07 Vol. 2 (Safety Evaluation), “Pressurized Water Reactor Sump Performance Evaluation Methodology,” December 2004.

3. “NRC Staff Review Guidance Regarding Generic Letter 2004-02 Closure in the Area of Strainer Head Loss and Vortexing” March 2008.

Appendix F
Downstream Effects Evaluation for the U.S. EPR

F.1 Introduction

Pressurized Water Reactor (PWR) containment buildings are designed to contain radioactive materials releases and facilitate core cooling in the event of a postulated loss-of-coolant accident (LOCA). The cooling process requires water discharged from the break to be collected in the in-containment refueling water storage tank (IRWST) for recirculation by the emergency core cooling system (ECCS). The IRWST contains numerous devices (weirs, strainer baskets, and screens) that protect the components of the ECCS from debris that could be washed into the IRWST. Fibrous debris could form a mat on either the basket screen or the strainer that would collect particulates, keeping them from being ingested into the ECCS. However, while the fiber bed is forming, or if the fiber bed does not completely cover the screens, particulates and some fibrous material may be ingested into the ECCS and subsequently flow into the reactor coolant system (RCS).

Concerns have been raised about the potential for debris ingested into the ECCS to affect long-term core cooling when recirculating coolant from the containment sump (NRC Generic Letter 2004-02 (Reference 1)). The fuel assembly bottom nozzles are designed with flow passages that provide coolant flow from the reactor vessel lower plenum into the region of the fuel rods. During operation of the ECCS to recirculate coolant from the IRWST, debris in the recirculating fluid that passes through the sump screen may collect on the bottom surface of the fuel assembly bottom nozzle, causing a flow resistance through this path. The collection of sufficient debris on the fuel assembly bottom nozzle is postulated to impede flow into the fuel assemblies and core. Other concerns have been raised with respect to the collection of debris and post-accident chemical products within the core itself. Specifically, the debris has been postulated to form blockages at intermediate spacer grids, thereby reducing the ability of the coolant to remove decay heat from the core. Similarly, chemical precipitants have been postulated to plate-out on fuel cladding, again resulting in a reduction of the ability of the coolant to remove decay heat from the core.

AREVA NP undertook a program to provide analyses and data on the effect of debris and chemical products on core cooling for the U.S. EPR plant when the ECCS is actuated. The objective of the program was to demonstrate reasonable assurance that sufficient long term core cooling (LTCC) is achieved for U.S. EPR plant to satisfy the requirements of 10 CFR 50.46(b)(5) with debris and chemical products that might be transported to the reactor vessel and core by the coolant recirculating from the IRWST. The debris composition includes particulate and fiber debris, as well as post-accident chemical products. This evaluation considered the design of the U.S. EPR plant, the design of the open-lattice fuel, the design and tested performance of the strainer baskets and sump screens, the tested performance of materials inside containment, and the tested performance of fuel assemblies in the presence of debris. Specific areas addressed in this evaluation include:

- Collection of debris on fuel assembly bottom nozzle or intermediate spacer grids,
- Production and deposition of chemical precipitants and debris on the fuel rod cladding.

The collection of debris in the fuel assembly bottom nozzle or at the spacer grids may be addressed by fuel assembly testing. The purpose of this testing, described in Section F.3, is to determine the mass of debris that can be deposited at the core entrance or at spacer grids that will not impede long-term core cooling flows to the core. These acceptance criteria will be used in part to demonstrate adequate flow for long-term decay heat removal.

An evaluation of the deposition of chemical precipitates and debris on the fuel rods was performed by applying U.S. EPR-specific design parameters to the U.S. EPR LOCA Deposition Analysis Model (EPRDM). This calculation, described in Section F.4, provides a conservative evaluation of:

1. The deposition thicknesses on fuel rod surfaces due to chemical and debris deposition.

2. The cladding temperatures under the buildup for up to 30 days following a LOCA.

F.2 Background

Immediately after the break opens, the RCS fluid is expelled as a jet to containment. The energy from this jet impacts structures near the break and generates debris through destruction of coatings and insulation. The amount of debris generated depends on the break location and size. The limiting amount of debris is generated by a full-area pipe break (refer to Section C.6.5). The discussion and transient descriptions in this document focus on large break LOCAs. Debris generated in smaller breaks is bounded by that of the large break LOCAs. The debris falls to the heavy floor and, depending on the size and density, transports to one of four holes in the heavy floor where it passes over the weirs around the openings, through the trash racks, to the retention baskets and, possibly, into the IRWST.

Within the first minute following the break, the ECCS actuates. The medium head safety injection (MHSI) and low head safety injection (LHSI) draw suction from the bottom of the IRWST. This ECCS flow in combination with the accumulator flow replaces the RCS liquid lost through the break and arrests any clad heatup. After the ECCS injection begins, the core level is recovered and the RCS is refilled to the break location. In the long term for any RCS pipe break, the two-phase mixture level is above the top of the core. The core decay heat is removed by ECCS injection. The core flow and vessel level depend on the break location, ECCS injection rate and configuration, and RCS cold leg liquid levels.

The ECCS in the U.S. EPR design operates in two configurations:

1. Cold leg injection.

2. Simultaneous hot and cold leg injection.

Depending on the break location, each configuration introduces debris to the core region at different locations and at different rates. Regarding the effect of debris ingestion on long-term core cooling, two periods of interest for the U.S. EPR are:

1. From debris arrival up to the time hot leg injection (HLI) is initiated at 60 minutes (Section F.2.1).

2. From the time of HLI at approximately 60 minutes up to the termination of core steaming (Section F.2.2).

F.2.1 Cold Leg ECCS Injection Period (from Debris Arrival to 60 Minutes)

In this first period from debris arrival until the switchover to HLI at approximately 60 minutes, the removal of core decay heat occurs as part of long-term core cooling. The minimum allowable core flow removes the decay heat energy.

During cold leg injection, MHSI and LHSI only inject into the cold legs. For cold leg pump discharge (CLPD) breaks (Figure F.2-1 and Figure F.2-2), the pumped ECCS injected into the intact cold legs provides liquid to make up for core boil-off. The ECCS liquid keeps the downcomer full to at least the bottom of the cold leg nozzles; any excess ECCS flows out of the broken cold leg through the break and back into the containment sump. The core mixture level is controlled by the manometric balance between the downcomer liquid level, the core level, and RCS pressure drop needed to pass the core generated steam to the break location. The situation is similar for cold leg pump suction (CLPS) breaks, although the downcomer liquid level may be higher depending on the relationship of the pump spillover elevation to the bottom of the CLPD piping.

For a break in the hot leg (Figure F.2-3), all the ECCS flow must pass through the core to exit the break. The core mixture level will be at least to the bottom of the hot leg nozzle elevation, and the core flow rate will equal the ECCS flow rate.

In either case, debris that enters the RCS will approach the core from the downcomer and RV lower plenum. Further, in order for the debris to be transported through the

RCS, it must be fairly well mixed in the ECCS fluid and be close to neutrally buoyant. Therefore, the debris is homogeneously mixed with the ECCS fluid such that the fraction of debris reaching the core inlet is proportional to the ratio of flow reaching the core inlet to the total ECCS flow rate.

F.2.2 Hot Leg ECCS Injection Period (after 60 Minutes)

The post-reflood peak containment pressure occurs at approximately 60 minutes into the transient when the LHSI HLI is initiated to suppress steaming from the core (Reference 17, Section 9). In accordance with NUREG-0800 (Reference 18, Section 6.2.1.1.A), containment pressure steadily decreases to below half the peak pressure at 24 hours after the accident. The boron precipitation analysis concluded that the required time to switch to HLI to prevent boron precipitation is later than one hour into the transient (Reference 19, Section 2.4.7). HLI at 60 minutes prevents boron precipitation. In this second period, from the time of HLI, the phenomenon of interest is the circulation of ECCS water within and throughout the core.

Sixty minutes after the break, the operator realigns the operating LHSI trains from injecting solely into the cold legs to the HLI mode, in which 75 percent of the LHSI water is injected into the respective hot legs. This realignment mitigates the possible build up of boric acid in the core, condenses steam in the upper plenum, and circulates ECC water throughout the core. In this configuration, MHSI and a portion of LHSI continue to inject into the cold legs. Consequently, ECC water is provided simultaneously to the cold and hot legs. This mode of operation is also known as HLI. The core flow patterns for this injection configuration are illustrated in Figure F.2-4.

An assessment of fluid mixing in the reactor during HLI shows the following: with the initiation of HLI, the cold ECCS water mixes with the steam-water mixture in the RV upper plenum and in the hot legs and flows down into the core region. If the RV mixture level is lower than the bottom of the hot leg, the cold water will interact with the steam in the upper plenum and in the hot leg resulting in substantial steam condensation. If the mixture level is in the hot leg and the stratified liquid level height is above the centerline of the hot leg then the ECCS water jet has less chance for steam-water interaction. In either case, as the water falls into the upper plenum, it spreads on top of 15 to 20 percent of the fuel assemblies per hot leg injection location and mixes with the re-circulating hot water and flows downwards. As the water flows down into the core region through the relatively low power periphery fuel assemblies, it suppresses the boiling in these fuel bundles as well as provides cross flows into the neighboring bundles. The downward flowing liquid region continues to grow until the steam production in all the bundles eventually ceases.

Following a cold leg break, the initiation of HLI at 60 minutes induces a reverse flow in the downcomer such that ECCS injected to the cold legs flows directly to the break. The only flow to the core is from the top via HLI. Debris that reaches the RCS will approach the core from the top.

Following a hot leg break, the HLI from the intact hot leg(s) mixes with steam and flow into the core as described above. The flow in the broken loop exits the break in the hot leg before reaching the core. Therefore, the net ECCS flow to the top of the core will be less than that seen for the cold leg break, where all of the HLI reaches the top of the core. At the same time, the ECCS injected to the cold legs can enter the core in the usual core flow direction. Debris that reaches the RCS will approach the core from both the top and bottom.

In both cases, in order for the debris to be transported through the RCS, it must be fairly well mixed in the ECC fluid and be close to neutrally buoyant. Therefore, the debris is homogeneously mixed with the ECCS fluid such that the ratio of debris reaching the core inlet or exit is proportional to the fraction of flow reaching the core inlet or exit to the total ECCS flow rate.

Figure F.2-1: Core Flow Patterns Following a Cold Leg Break During Cold Leg Injection

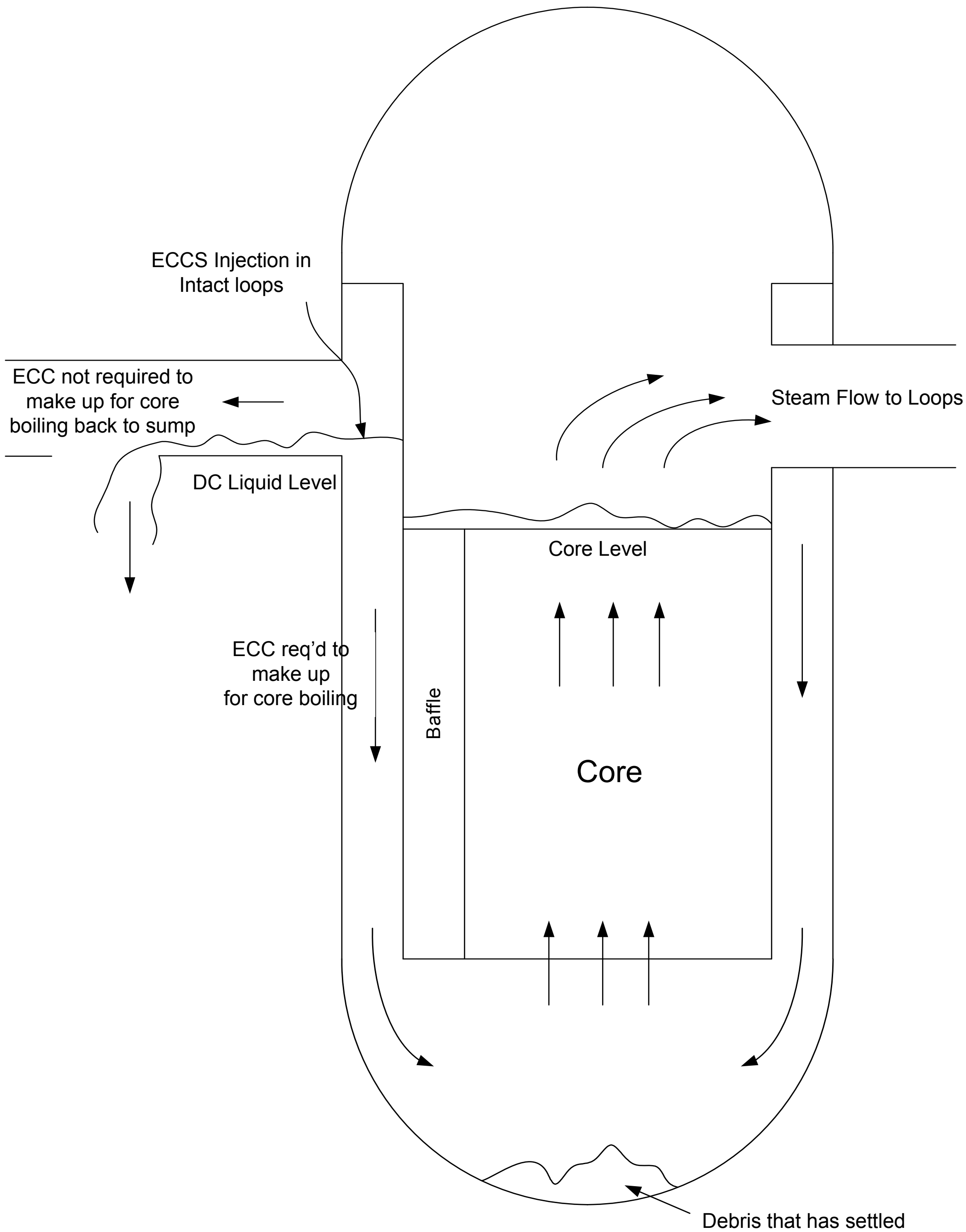

Figure F.2-2: Core Flow Patterns Following a Cold Leg Break During Cold Leg Injection (Another View)

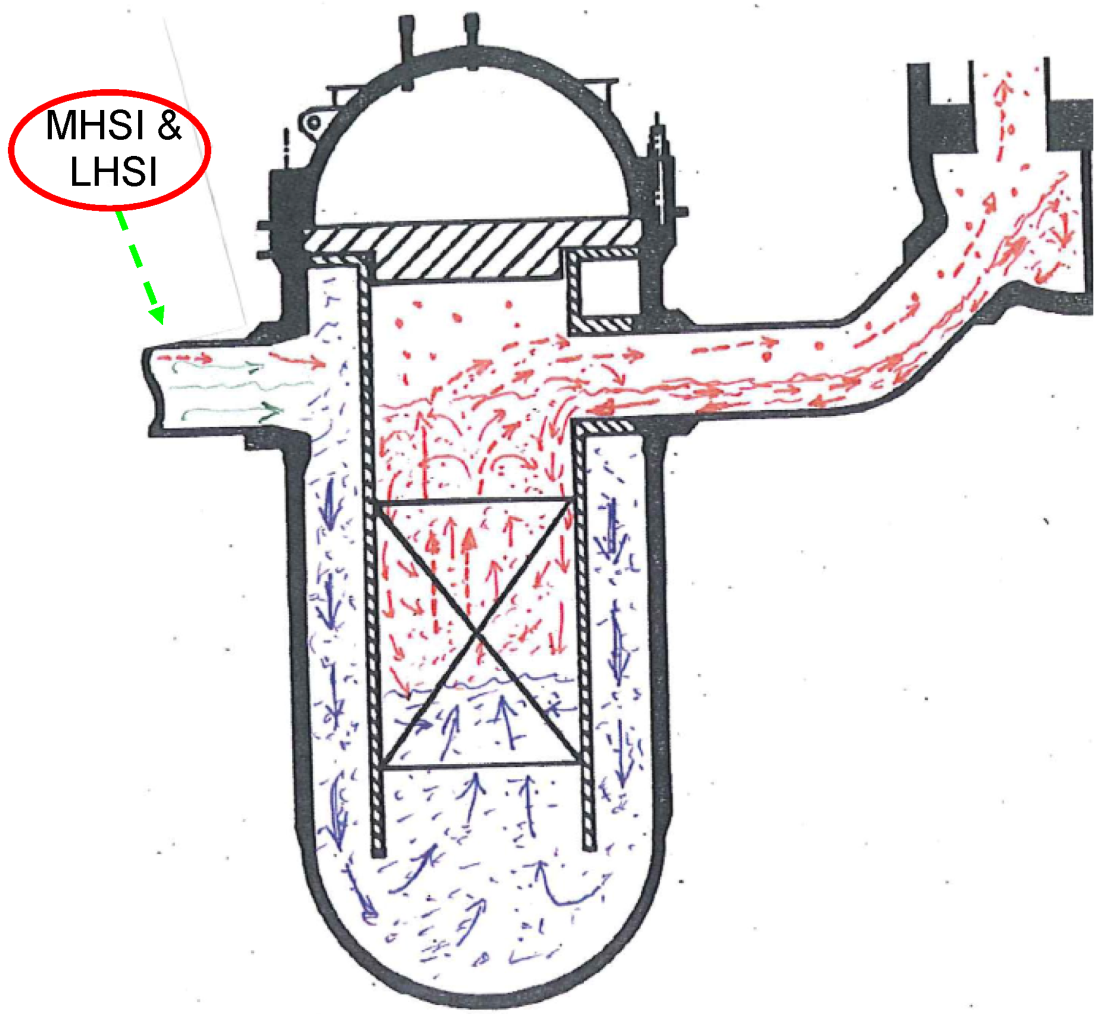

Figure F.2-3: Core Flow Patterns Following a Hot Leg Break During Cold Leg Injection

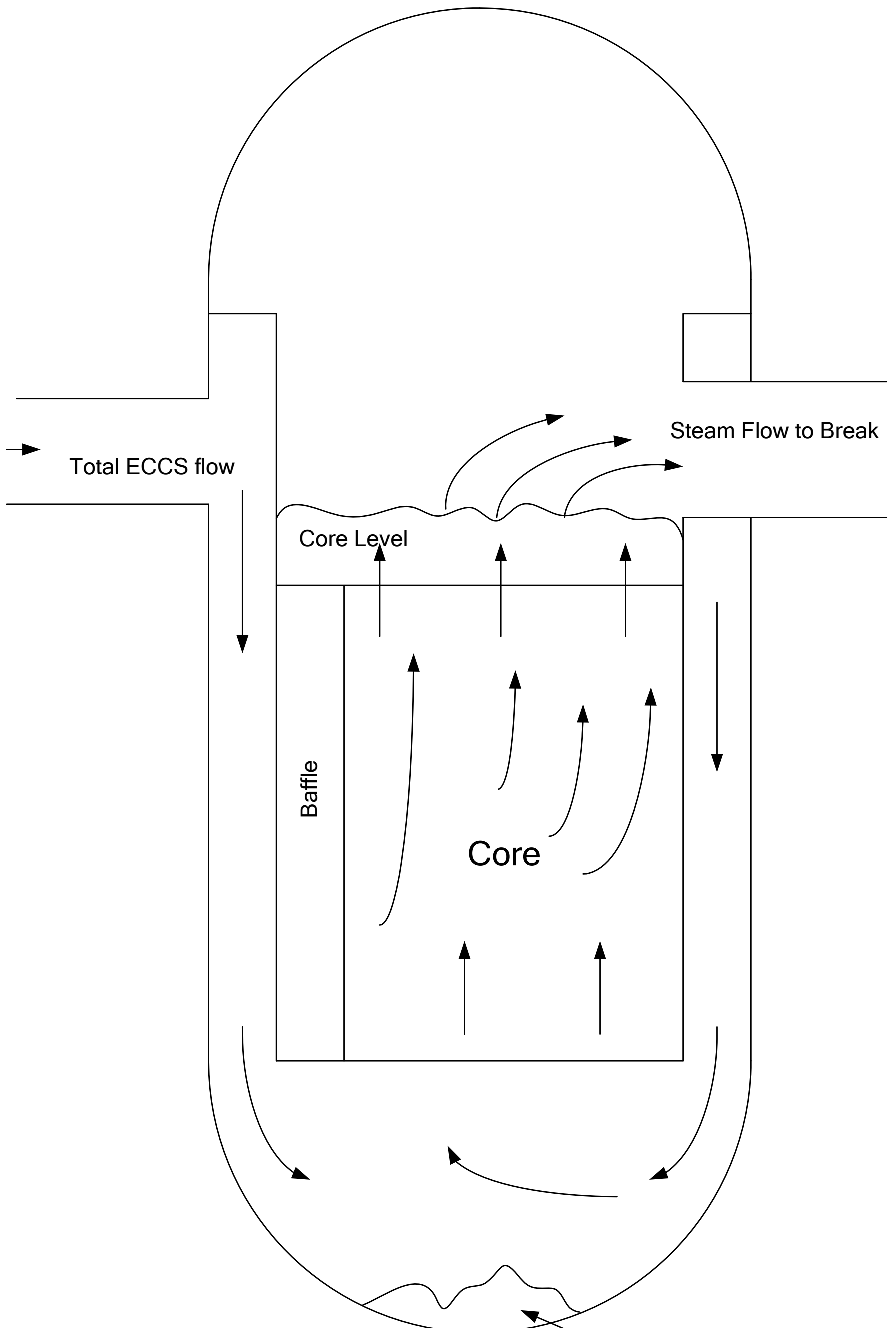

Figure F.2-4 Core Flow Patterns Following a Cold Leg Break During Simultaneous Injection

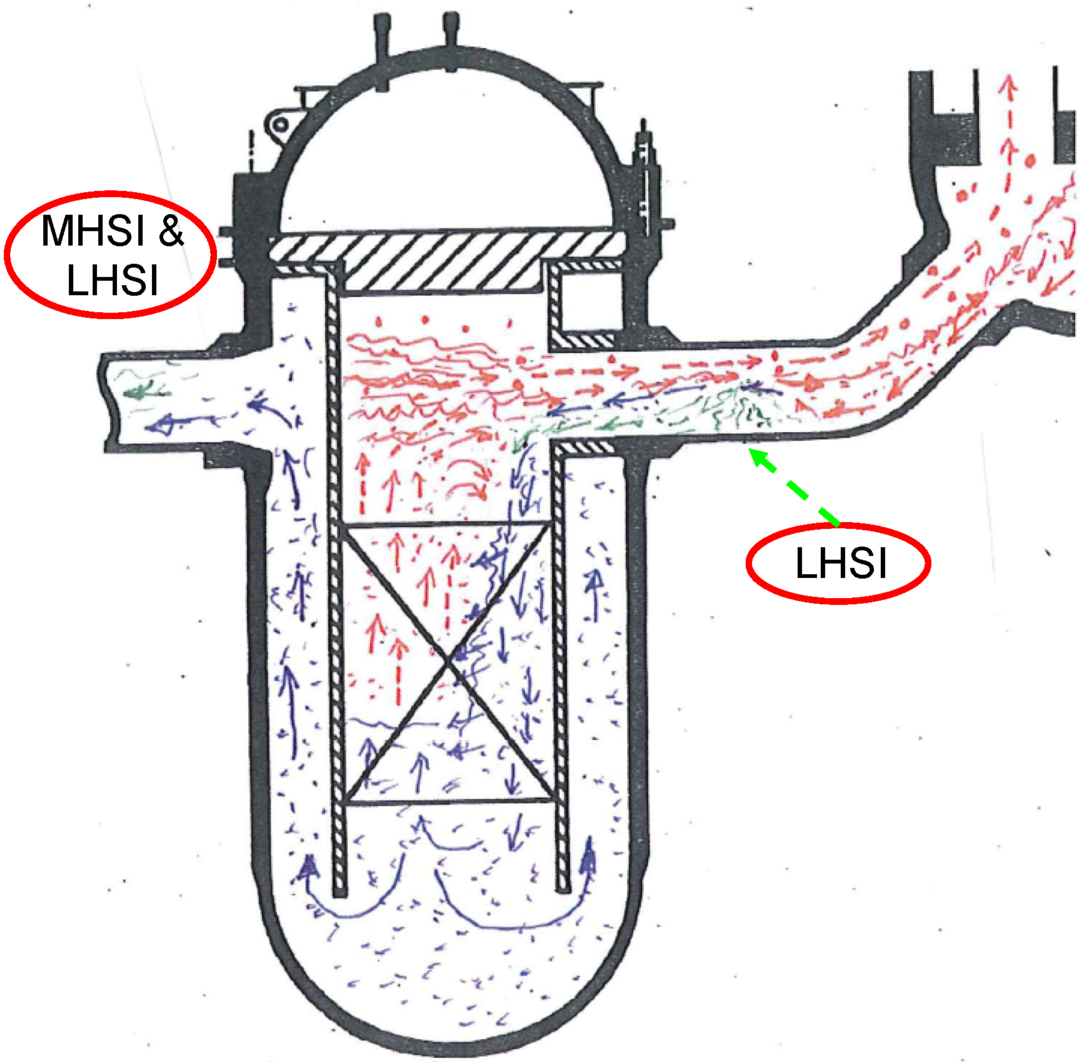

F.3 Debris Accumulation at Core Inlet or Intermediate Spacer Grids

Fuel assembly (FA) testing addressed the collection of debris in the fuel assembly bottom nozzle or at the spacer grids. The purpose of this testing is to justify acceptance criteria for the mass of debris that can be deposited at the core entrance or spacer grids and not impede long-term core cooling flows to the core. These acceptance criteria will be used to demonstrate adequate flow for long-term decay heat removal.

F.3.1 Approach

Darcy's equation (also referred to as the Darcy-Weisbach equation) suggests a flow squared relationship between the pressure drop and the flow rate for flow through or around an obstruction in the flow field.

$$\Delta P = \frac{K}{A^2} \cdot \frac{\omega^2}{288 \cdot \rho \cdot g_c} \qquad \text{(Equation F-1)}$$

where ΔP = differential pressure (psid)

K = form-loss coefficient

A = area upon which the form-loss coefficient is based (ft^2)

ω = flow rate (lbm/s)

ρ = density (lbm/ft^3)

g_c = gravitational constant (32.2 $lbm\text{-}ft/lbf\text{-}s^2$).

[ ]

F.3.2 Calculations

Cold-Leg Safety-Injection Period

Simultaneous Hot and Cold-Leg Safety-Injection Period

F.3.3 Containment Conditions

The containment conditions determine the pumped safety injection (SI) flow rate, the SI temperature, and the pressure for use with fluid properties.

F.3.3.1 *High Containment Pressure, SI Temperature*

The following calculations provide the containment pressure as a function of time for both the cold leg injection period and the simultaneous hot and cold leg injection period.

Cold Leg Pump Suction and Discharge Breaks

In a cold leg pump discharge break, the blowdown phase of the large break LOCA (LBLOCA) is similar in duration to a cold leg pump suction break and produces a similar containment pressure response (U.S. EPR FSAR, Tier 2, Section 6.2.1.3). However, the reflood and post-reflood phases of the cold leg pump discharge event are less limiting than the pump suction break. As such, the containment pressure response for the cold leg pump suction break is used in the evaluation of a cold leg break (maximum pressure as calculated for a suction break). Figure F.3-1 provides the containment pressure response for the cold leg pump suction break.

Hot Leg Break

A break in the hot leg piping is shown to produce the highest containment pressure (U.S. EPR FSAR, Tier 2, Section 6.2.1.3). As such, the containment pressure response for the hot leg break is also used in this evaluation. Figure F.3-1 provides the containment pressure response for the hot leg break (HLB), which has a peak pressure of 71 psia.

Figure F.3-1 Peak Containment Pressure Calculation Comparison

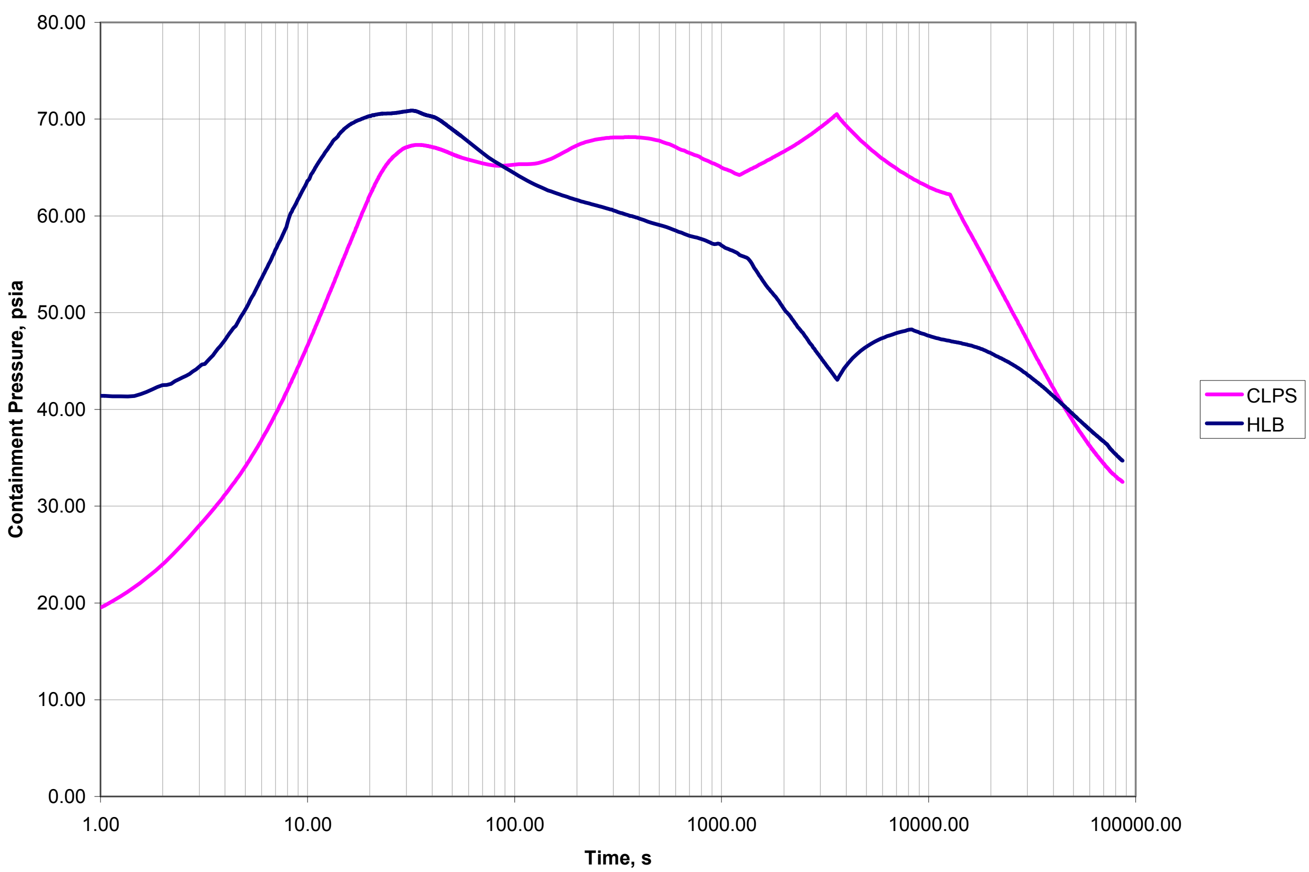

Figure F.3-2 IRWST and RHR Liquid Temperature Calculation Comparison

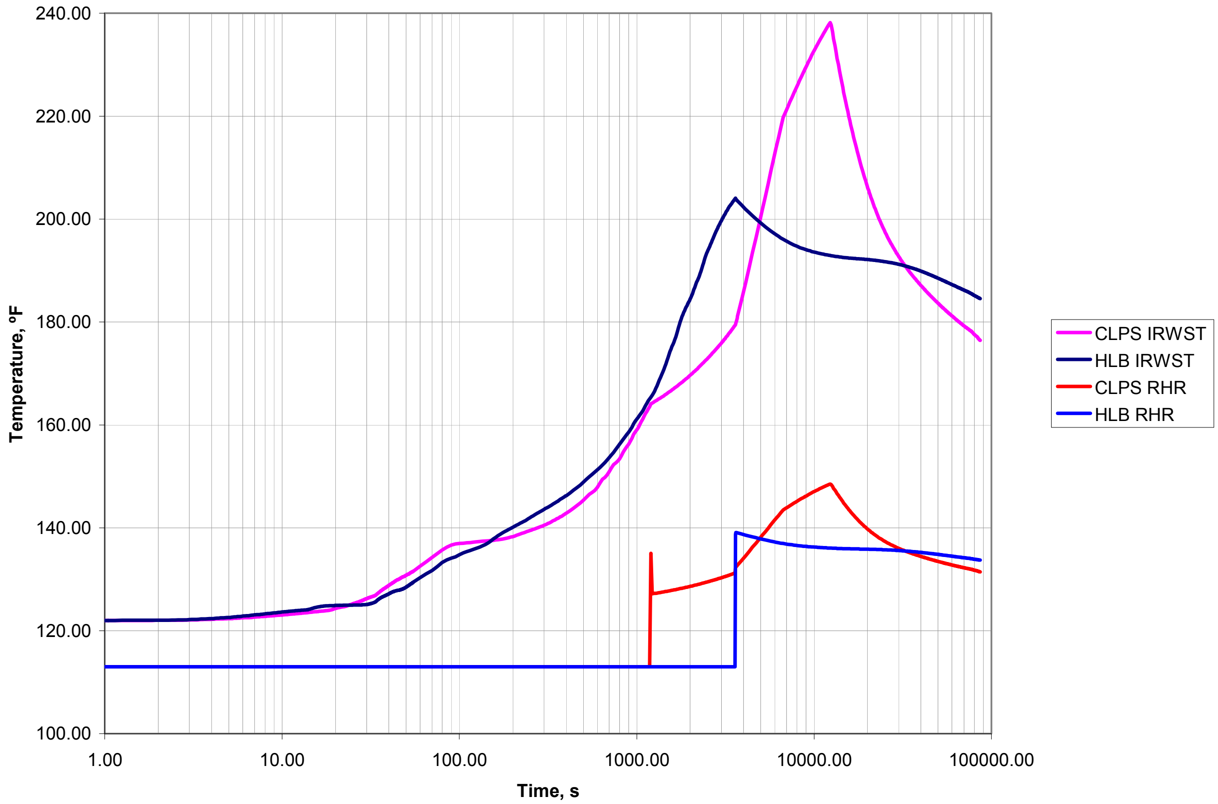

F.3.3.2 *Low Containment Pressure, SI Suction Temperature*

During Cold Leg Injection (from debris arrival up to 60 minutes)

[ ]

An estimate of the low containment pressure up to the time of the switchover to simultaneous hot and cold leg injection at 60 minutes uses the containment pressure calculation from three extended LBLOCA cases.

The results for the first 200 seconds presented in Figure F.3-4 suggest that the more conservative calculation ("min. vol. max. temp." and "max. vol. min. temp."), which uses an updated U.S. EPR ICECON model (ANP-10278P, Rev. 1, Reference 13), lies less than 15 psi below the three extended cases shown. At the time of switchover to simultaneous hot and cold-leg safety-injection, the extended cases show containment pressures of approximately 40 psi. Based on the 15 psi difference described above, using a containment pressure of 25 psia (40-15) for the entire cold leg injection period provides a conservative estimate of a minimum containment pressure.

To determine the effect of containment pressure on the downcomer void fraction assumption (Assumption 12), the results from the extended cases are compared to the results from the lower containment pressure cases. As shown in Figure F.3-5 and Figure F.3-6, downcomer void fraction is not sensitive to the range of pressures examined—approximately 30 psia to 45 psia at 900 seconds. While the two lower curves ("min. vol. max. temp." and "max. vol. min. temp.") stop at 200 seconds, they are expected to continue with the same shape as the other curves.

During Hot Leg Injection (>60 minutes)

Figure F.3-3 Effect of Sampling Range on ICECON Containment Pressure Calculation

Figure F.3-4 Comparison of ICECON Containment Pressure Calculations

Figure F.3-5 Comparison of Downcomer Void Fraction Calculations

Figure F.3-6 Comparison of Downcomer Void Fraction Calculations–with Fitted Line

F.3.4 Pumped Safety Injection Flow Rate

F.3.4.1 Effect on Debris Arrival Time

During the cold leg injection period, from debris arrival to 60 minutes, the pumped safety injection flow rate determines the debris arrival time into the core. Debris arrives at first opportunity, and all the debris that passes through the sump screens in the period of interest for each break and ECCS configuration is treated as if it arrives in the RCS at the first opportunity (Assumption 4). The debris laden fluid flows through the ECCS piping to the RCS and back through the break to the heavy floor. The time for debris to reach the RCS is estimated as the time it takes to turn over the liquid in the IRWST one time. While some amount of mixing might occur in the IRWST, it is assumed that no mixing occurs and all the fluid in the initial IRWST volume must pass through the system before debris arrives. This provides a reasonable estimate of the debris arrival time to the RCS, because:

1. Debris and fluid must accumulate on the heavy floor to a certain level before debris is introduced to the retaining baskets.

2. As the debris falls into the retaining baskets, it is only drawn through the basket screens by the suction of the ECCS pumps.

3. The distance from the retaining baskets to the sump screens is 12 to 20 feet, and there is little opportunity for mixing in this region.

The pumped safety injection flow is a function of the RCS pressure. From the perspective of determining an ECCS flow rate, the RCS pressure is approximately equal to containment pressure during the period of interest: greater than approximately 15 minutes after event initiation. As such, a high containment pressure yields a lower pumped SI flow rate relative to a low containment pressure. However, the differences in time of debris arrival into the core associated with containment pressure differences are small relative to differences in timing that result from the assumed number of operating trains of pumped SI.

Figure F.3-7 Debris Arrival Time Estimate

F.3.4.2 *Effect on Amount of Debris Delivered to the Core*

Assuming that the debris is homogeneously mixed in the ECCS fluid and that it is near neutrally buoyant; the fraction of the debris that reaches the core inlet is proportional to the ratio of ECCS flow that reaches the core inlet (Assumption 2). For example, if 70 percent of ECCS flow reaches the core, then only 70 percent of the debris reaches the core.

The methodology, in this document accounts for multiple sump turnovers within the period of interest, such that in the case of CLB/HLI, 100 percent of the total debris reaches the upper plenum.

F.3.4.3 *Effect on Available Driving Head*

A siphon situation exists in the steam generator when the smallest tube in the steam generator fills-up with water and spills-over. However, it is assumed that the siphon cannot hold in the relatively large area of the steam generator plenum such that the siphon breaks at the bottom of the steam generator tubesheet (Assumption 6). That is, the volumetric flow rate delivered by the pumped SI is insufficient to maintain the steam generator tubes water-solid. As such, the siphon breaks at the bottom of the steam generator tubesheet.

[ ]

F.3.5 Assumptions

[ ]

F.3.5.1 *Assumptions Applying to All Break and ECCS Configurations*

1. The test loop continually recirculates debris, thus providing multiple opportunities to catch debris on an obstruction and restrict flow. Depending on the break location and ECCS configuration, this is not likely to occur in the core. For example, following a hot leg break with cold leg injection, the fluid passes through the core and returns to containment where it must be re-filtered by the retention baskets and strainers before it re-enters the RCS.

2. Debris is homogeneously mixed with the ECCS fluid such that the fraction of debris reaching the core is proportional to the ratio of flow reaching the core to the total ECCS flow rate. For the debris to be transported through the RCS, it must be fairly well mixed in the ECCS fluid. Further, the transport of debris is

dependent on the ECCS injection configuration, break location, and debris buoyancy. For example, for cold-leg breaks with cold-leg safety injection in the period of interest for GSI-191, after core recovery, water can bypass directly to the break, supplying the core with only the water required to make up for boiloff. Debris that is positive in buoyancy will stay within the flow field at the top of the downcomer and proceed out the break. Debris that is negative in buoyancy will sink to the bottom of the vessel and accumulate. For this debris accumulation to be a concern, there must be enough of it to fill the lower head/lower plenum. Most of the neutrally buoyant debris will flow to the break because the dominant flow is toward the break. However, some of it could migrate to the lower plenum. The behavior of breaks within the pump suction piping is similar to cold leg pump discharge breaks except that the driving head for ECCS liquid is slightly greater.

For breaks in the hot leg, all of the ECCS flow passes through the downcomer and the core to the break. The velocities in the downcomer correspond to the ECCS charging rate. Debris that is negative in buoyancy will tend to sink to the bottom of the vessel and accumulate. Debris with neutral or slightly positive buoyancy will be carried with the ECCS flow to the lower head. Debris that is positive in buoyancy will tend to remain in the upper downcomer but, after accumulation, will be dragged to the lower plenum/lower head. Similar behavior is expected in the upper plenum during HLI. This assumption is used to determine the quantity of debris that reaches the core.

3. The core decay heat used in the cold-leg break with cold-leg safety injection evaluation is based on 1.2 times the ANS 1971/1973 standard. The decay heat used in the LBLOCA analyses of record to establish the core operating limits and show compliance with the first three criteria of 10 CFR 50.46 is the 1979 ANS standard. The ANS 1971/1973 standard produces a higher decay heat rate compared to the ANS 1979 standard. The decay heat rate is used to determine the core flow rate for a cold leg break. [

   ] (see Section F.3.7), the higher decay heat rate is conservative.

   The acceptable blockage determination for hot leg breaks with cold leg ECCS injection (HLB/CLI) and cold-leg breaks with simultaneous hot and cold leg ECCS injection use 1.2 times the ANS 1971/1973 standard plus RELAP5 default actinides.

4. The debris that passes through the sump screens during the period of interest for each break and ECCS configuration is treated as if it arrives in the RCS at the first opportunity. It takes a finite time for debris to transport from the break location to the RCS. Further, the mixing of fluid and debris on the heavy floor and the filtration of the retention baskets and strainers will cause the debris to arrive in the RCS over time. Therefore, having debris arrive at the first opportunity is conservative.

5. The maximum allowable fuel assembly blockage calculations are based on a fuel assembly-averaged minimum required core flow rate. The maximum allowable fuel assembly blockage is calculated based on the minimum core flow requirements.

6. A siphon situation exists in the steam generator when the smallest tube in the steam generator fills-up with water and spills-over (Section F.3.5.3). However, it is assumed that the siphon cannot hold in the relatively large area of the steam

generator plenum such that the siphon breaks at the bottom of the steam generator tubesheet. This assumption reduces the available driving head.

F.3.5.2 *Assumptions Specific to the Cold-Leg Safety-Injection Period:*

7. At the time in the transient when the GSI-191 downstream analyses are performed, the liquid entering the bottom of the core is subcooled. Core boiloff rate calculations neglect ECCS subcooling to provide conservative liquid properties. This assumption increases the required core flow, which drives-down the allowable core blockage.

8. Before debris arrival in the core in hot leg breaks with cold leg injection, the pumped safety injection is flowing through the core and boron precipitation effects are negligible. For hot leg breaks with cold leg injection, it is assumed that boron precipitate does not begin to form until debris accumulation impedes the core flow and the excess ECCS is reduced.

   Boron concentration effects for cold-leg breaks with cold-leg safety-injection are described in Assumption 16.

F.3.5.2.1 Assumptions Specific to the Hot-Leg Break with Cold-Leg Safety-Injection:

9. For a hot-leg break with ECCS injection into the cold legs only, the ECCS liquid removes core decay heat by liquid convection if enough flow is present to suppress core boiling. If sufficient blockage occurs at the core inlet, core boiling could occur. The core mixture level could decrease to just above the top of the core and still provide adequate core cooling. In this case, all flow at the core exit is saturated steam. This condition is limiting for maintaining core cooling in the cold leg injection period (Assumption 7). However, for the calculation of available driving head, core voiding is neglected, and the liquid level is assumed to be at the elevation of the break in the hot leg (e.g., the top of the hot leg for a top-slot break). This assumption increases the liquid head in the core for decay heat

removal flow rates. Therefore, this assumption reduces the available driving head and conservatively reduces the value of the allowable core blockage.

F.3.5.2.2 Assumptions Specific to the Cold-Leg Break with Cold-Leg Safety-Injection:

10. In the quasi-steady static-balance analysis, the two-phase flow analysis is based on the Cunningham-Yeh void fraction correlation that has been validated for use with the static-balance analysis using data from an electrically heated 7x7 rod bundle level-swell experiment at atmospheric pressure. The Cunningham-Yeh void-fraction correlation computes the axial distribution of void fraction in the core and upper plenum.

11. The static-balance analysis has a physically based criterion that defines three vented loop seals at 15 minutes (900 seconds), which is the time of debris arrival (Section F.3.4.1). Three vented loops is more conservative because the added pressure drop in the loops causes more depression of the core water levels in the static-balance analysis.

12. It is possible that all of the energy in the thick metal of the RV may not have been removed by this point in the transient, which can lead to boiling in the downcomer. The downcomer volume-average void fraction defines the two-phase gravity head in the downcomer. The maximum bounding value at the time of debris arrival, 15 minutes, is established from the results of representative S-RELAP5 computations for LBLOCAs as shown in Figure F.3-6. This assumption reduces the available driving head and results in a conservative core inlet blockage calculation. In the quasi-steady static-balance analysis, the downcomer void fraction decreases with time according to the fitted line shown in Figure F.3-6.

13. The cold leg break with cold leg injection (CLB/CLI) is considered to always have ample water to allow unrestricted flooding of the loop seals. The height of water in the downcomer is also assumed to be at the bottom of the cold leg pipe. While those assumptions are mutually exclusive, they are applied as

conservative choices to reduce the available driving head in the downcomer and to reduce the collapsed level in the core.

14. The quasi-steady static-balance analysis assumes a constant containment pressure of 71 psia, which is the highest pressure observed in Figure F.3-1. A higher pressure reduces core mixture level, which results in a conservative core blockage calculation.

15. The quasi-steady static-balance analysis assumes a top-peaked axial power shape in the core because this assumption reduces core mixture level, which results in a conservative core blockage calculation.

16. The quasi-steady static balance analysis includes the increased density of the water in the lower plenum and core caused by the concentration of boron with time. The increased water density produces more gravity head that causes the collapsed level in the core to decrease when balanced the gravity head in the downcomer. Therefore, this assumption results in a more conservative core blockage calculation. The boron concentration is conservatively taken to be 10,000 ppm at 15 minutes and increases with time (Reference 19).

17. Condensation pressure drop affects the interaction between the safety injection flow rate and the steam flow rate in the primary pipe at the injection point. Condensation produces a pressure increase, and turning the injection flow stream to align with the primary pipe flow rate produce a pressure loss, or a pressure gain, depending on the angle of injection and relative flow rates. A bounding, pressure loss at the SI point in terms of the steam momentum flux in the primary pipe is used in this analysis. Based on experimental data, the bounding pressure loss is prescribed as a function of the steam momentum flux:

$$\Delta P_{Cond} = f\left(\frac{\rho_g V_g^2}{g_c 144}\right) \quad psi$$

The term in parentheses is the steam momentum flux with units of psi. The functional relationship is:

$$f\left(\frac{\rho_g V_g^2}{g_c 144}\right) = \left\{\begin{array}{ll} 0.0; & \dfrac{\rho_g V_g^2}{g_c 144} < 0.1 \\ 0.13; & 0.10 \le \dfrac{\rho_g V_g^2}{g_c 144} \le 0.35 \\ 0.20; & 0.35 < \dfrac{\rho_g V_g^2}{g_c 144} \end{array}\right\} \quad psi$$

The above pressure loss is converted to an equivalent K/A^2 for condensation that is added to the loop flow resistance. Using the bounding pressure loss is a conservative assumption because it reduces the available driving head, which reduces the maximum core blockage.

18. The quasi-steady static-balance analysis also includes: a) steam flow resistance through the reactor coolant pump, b) steam flow resistance through the primary piping and steam generator (5 percent tube plugging), and, c) the pump is conservatively assumed to have a locked rotor for maximum resistance. The pressure drops and flow rates in the bypass, loops and vessel are fully resolved by an iterative process. This approach to loop flow resistance reduces the available driving head, which reduces the maximum core blockage.

F.3.5.3 *Assumptions Specific to the Simultaneous Hot and Cold-Leg Safety-Injection Period:*

19. The subcooled liquid enthalpy is used in calculating the maximum allowable core blockage in the simultaneous hot and cold-leg safety-injection period. The ECCS liquid properties are based on the IRWST liquid conditions and the containment pressure.

    MHSI draws suction directly from the IRWST, while LHSI passes through a heat exchanger before injection into the RCS. Therefore, the temperatures of the injected MHSI and LHSI differ. The liquid enthalpy in break scenarios in the HLI period considers that a mixture of MHSI and LHSI flows to the core inlet, while LHSI injected to the hot leg flows downward through the top of the core. The subcooled liquid enthalpy from the downcomer side, which comprises a mix of MHSI and LHSI flow, is different from the subcooled liquid enthalpy from the HLI side, which comprises only LHSI flow.

20. This assumption addresses hot-leg breaks during the hot-leg injection period (HLB/HLI). In a hot-leg break with cold-leg safety injection just prior to the switchover to simultaneous hot and cold-leg injection and just prior to debris arrival, the top of the active fuel is covered by flowing ECCS liquid and core boiling is suppressed. This initial core condition persists when the safety injection is switched simultaneous hot and cold-leg injection. The mechanism by which the core level decreases is if there is insufficient flow to match core boiloff. That is, if the blockage is insufficient to reduce the flow to core boiloff, then core steaming is suppressed. As such, this break and ECCS configuration is addressed by HLB/CLI.

F.3.6 Available Driving Head

The following provides a description of the dimensions used in the calculations below.

Distance from cold-leg centerline to top of active fuel, in	85.04
Length of active fuel, in	165.35
Inside diameter of cold leg and hot leg, in	30.71
Elevation from cold leg centerline to the bottom of the SG tubesheet, ft	9.3364

Hot Leg Breaks with Cold Leg Injection

Following a hot leg break with ECCS injection into the cold legs only, the ECCS must pass through the core to reach the break. The driving force is the manometric balance between the liquid in the downcomer and core. Should a debris bed begin to build up in the core, the liquid level will begin to build in the cold legs and steam generator (SG). As the level begins to rise in the SG tubes, the elevation head to drive the flow through the core increases as well. The driving head reaches its peak at the shortest SG tube spillover elevation. However, it is assumed that the siphon break occurs at the bottom of the SG tubesheet (Assumption 6).

The hot leg diameter is 30.71 in and the distance from the hot leg centerline to the top of the active fuel is 85.04 in. As shown below, subtracting the inside radius of the hot leg from the 85.04 in dimension, implies a break at the bottom of the hot leg piping.

If the breaks are at the top of the hot leg piping, then:

A sample calculation showing how this information is used is presented in Table F.3-1 and in Figure F.3-10.

Table F.3-1 Acceptance Criterion based on CLPS Pressure, Top Slot Break – HLB/CLI

Time	Figure F.3-1 peak cont-press	Decay Heat			$h_{fg}(P_{CONT})$	$\rho(P_{CONT})$
	Containment Pressure	RELAP5 Total	Q_{DH} (full power = 4612 MW)			
minutes	psia	P/P0	MW	BTU/s	BTU/lbm	lbm/ft^3
5.00E+00	68.09901	0.034447527	1.59E+02	150619.48	909.21	57.26
1.00E+01	67.1009	0.0294031	1.36E+02	128563.06	909.94	57.29
1.50E+01	65.46774	0.027181406	1.25E+02	118848.85	911.16	57.35
2.00E+01	64.26317	0.025577246	1.18E+02	111834.78	912.08	57.39
2.50E+01	65.21294	0.024224789	1.12E+02	105921.25	911.36	57.35
3.00E+01	66.12526	0.023047546	1.06E+02	100773.83	910.67	57.32
3.50E+01	66.90987	0.022015156	1.02E+02	96259.78	910.08	57.30
4.00E+01	67.67664	0.02110745	9.73E+01	92290.896	909.52	57.28
4.50E+01	68.43301	0.020307831	9.37E+01	88794.616	908.96	57.25
5.00E+01	69.14865	0.01960205	9.04E+01	85708.636	908.44	57.23
5.50E+01	69.83832	0.018977775	8.75E+01	82979.036	907.94	57.21
6.00E+01	70.5202	0.018424317	8.50E+01	80559.079	907.45	57.19

Cold-Leg Breaks with Hot-Leg Safety Injection

Within one hour after the LOCA, the operators initiate hot leg injection for boric acid precipitation control and steam suppression in the core. Following a cold leg break, the HLI introduces debris at the top of the core. Debris introduced via the HLI likely is captured at the uppermost spacer grid, which is approximately at the location of the top of the active fuel. If sufficient debris accumulates to retard flow, the liquid level above the debris bed begins to build, increasing the available driving head. If the blockage is substantial enough, flow is either:

1. Diverted through the heavy reflector region and flows to the core inlet.

2. Liquid level begins to accumulate in the upper plenum and hot leg.

If flow is diverted to the heavy reflector region, debris build up may occur at the core inlet. Testing for cold and hot leg breaks with cold leg injection bounds this situation. If liquid begins to build into the hot legs, the maximum driving head achieved corresponds to the shortest SG tube spillover elevation. However, it is assumed that the siphon break occurs at the bottom of the SG tubesheet (Assumption 6).

The available driving head for cold-leg breaks with hot-leg safety injection is defined as follows:

[ ]

A sample calculation showing how this information is used is presented in Table F.3-2. and in Figure F.3-11.

Table F.3-2 Acceptance Criterion based on Challenging Subcooling – CLB/HLI

Time	Figure F.3-1 peak pressure	Decay Heat			Δh	$\rho(P_{CONT})$
	Containment Pressure	RELAP5 Total	Q_{DH} (full power = 4612 MW)			
minutes	psia	P/P0	MW	BTU/s	BTU/lbm	lbm/ft^3
6.00E+01	43.12962	0.018424667	8.50E+01	80560.607	94.39	58.17
6.03E+01	43.06085	0.018390042	8.48E+01	80409.211	94.39	58.17
6.07E+01	43.12548	0.018355698	8.47E+01	80259.047	94.39	58.17
6.10E+01	43.23731	0.018321626	8.45E+01	80110.067	94.39	58.17
6.13E+01	43.33813	0.018287816	8.43E+01	79962.237	94.39	58.16
6.17E+01	43.43324	0.018254262	8.42E+01	79815.525	94.39	58.16
6.50E+01	44.23199	0.017932551	8.27E+01	78408.864	94.39	58.12
6.83E+01	44.82075	0.017634602	8.13E+01	77106.102	94.39	58.10
7.17E+01	45.30239	0.017358323	8.01E+01	75898.09	94.39	58.08
7.50E+01	45.70731	0.017101848	7.89E+01	74776.671	94.39	58.06
7.83E+01	46.04952	0.016863297	7.78E+01	73733.624	94.39	58.05
8.17E+01	46.34065	0.0166412	7.67E+01	72762.518	94.39	58.04
8.50E+01	46.59052	0.016434068	7.58E+01	71856.847	94.39	58.03
8.83E+01	46.81067	0.016240691	7.49E+01	71011.321	94.39	58.02
9.17E+01	47.00196	0.016059671	7.41E+01	70219.823	94.39	58.01

Figure F.3-8 Cold Leg Break with Hot Leg Safety Injection

F.3.7 Cold-Leg Breaks with Cold-Leg Safety-Injection

Figure F.3-9 Quasi-Steady Static Balance Approach to CLB/CLI - Core Water Levels

F.3.7.1 *Summary*

Figure F.3-10 HLB/CLI Acceptance Criteria

Figure F.3-11 CLB/HLI Acceptance Criteria

F.3.8 Quantity of Debris

The quantity of debris generated following a LOCA was evaluated for a number of break locations. The results are presented in Appendix C and summarized in Table F.3-3. The amount of debris that is generated on a per fuel assembly basis, considering 241 fuel assemblies, is also shown on Table F.3-3. A test was performed to determine the amount of fiber that passes through the retaining baskets and strainers and might reach the RCS and core. The results of this test showed that 69.6 percent of the fiber passes through the sump strainer over a 30 day period (Appendix E). The particulate (including Microtherm) is assumed to pass through the sump screen and reach the core. The amount of debris reaching the RCS considering these bypass fractions is also shown on Table F.3-3.

Microtherm is a granular insulation and a particulate (Reference 10, Vol. 1, p 3-66). Table F.3-3 shows that the total amount of Microtherm is 12 lbm, compared to 1474.8 lbm of particulates. The Microtherm debris load is less than one percent of the particulate loading and is insignificant

The debris quantities listed in Table F.3-3 and calculated in the following subsections represent the total amount of debris that will reach the RCS and core over a 30 day period. For testing, it is conservatively assumed that this quantity of debris reaches the core instantaneously (see Assumption #4).

Table F.3-3 Summary of Maximum Debris Generated from All Break Locations

Debris Description	Total Amount Generated (Amounts from Table C.6-10)	Total Amount per FA assuming [ ] Bypass of Baskets & Strainers
	M_{total}	(M_{total})/241*bypass
Fiber (Nukon + latent debris + miscellaneous)	10.2 lbm	[ ]
Particulates (qualified coatings + unqualified coatings + latent debris + miscellaneous)	1474.8 lbm	[ ]
Microtherm (Note)	12 lbm	[ ]
Note: 1.00 ft^3 of Microtherm as shown in Appendix C. The density of as-fabricated Microtherm is between 5 and 12 lbm/ft^3 (Ref. 10). The higher value is used for conservatism.		

F.3.8.1 *Chemical Precipitates*

Following the LOCA, the chemistry of the fluid in the IRWST and the core could produce chemical precipitates which could affect the pressure drop in a debris bed. The testing used aluminum oxyhyroxide (AlOOH) consistent with the testing summarized in Reference 7.

Studies were performed to identify the specific compounds and quantities of materials that may precipitate within the U.S. EPR reactor containment pool following a LOCA (Appendix D). The precipitates that are predicted include sodium aluminum silicate, calcium phosphate, and aluminum hydroxide. Sodium aluminum silicate is a hazardous material and not available for testing. AlOOH has been shown to be conservative compared to actual precipitates that might form (Reference 8). Therefore, testing with AlOOH is appropriate. The quantities of precipitate that can be tolerated should be determined by testing.

F.3.9 Testing Process and Approach

Following a LOCA, the core void fractions and the flow patterns into and within the core are variable and complex. To simplify the testing process, Assumptions #1 and #4 (Section F.3.5) are applied for simplification and conservatism.

F.3.9.1 *Debris Amounts and Order of Debris Addition for Each ECCS Configuration*

Fuel assembly testing experience indicates that the particulates and chemical precipitates are small debris types that readily pass through the debris filters or fuel assemblies. The fibrous debris content is more readily trapped and could form a debris bed that is capable of capturing the smaller debris types. If particulates are present, they can fill the interstitial gaps among the fibers and decrease the porosity of the debris bed, which increases the pressure drop.

Having all of the particulates available in the test loop from the start of the test allows the particulates to fill the openings in the fiber bed as the bed forms. This order of debris addition is adopted to maximize the pressure drop of the debris bed by minimizing the porosity of the debris bed as it forms.

Testing indicates that using lower particulate to fiber ratios result in higher head losses, mainly because of chemical precipitate addition. An evaluation of test results concluded that the highest fuel assembly pressure drop occurred in cases with a particulate to fiber ratio (p:f) of 1:1. Therefore, the fuel assembly testing was performed with a p:f of 1:1 using [ ] grams of fiber (rounded up from [ ] grams) for all ECCS configurations.

The chemical precipitates are added after the particulates and fiber because they do not form until well into the transient. The chemical precipitates are expected to form a layer on top of the established debris bed and could possibly compress the bed, further increasing the pressure drop of the bed. Testing has indicated that the chemical precipitates have a limited effect on the overall pressure drop through the debris bed. That is, the initial formation of the chemical precipitates causes an increase in the pressure drop. However, after a small quantity has been introduced, the pressure drop stops increasing and additional chemical precipitates do not significantly affect the pressure drop. Based on this knowledge, this order of debris addition, particulate first, fiber second, and chemical precipitates last, is applied to the fuel assembly testing.

F.3.9.1.1 Hot Leg Break with Cold Leg Injection (< 60 Minutes)

Table F.3-4 presents the quantity and composition of solids formed by chemical precipitation within the first hour after the initiating event. Since the switchover to simultaneous hot and cold leg ECCS injection occurs one hour after the initiating event, only those amounts formed within the first hour are used in testing for this configuration.

The debris quantities and order of addition are summarized in Table F.3-5.

Table F.3-4 Quantity and Composition of Total Solids at One Hour

	Total Solids all values in kg unless otherwise specified (Appendix D, Table D.3-10)			
Comments	**Time, hrs**	**$Ca_3(PO_4)_2$**	**AlOOH**	**$NaAlSi_3O_8$**
	0.92	16.26	0.22	23.95
	1.58	17.34	0	25.54
Calculated by linear interpolation between 0.92 and 1.58 hrs	1	16.39	0.19	24.14
See Note 1 - combining $NaAlSi_3O_8$ quantity with AlOOH quantity			24.33	
Total amount per fuel assembly (1/241 fuel assemblies), kg		0.068	0.101	
Total amount per fuel assembly (1/241 fuel assemblies), g		68	101	

Note:

1. Sodium aluminum silicate is a hazardous material and not available for testing. In addition, tests with sodium aluminum silicate surrogate show that it is not quite as efficient as aluminum hydroxide in increasing head loss.

Table F.3-5 HLB/CLI Debris Amounts and Addition Sequence

		Composition, g					
Debris Addition Order	Description	SiC	$Ca_3(PO_4)_2$	AlOOH	Fiber	Total, g	Comments
1	Particulates	[ ]				[ ]	
2	Fiber				[ ]	[ ]	Added in [ ] increments, with a [ ] final increment
3	Chemicals		68	101		169	Added in 4 increments

F.3.9.1.2 Cold Leg with Cold Leg Injection (< 60 Minutes)

Section F.2.1 explains that the required ECCS flow into the core is the flow required to replace the core boil-off due to decay heat removal. Assuming that the debris is homogeneously mixed in the ECCS fluid and that it is near neutrally buoyant (Assumption #2), the fraction of the debris that reaches the core inlet is proportional to the fraction of ECCS flow that reaches the core inlet.

With this approach, it is estimated that between 5 and 16 percent of the debris reaches the core inlet depending on total pumped ECCS injection flow rate. Table F.3-6 uses 16 percent and conservatively estimates approximately four sump turnovers between the time of initial debris arrival at 15 minutes until the switchover to simultaneous hot and cold leg injection at one hour. This conservatism uses a short sump turnover time to deliver more debris to the core. The result shown in Table F.3-6 estimates that **[ ]** grams of fiber will reach the core during this time. However, this test is performed with **[ ]** grams of fiber.

The debris quantities and order of addition summarized in Table F.3-5 also applies to this test configuration.

Table F.3-6 CLB/CLI Debris Amount

Initial Amount of Fiber Available, g				[ ]
Percent of Pumped ECCS Injected to Cold Leg (%dep)				16%
Sump Turnover Number	Time, min	Amount of Fiber Available, g	Amount of Fiber Deposited, g	Amount of Fiber Remaining, g
		Mavail	(Mavail)*(%dep)	(Mavail)*(1-%dep)
1, initial arrival at core inlet	15	[ ]	[ ]	[ ]
2	30	[ ]	[ ]	[ ]
3	45	[ ]	[ ]	[ ]
4	60	[ ]	[ ]	[ ]
Total amount deposited, g			[ ]	

F.3.9.1.3 Hot Leg Break with Hot Leg Injection (> 60 Minutes)

As described in Section F.3.9.2.3, this test is addressed indirectly by hot leg breaks with cold leg injection. As a result, the debris amount for the hot leg break with cold leg injection test also applies to this configuration.

F.3.9.1.4 Cold Leg Break with Hot Leg Injection (> 60 Minutes)

Fuel assembly testing for this configuration conservatively uses the 30 day debris load. Table F.3-7 presents the quantity and composition of solids formed by chemical precipitation during the 30 day mission time. The debris quantities and order of addition are summarized in Table F.3-8.

Table F.3-7 Quantity and Composition of Total Solids at 30 Days

	Total Solids			
	all values in kg unless otherwise specified (Appendix D, Table D.3-10)			
Comments	Time, hrs	$Ca_3(PO_4)_2$	$Al(OH)_3$ (Note 2)	$NaAlSi_3O_8$
	720	76.55	11.3	53.44
See Note 1 - combining $NaAlSi_3O_8$ quantity with AlOOH quantity			64.74	
Total amount per fuel assembly (1/241 fuel assemblies), kg		0.318	0.269	
Total amount per fuel assembly (1/241 fuel assemblies), g		318	269	

Note:

1. Sodium aluminum silicate is a hazardous material and not available for testing. In addition, tests with sodium aluminum silicate surrogate show that it is not quite as efficient as aluminum hydroxide in increasing head loss.

2. Aluminum precipitates as aluminum hydroxide at lower temperatures and as aluminum oxyhydroxide at higher temperatures. Using AlOOH is reasonable for the fuel assembly testing.

Table F.3-8 CLB/HLI Debris Amount and Addition Sequence

		Composition, g					
Debris Addition Order	Description	SiC	$Ca_3(PO_4)_2$	AlOOH	Fiber	Total, g	Comments
1	Particulates	[ ]				[ ]	
2	Fiber				[ ]	[ ]	Added in [ ] increments, with a final [ ] increment
3	Chemicals		318	269		587	Added in ten increments

F.3.9.2 *Initial Testing Flow Rate*

This section describes how the acceptance criteria are implemented in the fuel assembly testing. The test begins with an initial flow rate that is typical of what is expected in the plant during a particular break and ECCS configuration prior to debris arrival. As debris arrives and accumulates in the fuel assemblies, the flow through the core starts to decrease. In the test, the flow rate is reduced to maintain the fuel assembly pressure drop within test facility limits.

This section also addresses the implication of using a low initial flow rate instead of a high initial flow rate on the acceptance criteria. This affects only breaks and ECCS configurations prior to switchover to simultaneous hot and cold leg injection. In breaks and ECCS configurations after the switchover, it is assumed that debris arrives at the instant of switchover.

Sump turn-over times of 29 and 154 minutes (2.57 hours) are calculated by dividing the technical specification minimum IRWST liquid volume of 500,342 gal by the maximum and minimum ECCS flow rates of 17,200 gpm and 3250 gpm, respectively. This means that debris generated during a LOCA is estimated to reach the core or RCS between 29 and 154 minutes after the break. Accounting for unknowns in the transportation process, an additional measure of conservatism is taken by assuming the earliest time that debris can reach the core is 15 minutes (≈ 29 mins/2). In contrast, using a minimum initial test flow rate implies that debris does not arrive at the core until well into the simultaneous hot and cold leg injection phase. In the period from the time of debris arrival until the switchover to hot leg injection at 60 minutes, the phenomenon of interest to long term core cooling is the removal of core decay heat. That is, the minimum required core flow is the flow rate that matches core boil-off. Table F.3-1 calculates the minimum flow required for decay heat removal as a function of time and shows that less flow is required as time increases.

The effect of lower flow rate on the acceptance criteria can be seen by examining **[ ]** (shown below). Using a higher value for the required flow rate produces a lower allowable core blockage. In contrast, using a lower value for the required flow produces a higher allowable core blockage. Therefore, a lower allowable core blockage is appropriate for testing.

[ ]

Incorporating this consideration, the initial test flow rate for each break and ECCS configuration is described in the subsections below. Each configuration is described in terms of the time of switchover to simultaneous hot and cold leg ECCS injection at 1 hour after the initiating event. The initial test flow rate will represent an average fuel assembly flow rate just prior to debris arrival.

F.3.9.2.1 Hot Leg Break with Cold Leg Injection (< 60 Minutes)

All of the injected ECCS passes through the core to reach the break. The maximum flow through the core is then the maximum ECCS flow rate: 17,200 gpm, which assumes all pumps and trains are operating. Based on the maximum ECCS flow rate, a fuel assembly-averaged flow rate is then 71.4 gpm (17,200 gpm / 241).

Once the measured flow and pressure stabilize after the final debris addition, the test system is reconfigured to allow reverse flow through the fuel assembly. The purpose of this portion of the test is to demonstrate the fragility of the debris bed and the capacity of the hot leg injected flow to disturb the debris accumulation.

During simultaneous hot and cold leg ECCS injection, approximately **[ ]** percent of the injected ECCS is injected into the hot leg. A fuel assembly-averaged flow rate is then **[ ]** gpm (71.4 gpm * **[ ]** percent), which is rounded up to **[ ]** gpm (percentage of hot leg flow estimated in Table F.3-9). However, only a fraction of this flow rate is needed to disrupt and dislodge the debris bed that may have formed.

Table F.3-9 Ratio of Hot Leg ECCS Injection to Cold Leg ECCS Injection

Flow Into RCS Hot Leg, gpm	**Flow Into RCS Cold Leg, gpm**	
HL_{TOT}	CL_{TOT}	$HL_{TOT}/(HL_{TOT}+CL_{TOT})$
2157	1431	0.60
1837	1319	0.58
1863	1339	0.58
1997	1490	0.57
	Average	**0.58**

F.3.9.2.2 Cold Leg Break with Cold Leg Injection (< 60 Minutes)

Section F.2.1 explains that the net ECCS flow into the core is only what is required to make up for core boil-off that removes the decay heat.

The required flow rate for this test is **[ ]** gpm (Table F.3-1, Time=15 minutes). However, this test is performed at a slightly higher flow rate to avoid testing close to the lower range of the flow measurement instrument.

F.3.9.2.3 Hot Leg Break with Hot Leg Injection (> 60 Minutes)

Section F.2.2 explains that the phenomenon of interest for this break and ECCS configuration is the suppression of core steaming. Section F.3.2 conservatively treats the hot leg injected flow as not contributing to the flow required to suppress core steaming. That is, the allowable core blockage is determined relying only on flow from the bottom of the core to suppress core steaming.

The test for hot leg breaks with cold leg injection includes a reverse flow component to the test. The expectation is that only a small amount of reverse flow is needed to disrupt and dislodge the resulting debris bed.

Therefore, in hot leg breaks with hot leg injection, debris entrained in the flow delivered to the core inlet must overcome reverse flow via hot leg injection before accumulation can occur. The reverse flow component described in Section F.3.9.2.1 demonstrates that this accumulation is not achievable, and that this configuration need not be tested. Therefore, no initial test flow rate is defined.

F.3.9.2.4 Cold Leg Break with Hot Leg Injection (>60 Minutes)

All of the ECCS injected into the hot leg passes through the core to reach the break. The maximum flow through the core is then the maximum hot leg injection flow rate.

The hot leg injection flow rate ranges from **[ ]** This test will be performed at **[ ]** to understand the effect of the differences in the initial flow rate on debris bed formation. The minimum test flow rate of **[ ]** gpm was selected because:

- It is approximately equal to the bottom range of hot leg injected flow.
- It allows for better comparison to cold leg injection tests run at **[ ]** gpm.

F.3.10 Conclusion

[ ]

An evaluation of in-vessel, downstream effects are performed in a separate effects fuel assembly tests using the approach in this section to demonstrate that adequate long-term core cooling is provided. This method addresses the collection of debris in the fuel assembly bottom nozzle or at the spacer grids, and justifies the acceptance criteria for the debris mass that can be deposited at the core entrance or spacer grids and not impede long-term core cooling flows to the core.

F.4 Deposition of Chemical Precipitates and Debris on Fuel Rods (EPRDM)

Analysis and testing provides insight into the chemical processes that may occur in post-accident containment sump fluids (see Appendix D). This work used the results of OLI StreamAnalyzer™ analyses as validated by autoclave testing to identify the chemical reactions expected to generate the most precipitate, through the application of simplified configurations of individual insulation types, buffer solutions, and post-accident temperatures.

Two specific chemical compounds precipitated during this testing depending on the debris mixture and test parameters. The results of the analysis and test program indicated that the predominant chemical precipitates for the U.S. EPR plant design were sodium aluminum silicate ($NaAlSi_3O_8$) and calcium phosphate ($Ca_3(PO_4)_2$). Therefore, the chemical model considers only the release rates of the principal elements guiding the formation of these precipitate compounds: aluminum, calcium and silicon. Some aluminum oxyhydroxide (AlOOH) was formed, but the mass was small compared to sodium aluminum silicate and calcium phosphate and will be considered negligible for this calculation.

In order to perform analyses that will provide information on chemical or physical deposition on fuel rods and the subsequent effect on core cooling once ECCS flow is established, a method based on the OLI StreamAnalyzer™ output and test results is required. This calculation provides a conservative evaluation of (1) deposition thicknesses on fuel rod surfaces due to chemical and debris deposition and (2) to determine the cladding temperatures under the buildup for up to 30 days following a LOCA.

F.4.1 Acceptance Criteria

The following measures were developed to demonstrate compliance with the long-term core cooling acceptance criteria defined in 10 CFR 50.46(b)(5).

F.4.1.1 *Decay Heat Removal*

Cladding temperatures at or below 800°F maintain the cladding within the temperature range where additional corrosion and hydrogen pickup over a 30 day period will not have a significant effect on cladding properties. At temperatures greater than 800°F, rapid nodular corrosion and higher hydrogen pickup rates that can reduce cladding mechanical performance. Long-term autoclave testing has been performed to demonstrate that no significant degradation in cladding mechanical properties would be expected due to a localized hot spot. This testing demonstrated that the increase in oxide thickness and hydrogen loading was limited at temperatures of less than 800°F for periods of 30 days. With limited corrosion and hydrogen pickup, the impact on cladding mechanical performance is not significant. Therefore, no significant degradation in cladding properties would occur due to 30-day exposure at 800°F, and there would not be any adverse impact on core cooling ability. Based on the autoclave results, maintenance of a maximum cladding temperature below 800°F is one measure to demonstrate long-term core cooling capability.

F.4.1.2 *Deposition Thickness*

If the calculation using plant-specific conditions results in a total deposition thickness (including existing oxide and crud layers) below 50 mils (1270 microns), the acceptance criteria within 10 CFR 50.46(b)(5) is satisfied.

The spacing between fuel rods is calculated by subtracting the fuel rod outside diameter from the fuel rod pitch. The fuel rod OD is 0.374 inches. The fuel rod pitch is 0.496 inches. The spacing between fuel rods is then 0.122 in, or 122 mils. Complete blockage in this space constitutes half the spacing between fuel rods: 61 mils. Restricting the total deposition buildup on any rod (including existing oxide and crud layers) to 50 mils will maintain an open rod-to-rod gap. Therefore, for the purposes of this evaluation, this deposition limit is considered an acceptance criterion.

F.4.2 Analytical Methodology

The U.S. EPR LOCA deposition model (EPRDM) incorporates deposition and heat transfer calculations to determine the effect of fibrous, particulate, and chemical debris that passes through the IRWST baskets and/or sump screens, enters the reactor vessel, and deposits on the fuel rods. Figure F.4-1 shows the basic layout of the U.S. EPR reactor section in the vicinity of a typical LOCA break. Materials upstream of the sump strainer are affected by the liquid in the sump and are subject to degradation effects. Once the ECCS is actuated and suction begins from the IRWST, bypassed materials and ions freed by dissociation of materials upstream of the strainer may reach the reactor vessel. In the presence of boiling in the core, these materials may be deposited on the fuel rods and build up an insulating layer that could inhibit core cooling by (1) degrading the heat transfer from the fuel rod or (2) closing the gap between fuel rods.

The EPRDM assumes that oxide and crud layers exist on fuel surfaces prior to the initiation of a LOCA. The model also conservatively assumes that all deposition occurs through the boiling process if conditions at each node predict that boiling will occur. The rate of deposition is governed by the steaming rate as all impurities are assumed to transport into the deposit through large pores (i.e., boiling chimneys) in the crud deposit at this rate (see Figure F.4-2). Deposition occurs as impurities transport into the crud deposit with the flow of reactor coolant. Certain resultant chemical species will be forced to precipitate as they cannot exit through the top of the chimney with the newly converted steam phase. Small particulates and already formed precipitates are also assumed to be drawn into and merge with the growing deposit scale.

In the EPRDM model, chemical deposition on the fuel rods is directly proportional to boiling. Therefore, at any point along the height of the fuel rod, more boiling means more deposition and no boiling means no deposition. As discussed in Section F.2, the break/ECCS configuration that presents the most boiling is a cold leg break with cold side injection. However, as discussed in Section F.2, the boiling in this break/ECCS configuration decreases and eventually stops after Hot Leg Injection is initiated at 60 minutes. While it is not credible that this break/ECCS configuration continues during the long-term cooling period of 30 days, assuming so provides conservative results and therefore provides the basis for this analysis.

The EPRDM allows division of the core into specific region and elevation locations with various parameters including relative power, number of rods, initial cladding and crud thicknesses, and average depth within the core. The final deposition thickness is predicted for each core location using the overall core thermal power and the relative power and area for each specific core location. The cladding temperature is then calculated based on heat transfer through the final determined scale and deposition thickness. This is not a finite difference type of analysis; the relative factors of each core location are simply used to modify the numbers that would be calculated if all core locations are assumed equivalent.

The methodology assumes that fluid in the IRWST and reactor is well mixed, and that the dissolution of calcium, aluminum or silicon from one material will not inhibit the dissolution of calcium, aluminum or silicon from another material by the common ion effect. No species-specific interactions that could potentially influence crystal nucleation and growth are considered. As a result, reactions that inhibit precipitation are not replicated, thereby making the calculation results conservative. In reality, the presence of other ions in the solution would reduce the dissolution rate compared to the dissolution rate of a single ion solution. Credit is not taken for local corrosion inhibition effects by any materials present following the accident.

Figure F.4-1 Flows During a LOCA Cold Leg Break

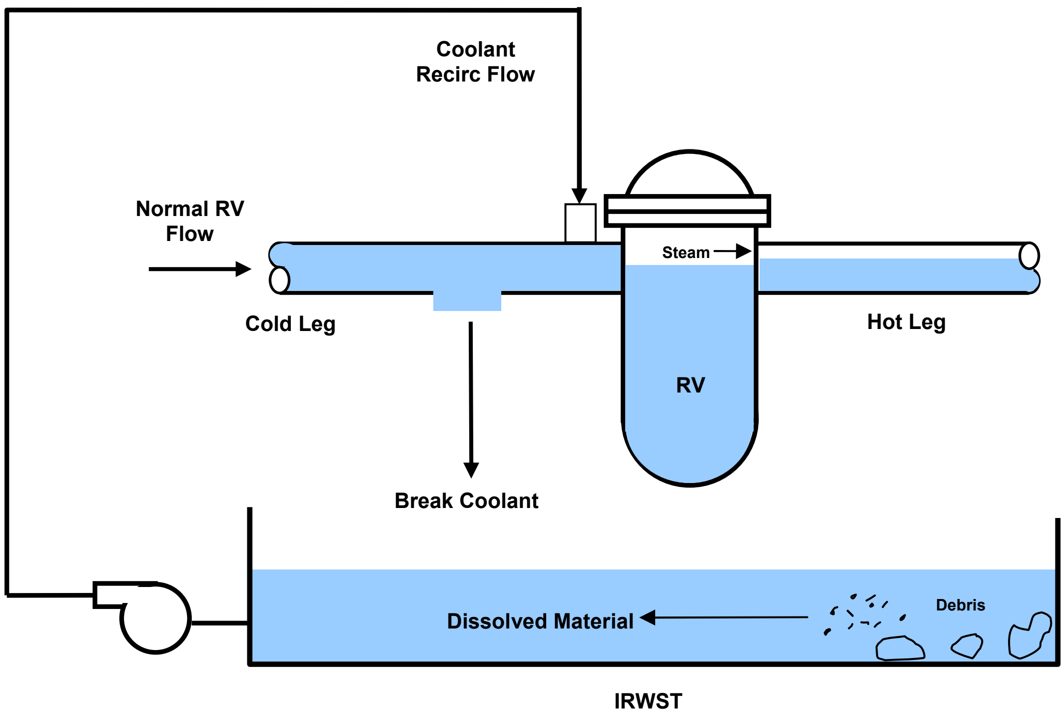

Figure F.4-2 Boiling Chimney Deposition Effect

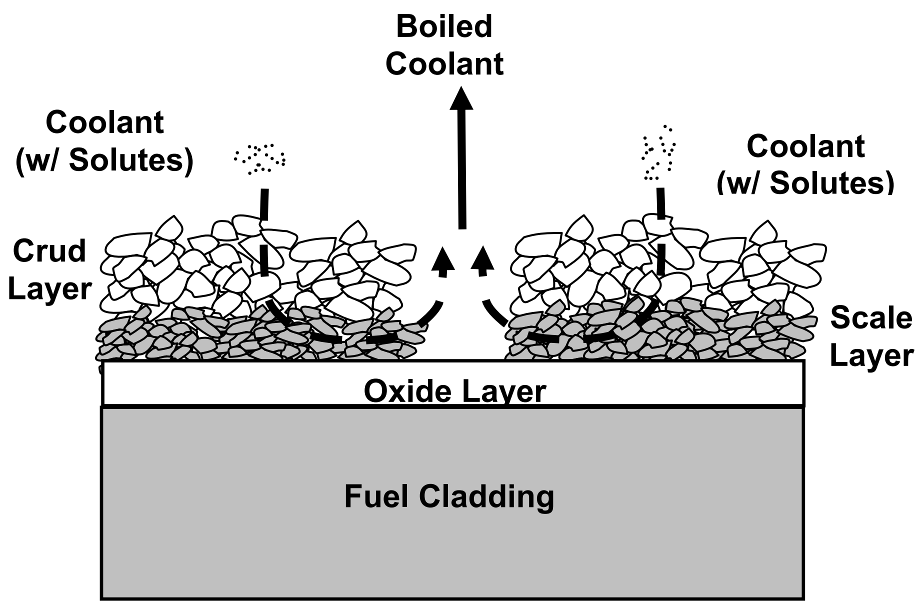

F.4.3 Assumptions

The following assumptions are made in the calculation methodology to provide a conservative estimate of the fuel rod cladding temperature and the amount of scale deposits formed within the core.

1. All large debris is trapped upstream of the reactor vessel and only material dissolved in the coolant or small enough to transport (i.e., small fibers and small particulates) is assumed to form deposits within the core.

2. The types of reactive elements assumed to be within the containment are: Aluminum, Calcium, Silicon, Fiber, and Miscellaneous Particulates.

3. Scale distribution within the core will be proportional to the relative power of each core section.

4. Coolant saturation pressure is the same as pure water. Impurities present in the coolant are non-volatile and will have the effect of raising the boiling point above pure water. Thus, the amount of boiling will be overestimated for each point along the height of the fuel rod and provides a conservative estimate of scale thickness.

5. All dissolved elements for the entire coolant volume are deposited only on the fuel rod cladding and are not reduced or redistributed due to possible flow effects within the core. This is conservative since deposits will form on all of the surfaces exposed to coolant, which would distribute the scale deposits over a larger area and reduce the fuel rod cladding scale thickness.

6. All dissolved material will be deposited at a rate equal to a deposition rate multiplied by the dissolved material concentration. When the temperature at the oxide/crud interface is below the boiling point, deposition is assumed to occur via convective deposition rather than by boiling. The non-boiling rate of deposit build-up is proportional to heat flux and is 1/80th of that of boiling deposition at the same heat flux. This ratio is based on empirical data for mixed calcium salts under boiling and non-boiling conditions (Reference 9).

7. Fluid exiting the RV is assumed to be pure steam. In an actual accident scenario, this steam would carry some of the dissolved material out of the coolant steam and reduce the amount of deposited material and scale thickness thus giving conservative results.

8. The calculations assume an increase in deposit volume (or indirectly, mass) during precipitation due to the incorporation of species, such as the waters of hydration or boric acid. However, specific compounds are not assumed. This is done by specifying a deposit density that is sufficiently low to bound possible hydrates and adsorbed species (e.g., 12.5 lbm/ft^3 – See Section F.4.4.3).

9. Flow is not modeled explicitly. Instead, a generic heat transfer coefficient of 400 W/m^2-K (70 BTU/ft^2-°F) was assumed for the transfer of heat between bulk coolant within the fuel channels and the surface of the deposits. This is an appropriate heat transfer coefficient for convective flow within natural circulation systems.

10. The methodology assumes that fluid in the IRWST and reactor is well mixed, and that the dissolution of calcium, aluminum or silicon from one material will not inhibit the dissolution of calcium, aluminum or silicon from another material by the common ion effect.

11. The fiber transport rate is set so that all fiber that is not trapped by the sump strainers is deposited into the core within an hour. This is conservative because early deposition of fiber will increase the overall deposition thickness which reduces the heat transfer away from the rod and increase the oxide/crud layer boundary temperature. The saturation pressure used to predict boiling rate is based on this temperature and will increase. The boiling rate will be overpredicted resulting in conservative output results. Fiber is treated as an element in solution for deposition purposes.

12. Particulates in the coolant are treated as a uniformly distributed solute and deposited in the same manner as dissolved elements.

13. All heat emanates radially from the fuel rods; the top and bottom inactive surfaces of the fuel rods do not add heat to the coolant and do not need to be added to the effective surface area of the rod. This is conservative because the full thermal power of the rod is confined to the active rod surface area resulting in a higher cladding temperature.

14. Fuel rod cladding is treated as a linear wall for heat transfer purposes instead of as a cylindrical heat transfer surface. This gives conservative results because the thermal resistance of a radial wall is less than that of a flat wall.

15. For the purpose of calculating pressure at each elevation along the height of the fuel rod, the coolant density used is the liquid density at the coolant temperature. This is a reasonable approximation of the coolant density at these elevations.

16. Element solubility in the coolant solution is assumed to be zero to provide additional conservatism by allowing the total amount of the elements in solution to be deposited as scale instead of only the amount above the solubility limit.

17. Section F.4 states that some aluminum oxyhydroxide (AlOOH) was formed as a precipitate compound but that the mass was small compared to sodium aluminum silicate and calcium phosphate. Hence, aluminum hydroxide is assumed to be negligible in this calculation.

18. For a single time step, every elevation of the core is at the same concentration. Physically, the concentrations at the higher elevations would be reduced to deposition on the fuel rods at the lower elevations. Since the amount of deposition is proportional to the concentration this is a conservative assumption which results in greater depositions.

19. No credit is taken for the increase in surface area due to deposition on the rods. Since the scale thickness is volume of the deposit divided by the area, this conservatively increases the reported thickness. Additionally, the area is used to determine the thermal resistance. With a lower area, the thermal resistance is

higher and the temperature increase across the oxide is greater, resulting in more boiling and more deposition (Assumption 1).

F.4.4 Inputs

F.4.4.1 *Liquid Volumes*

In the EPRDM calculation, the mass of two liquid volumes are important: (1) the reactor vessel core region liquid volume and (2) the IRWST volume during recirculation. While suction from the IRWST begins immediately upon ECCS initiation, debris is not expected to reach the core before approximately 30 minutes following the LOCA (Section F.3.4.1). To provide additional conservatism, this time was reduced to 15 minutes, which is consistent with the time assumed in Section F.3.4.1. At this time, the RCS fluid has been expelled and the accumulators and ECCS have refilled the core. Parameters calculated before the initial coolant recirculation time (< 15 minutes) are not considered to be accurate due to an expected transient time where the coolant is transitioning to a boiling state.

The input in EPRDM for the initial reactor vessel core region liquid volume (or mass) is not directly related to any specific transient analysis. If EPRDM was purely mechanistic, this input would be defined as the steady-state reactor vessel core region volume. However, this volume is actually the reactor vessel core region volume that is reached after the initial blowdown and refill phase of the LOCA when the core has been recovered. This quasi-steady volume is commonly known as the long-term core mixing volume and is consistent with the mixing volume used for boric acid precipitation analyses.

This volume is important for determining the concentration of chemicals in the core. From the boric acid precipitation analysis, the Core Region Mixing Volume is 542 ft^3. This is the volume consistent with the scenario described in Section F.2.1 for a cold leg break with cold side injection.

Since the core is boiling, the mass is calculated based on the density at saturation conditions. The average core liquid density is 60.495 lbm/ft^3. However, since a smaller density leads to smaller liquid mass which increases the chemical concentration the smaller density value of 57 lbm/ft^3 will be used. Therefore:

*Reactor Vessel Core Region Liquid Mass = 542 ft^3 * 57 lbm/ft^3*

= 30,894 lbm (14,013.3 kg)

The input in EPRDM for the initial volume of the IRWST, represents the IRWST volume in the post-accident period when SI is operating in recirculation mode. This volume is important for determining the concentration of chemicals in the IRWST. Choosing a smaller liquid volume will result in a higher chemical concentration and provide a conservative result. The minimum initial IRWST liquid volume (based on the minimum IRWST level for SIS NPSH during LOCA recirculation) is 57,916 ft^3 (433,242 gal). (Note that this value is below the Technical Specification minimum value of 500,342 gallons. The smaller volume increases the concentration of the liquid transported to the core, and is therefore conservative for the deposition model.)

The liquid density is based on the IRWST liquid conditions following the LOCA. A lower liquid density will reduce the mass of liquid for a given liquid volume, which will increase the chemical concentration. The lowest density that corresponds to a temperature of 246.2 °F would be the liquid density at saturation. The saturation density corresponding at 246.2 °F is 58.93 lbm/ft^3.

For consistency with the Section F.3.5.2.2 calculation, a density of 57.186 lbm/ft^3, corresponding to the peak containment pressure of 71 psia, is used. This equates to a mass of:

$$m_{IRWST} = \rho V = 59.186 \frac{lbm}{ft^3} \cdot 57{,}916\, ft^3 = 3{,}311{,}984.4\ lbm\ (1{,}502{,}292.6\, kg)$$

F.4.4.2 *Fiber and Particulate Quantities and Densities*

The elemental quantities reported in Appendix D were determined based on 257 ft^2 exposed concrete on the heavy floor following a LOCA. Further, all debris is assumed to be available for dissociation immediately following the break. The only elements assumed to be released in the IRWST are aluminum, calcium, and silicon.

The EPRDM provides an optional input to add an additional amount of aluminum to the debris in the IRWST to provide conservatism in the analysis. However, debris composed of aluminum alloys (as opposed to the aluminum released from debris such as concrete) was not included in the list of predicted debris so this input was not used in the calculation of the maximum deposit thickness.

Table F.3-3 indicates that a total of [ ] of fiber per fuel assembly (241 fuel assemblies total) may bypass the strainers and reach the RCS. This fiber mass is only [ ] of the total fiber debris generated in containment. This calculation conservatively assumes that 100 percent of the fiber debris generated, 10.2 lbm, is able to pass through the screens. The fiber transport rate is set so that the fiber that is not trapped by the sump strainers is deposited into the core within an hour. Because a conservative fiber amount bypass is assumed, this translates to 10.2 lbm of fiber debris. This rate can be calculated as: 10.2 lbm / 3600 s = 0.003 lbm/s. The as-fabricated density of Nukon fiber is 2.4 lbm/ft^3 (Reference 10, Vol. 1, Table 3-2). However, the material density of fibrous material may be as high as 162 lbm/ft^3. A lower fiber density leads to a higher deposit thickness. A higher deposit thickness leads to a higher surface temperature. Thus, using the smaller, as-fabricated fiber density for Nukon is appropriate for this evaluation.

A total of 100 percent or [ ] of generated particulate and [ ] of generated Microtherm may bypass the strainers. Microtherm is treated as a particulate (10, Vol. 1, p 3-66). The total mass of particulates of [ ] represents Microtherm and particulates. This amount is conservatively higher than the amount reported in Appendix C, [ ]. Particulates in containment comprise various material types with densities ranging from 94 lbm/ft^3 to 457 lbm/ft^3 (10, Vol.1, Table 3-3). A value of 100 lbm/ft^3 is selected to represent particulates.

The fiber and particulate densities are used to determine the thickness of the fiber layer and the particulate debris deposit layer. Table F.4-1 shows a summary of these mass and density inputs.

F.4.4.3 *Scale Density*

The densities for the calcium carbonate and calcium hydroxide deposits formed under boiling conditions are approximated based on reported densities for calcium carbonate, magnesium hydroxide, and calcium hydroxide deposits. Densities of 147 to 155 lb/ft^3 (2350 to 2640 kg/m^3) have been reported for calcium carbonate, magnesium hydroxide, and calcium hydroxide deposits formed under boiling conditions (Reference 11, p. 231). Since calcium, aluminum, and silicon may bond with other RCS chemicals such as phosphate and borate, this number should be reduced significantly to introduce conservatism into the prediction of LOCA scale thickness.

A lower density leads to a thicker deposit thickness, which is conservative for this evaluation, because it results in a higher surface temperature. Measurements on cross-sectioned calcium sulfate scale have shown that the density varies from 12.5 to 106 lbm/ft^3 (200 to 1700 kg/m^3) across the thickness of the deposit (Reference 12, Fig. 11). Using the lowest density in this range, 12.5 lbm/ft^3 (200 kg/m^3), introduces conservatism to the calculation. Although this value is conservative for a variety of values scale thickness, it is desirable to incorporate a more representative value. This also allows for a more direct comparison to experimental data.

F.4.4.4 *Mission Time*

To address the extended time period required in 10 CFR50.46(b)(5), (Reference 10, Volume 2, Section 2.0, paragraph 2) states: “For this evaluation of PWR recirculation performance, the staff considers this extended time to be 30 days, and requires cooling by recirculation of coolant using the ECCS sump.”

Therefore, this evaluation assumes that the mission time for the ECCS operation is thirty (30) days and that only the quantity of precipitate that is generated up to that point must be calculated for use in head loss and downstream analyses.

F.4.4.5 *IRWST Liquid Temperature*

Use of a higher value for the IRWST liquid temperature increases the boiling and deposition on the fuel rods. Therefore, the fluid temperature as a function of time is based on a calculation of the maximum temperature for the IRWST liquid during a LOCA. The IRWST temperature profile used for this evaluation is provided in Table F.4-2.

F.4.4.6 *Reactor Coolant Temperature*

Reactor coolant temperatures were obtained by increasing the IRWST liquid temperatures by 5°F. This temperature is used to determine the core pressure and the core boiling rate. To prevent a non-physical pressure being calculated due to a low IRWST temperature, however, the pressure value is no lower than atmospheric. The RV upper plenum pressure is higher than containment pressure, because the steam must travel through the loops to the break during the cold leg injection period. Increasing the RV coolant temperature by 5°F effectively increases the core region pressure by approximately 5 psi, which bounds the expected pressure drop through the loops. The core coolant temperature is uniform such that the core coolant temperature at every elevation is equal to the IRWST temperature plus the specified temperature increase. The IRWST temperature profile used for this evaluation to calculate the RV temperature profile is provided in Table F.4-2.

F.4.4.7 *Coolant Flow Balance*

The coolant flows of concern for this analysis are the IRWST recirculation flow and the core reactor vessel steam boiloff rate. As coolant in the reactor boils and condenses into the coolant stream, it is conservatively assumed that all impurities remain in the reactor vessel. In actual operation, some of the impurities would be carried out of the reactor vessel, thus reducing the amount of scale deposited in the reactor vessel. As a consequence of this conservative approach, the pure steam generated in the core condenses in the RCS coolant, returns to the IRWST through the break, and adds to the IRWST coolant volume, which reduces the impurity concentration in the IRWST.

F.4.4.8 *Total Mass of Released Elements Dissolved in the IRWST*

The total amount of released elements dissolved in the IRWST was obtained by analysis. The results from Appendix D, Table D.3-10 used in the EPRDM analysis are summarized in Table F.4-2.

F.4.4.9 *Core Data*

To calculate the amount of chemical precipitation in the core, specific core design parameters must be defined. These input parameters are discussed in this section.

The initial core power is selected to maximize boiling in the core. The value used in this calculation is 4,612 MWt (4,590 MWt + 22 MWt uncertainty). The core decay power fraction defines how the power output of the reactor is reduced over time. The model used is based on a curve-fit to the ANS 1971 standard plus 20 percent and includes actinides.

The fuel is represented by five radial regions: a hot rod, hot assembly, surrounding assemblies, average-core assembly and lower powered, outer assemblies. This is consistent with the LOCA linear heat rate limit analyses. Axially, each radial region is divided into 52 nodes. The relative power for 52 positions along the length of the fuel rods (i.e., axial power shape is consistent with that used in the highest PCT case in the 124 case RLBLOCA analysis (Reference 13, Appendix A).

A nominal fuel rod OD, 0.374 inches, is used in all cases. The total active fuel rod length is 165.354 inches.

Oxidation and crud formation during normal operation are also considered in the analysis. The model assumes a limiting oxide thickness of 35 microns (1.38 mils). This thickness includes the crud layer thickness. Because the crud and oxide thickness reference input is combined with no indication of relative amounts of each, the thermal conductivity used for the oxide/crud layer will be set to the lowest value of thermal conductivity present. A lower value will give less heat transfer and conservatively higher temperature predictions. The thermal conductivity of zirconium oxide (ZrO_2) expected to be present on fuel surfaces at the time of the accident is taken as 1.6 W/m-K (Reference 14, p. 435). The thermal conductivity of the crud layer can be as low as 0.17 W/m-K (Reference 15). This value assumes that the surrounding fluid is saturated steam. If the surrounding fluid is liquid water, as is expected for the accident, the thermal conductivity is higher and ranges between 0.46 BTU/h-ft-ºF (0.80 W/m-k) and 0.50 BTU/h-ft-ºF (0.87 W/m-K). Therefore, use of the saturated steam value is conservative since a lower value will result in less heat transfer and a higher surface temperature. Since this value is lower than the actual oxide layer thermal conductivity, 0.17 W/m-K will be used for the combined oxide-crud layer in this calculation. The oxide and crud thickness at any location in the core is dependent on the temperature achieved during a LOCA, which, in turn, is partly dependent on the time that the fuel rod has been in service and the axial and radial power. These variations result in oxide thicknesses that are less than the maximum value. EPRDM has the capability to model these variations. However, the analyses conservatively set the relative oxide and crud thickness fraction at each core location to 1.0 such that all locations start with the maximum oxide and crud thickness.

F.4.4.10 *Scale Deposit*

The two types of precipitates predicted to form out of solution are calcium phosphate, $Ca_5(PO_4)_2$, and sodium aluminum silicate, $NaAlSi_3O_8$ (Appendix D). Of these, sodium aluminum silicate is more insulating with thermal conductivity values as low as 0.2 W/m-K (Reference 16). Thus, for a bounding calculation, choosing sodium aluminum silicate is appropriate. However, for conservatism, a value of 0.1 W/m-K has been used in this evaluation for the thermal conductivity of any LOCA scale in all cases.

F.4.4.11 *Distance from Hot Leg Inlet to Top of Pellet Stack*

The distance between the hot leg centerline to the top of the pellet stack in the U.S. EPR design is 85.04 inches or 2160 mm. The hot leg inner diameter is 30.71 inches or 780 mm. Subtracting the hot leg radius from this distance gives the distance from the hot leg inlet to the top of the pellet stack as 69.685 inches.

Table F.4-1 Debris Inputs

Debris Material	Density (lb/ft^3)	Mass (lbm)	Mass (kg)	Section
Additional Aluminum Debris	0	0	0.0	F.4.4.2
Bypassed Fiber	2.40	10.2	4.6	F.4.4.2
Bypassed Particulate (includes Microtherm)	100.00	1486.8	674.4	F.4.4.2
Scale Deposit Density	12.5			F.4.4.3

Table F.4-2 Inputs for IRWST Temp and Mass Releases

Time - hr (total)	IRWST Temp. (ºF)	Total Released Al (kg)	Total Released Ca (kg)	Total Released Si (kg)
0	122	0	0	0
0.25	154.8	1.88	6.78	4.77
0.58	178.8	2.54	6.8	6.31
0.92	194.5	2.63	6.82	7.9
1.58	216.3	2.81	6.89	8.42
1.92	224.5	2.91	6.91	8.47
2.25	231.4	3	6.94	8.55
3.31	246.2	3.3	7.07	8.8
4.5	221.5	3.62	7.19	9
6.5	203.2	4.17	7.33	9.24
9.5	193.1	4.97	7.54	9.55
13.5	187	6.06	7.78	9.91
20	181.6	7.81	8.14	10.41
31.5	180	7.9	8.77	11.29
37.5	170	7.93	9.05	11.62
49.5	160	8	9.5	12.15
60	160	8.04	9.9	12.59
80	160	8.14	10.66	13.48
120	160	8.22	11.89	13.71
240	160	8.47	15.55	14.41
360	160	8.71	19.14	15.12
480	160	8.96	22.91	15.82
600	160	9.21	26.52	16.54
720	160	9.45	30.13	17.25

Table F.4-3 Coolant/Miscellaneous Material Inputs

Parameter	Units	Value	Section
IRWST Coolant Density	lbm/ft^3	57.186	F.4.4.1
Initial IRWST Coolant Volume	ft^3	57,916.0	F.4.4.1
Initial IRWST Coolant Mass	lbm	3,311,984.4	F.4.4.1
Initial IRWST Coolant Mass	kg	1,502,292.6	F.4.4.1
RV Core Region Coolant Density	lbm/ft^3	57.00	F.4.4.1
Initial RV Core Region Coolant Volume	ft^3	542.0	F.4.4.1
Initial RV Core Region Coolant Mass	lbm	30,894.0	F.4.4.1
Initial RV Core Region Coolant Mass	kg	14,013.3	F.4.4.1
Fiber Screen Bypass Rate	lbm/s	0.003	F.4.4.2
Initial Recirculation Time	min	15	F.3.4.1

Table F.4-4 Reactor Core Parameters

Variable	Value	Units	Section
Reactor Power	4,612	MWt	
Oxide/Crud Thermal Conductivity	0.17	W/m-K	F.4.4.2
Scale Deposit Thermal Conductivity	0.1	W/m-K	F.4.4.10
Fuel Rod OD	0.374	Inches	
Fuel Rod Height	165.354	Inches	
Distance from Hot Leg Inlet to Top of Pellet Stack	69.685	Inches	F.4.4.11
Average Initial Cladding Oxide/Crud Thickness	35	Microns	F.4.4.2
Number of Regions	5	Regions	
Number of Elevation Sections	52	Elevations	

F.4.5 Results

The methodology and assumptions for the deposition of chemical precipitates and debris on fuel rods are applied to calculate peak cladding temperatures throughout the core, and the final magnitude of LOCA scale thickness predicted for each analyzed node.

Table F.4-5 through Table F.4-9 shows the results of the EPRDM calculation.
Table F.4-6 through Table F.4-9 shows the final amount of material deposition thickness predicted for each analyzed node post-LOCA. The maximum total deposit thickness is 15.47 mils, which is below the acceptable limit of 50 mils. For each node, the acceptance criteria were met throughout the calculation.

The EPRDM calculation with U.S. EPR-specific information calculates a peak cladding temperature of 375°F (refer to Table F.4-5 at 3.31 hours). This peak temperature is well below 800°F. The final total deposit thicknesses were calculated to be well below 50 mils (1270 microns).

Therefore, the results of this calculation, applying conservative assumptions, shows that chemical precipitation and deposition will not prevent adequate removal of core decay heat and the long-term core cooling criterion of 10 CFR 50.46(b)(5) is met.

Table F.4-5 EPRDM Output For Each Time Step

Time	Al Conc (ppm)		Ca Conc (ppm)		Si Conc (ppm)		Fiber Conc (ppm)		Particulate Conc (ppm)		Region of Max Scale Thk	Elev. of Max Scale Thk	Max Scale Thk (microns)	Max Fuel Cladding Temp (°F)
Hours	RV	IRWST	RV	IRWST	RV	IRWST	RV	IRWST	RV	IRWST				
0.00	0.00	0.00	0.00	0.00	0.00	0.00	0.00	0.00	0.00	0.00				
0.25	0.00	1.25	0.00	4.51	0.00	3.18	0.00	3.08	0.00	448.92				
0.58	1.56	1.70	4.48	4.53	3.90	4.21	29.12	2.05	432.43	433.11	1	43	16.84	352.2
0.92	1.73	1.75	4.53	4.54	4.93	5.24	32.50	1.03	423.08	419.28	1	43	35.16	353.5
1.58	1.85	1.87	4.58	4.59	5.55	5.61	1.72	0.00	399.97	396.24	1	43	61.02	362.2
1.92	1.91	1.94	4.59	4.60	5.62	5.64	0.08	0.00	389.86	386.22	1	43	65.32	364.4
2.25	1.97	2.00	4.61	4.62	5.67	5.69	0.00	0.00	380.40	376.85	1	43	69.23	367.6
3.31	2.17	2.20	4.69	4.71	5.84	5.86	0.00	0.00	353.56	350.26	1	43	80.43	375.0
4.50	2.38	2.41	4.78	4.79	5.97	5.99	0.00	0.00	327.65	324.60	1	43	91.45	344.9
6.50	2.74	2.78	4.87	4.88	6.14	6.15	0.00	0.00	292.12	289.39	1	43	106.96	319.6
9.50	3.27	3.31	5.01	5.02	6.34	6.36	0.00	0.00	251.19	248.96	1	43	125.80	302.0
13.50	3.98	4.03	5.16	5.18	6.57	6.60	0.00	0.00	212.41	210.83	1	43	145.97	289.8
20.00	5.10	5.20	5.37	5.42	6.87	6.93	0.00	0.00	173.84	173.32	1	43	172.38	279.7
31.50	5.21	5.26	5.77	5.84	7.43	7.52	0.00	0.00	134.48	134.38	1	43	209.31	275.0
37.50	5.18	5.28	5.90	6.02	7.57	7.73	0.00	0.00	120.74	121.80	1	43	225.36	263.9
49.50	4.55	5.33	5.33	6.32	6.83	8.09	0.00	0.00	97.73	113.03	1	43	252.57	251.5
60.00	3.43	5.35	4.07	6.59	5.20	8.38	0.00	0.00	73.23	112.69	1	43	269.18	248.8
80.00	2.31	5.42	2.84	7.10	3.61	8.97	0.00	0.00	48.84	112.32	1	43	289.79	243.4
120.00	1.40	5.47	1.87	7.91	2.28	9.13	0.00	0.00	29.08	111.96	1	43	311.76	234.4
240.00	0.77	5.64	1.31	10.35	1.31	9.59	0.00	0.00	15.50	111.39	1	43	343.17	221.7
360.00	0.23	5.80	0.44	12.74	0.39	10.06	0.00	0.00	4.49	111.24	1	43	356.34	215.9
480.00	0.03	5.96	0.05	15.25	0.04	10.53	0.00	0.00	0.49	111.24	1	43	357.95	211.4
600.00	0.00	6.13	0.01	17.65	0.01	11.01	0.00	0.00	0.06	111.24	1	43	357.96	207.9
720.00	0.00	6.29	0.00	20.06	0.00	11.48	0.00	0.00	0.01	111.24	1	43	357.96	205.1

Table F.4-6 EPRDM Output For Core Elevations 1-13

Elevation	1	2	3	4	5	6	7	8	9	10	11	12	13
Region (Scale Thickness in microns)													
1	5.32	23.40	46.42	64.91	81.97	94.23	97.98	101.47	105.78	109.92	112.74	114.26	115.71
2	4.98	21.69	43.56	60.66	72.23	83.11	90.21	96.46	100.51	104.44	107.11	108.57	109.93
3	3.44	14.01	26.35	37.63	44.49	47.69	49.85	52.21	55.16	58.02	60.01	61.08	62.07
4	3.05	12.16	22.63	31.98	37.94	40.84	43.02	44.95	47.35	49.79	51.47	52.41	53.27
5	1.54	5.28	9.29	12.22	14.19	15.21	15.71	16.51	17.17	18.08	18.80	19.03	19.29
Region (Scale Thickness in mils)													
1	0.21	0.92	1.83	2.56	3.23	3.71	3.86	4.00	4.16	4.33	4.44	4.50	4.56
2	0.20	0.85	1.71	2.39	2.84	3.27	3.55	3.80	3.96	4.11	4.22	4.27	4.33
3	0.14	0.55	1.04	1.48	1.75	1.88	1.96	2.06	2.17	2.28	2.36	2.40	2.44
4	0.12	0.48	0.89	1.26	1.49	1.61	1.69	1.77	1.86	1.96	2.03	2.06	2.10
5	0.06	0.21	0.37	0.48	0.56	0.60	0.62	0.65	0.68	0.71	0.74	0.75	0.76
Region (Total Deposit Thickness in mils)*													
1	1.59	2.30	3.21	3.93	4.61	5.09	5.24	5.37	5.54	5.71	5.82	5.88	5.93
2	1.57	2.23	3.09	3.77	4.22	4.65	4.93	5.18	5.34	5.49	5.59	5.65	5.71
3	1.51	1.93	2.42	2.86	3.13	3.26	3.34	3.43	3.55	3.66	3.74	3.78	3.82
4	1.50	1.86	2.27	2.64	2.87	2.99	3.07	3.15	3.24	3.34	3.40	3.44	3.48
5	1.44	1.59	1.74	1.86	1.94	1.98	2.00	2.03	2.05	2.09	2.12	2.13	2.14
Region (Final Fuel Cladding Temp in deg. F)													
1	166.18	168.59	170.89	172.68	173.94	174.69	175.06	175.45	175.95	176.42	176.75	176.92	177.09
2	166.13	168.43	170.60	172.27	173.33	174.01	174.44	174.89	175.35	175.79	176.10	176.26	176.42
3	165.83	167.48	168.93	170.02	170.68	171.02	171.23	171.46	171.74	172.02	172.21	172.31	172.41
4	165.76	167.24	168.53	169.48	170.06	170.35	170.54	170.74	170.98	171.22	171.39	171.48	171.56
5	165.40	166.17	166.81	167.25	167.51	167.63	167.71	167.80	167.90	168.01	168.08	168.11	168.15
Region: Boiling in node at end of computer run?													
1	N	N	N	N	N	N	N	N	N	N	N	N	N
2	N	N	N	N	N	N	N	N	N	N	N	N	N
3	N	N	N	N	N	N	N	N	N	N	N	N	N
4	N	N	N	N	N	N	N	N	N	N	N	N	N
5	N	N	N	N	N	N	N	N	N	N	N	N	N

* Scale Thickness + 1.38 mils (Average Initial Cladding Oxide/Crud Thickness)

Table F.4-7 EPRDM Output For Core Elevations 14-26

Elevation	14	15	16	17	18	19	20	21	22	23	24	25	26
Region (Scale Thickness in microns)													
1	118.43	122.88	128.24	133.74	138.81	143.57	149.55	157.44	166.55	175.15	190.38	203.35	215.61
2	112.49	116.73	121.75	126.51	130.42	134.81	140.42	147.87	156.56	164.83	171.76	178.70	194.95
3	64.05	67.24	71.58	78.59	84.69	90.59	96.41	100.50	105.28	109.82	113.71	117.09	120.87
4	54.94	57.68	60.97	64.09	66.72	69.18	73.81	81.91	91.86	97.84	101.28	104.28	107.61
5	19.99	20.72	21.88	23.29	24.03	24.82	26.09	27.72	29.56	31.04	32.66	34.15	35.78
Region (Scale Thickness in mils)													
1	4.66	4.84	5.05	5.27	5.46	5.65	5.89	6.20	6.56	6.90	7.50	8.01	8.49
2	4.43	4.60	4.79	4.98	5.13	5.31	5.53	5.82	6.16	6.49	6.76	7.04	7.68
3	2.52	2.65	2.82	3.09	3.33	3.57	3.80	3.96	4.14	4.32	4.48	4.61	4.76
4	2.16	2.27	2.40	2.52	2.63	2.72	2.91	3.22	3.62	3.85	3.99	4.11	4.24
5	0.79	0.82	0.86	0.92	0.95	0.98	1.03	1.09	1.16	1.22	1.29	1.34	1.41
Region (Total Deposit Thickness in mils)*													
1	6.04	6.22	6.43	6.64	6.84	7.03	7.27	7.58	7.94	8.27	8.87	9.38	9.87
2	5.81	5.97	6.17	6.36	6.51	6.69	6.91	7.20	7.54	7.87	8.14	8.41	9.05
3	3.90	4.03	4.20	4.47	4.71	4.94	5.17	5.33	5.52	5.70	5.85	5.99	6.14
4	3.54	3.65	3.78	3.90	4.00	4.10	4.28	4.60	4.99	5.23	5.37	5.48	5.61
5	2.16	2.19	2.24	2.29	2.32	2.36	2.41	2.47	2.54	2.60	2.66	2.72	2.79
Region (Final Fuel Cladding Temp in deg. F)													
1	177.41	177.94	178.58	179.20	179.74	180.25	180.89	181.76	182.79	183.78	184.98	186.05	187.16
2	176.72	177.21	177.81	178.37	178.84	179.31	179.91	180.71	181.67	182.59	183.39	184.13	185.34
3	172.60	172.91	173.29	173.73	174.10	174.47	174.88	175.34	175.89	176.41	176.86	177.26	177.70
4	171.72	171.98	172.30	172.61	172.86	173.09	173.43	173.93	174.54	175.05	175.43	175.77	176.15
5	168.22	168.32	168.46	168.58	168.68	168.77	168.90	169.05	169.24	169.41	169.56	169.70	169.85
Region: Boiling in node at end of computer run?													
1	N	N	N	N	N	N	N	N	N	N	N	N	N
2	N	N	N	N	N	N	N	N	N	N	N	N	N
3	N	N	N	N	N	N	N	N	N	N	N	N	N
4	N	N	N	N	N	N	N	N	N	N	N	N	N
5	N	N	N	N	N	N	N	N	N	N	N	N	N

*** Scale Thickness + 1.38 mils (Average Initial Cladding Oxide/Crud Thickness)**

Table F.4-8 EPRDM Output For Core Elevations 27-39

Elevation	27	28	29	30	31	32	33	34	35	36	37	38	39
Region (Scale Thickness in microns)													
1	228.96	242.84	255.58	265.82	273.74	281.46	291.16	303.03	315.41	325.30	331.67	335.95	340.56
2	210.74	225.95	238.88	248.90	256.54	263.89	272.96	283.96	295.46	305.04	311.60	316.20	321.30
3	125.63	131.14	137.61	142.92	147.09	151.15	156.15	162.24	168.45	173.48	176.86	182.94	189.61
4	111.79	116.62	121.32	125.13	128.11	130.97	135.39	140.75	146.31	150.85	153.96	156.13	158.60
5	37.73	39.94	42.06	43.82	45.14	46.40	48.07	50.09	52.20	53.96	55.14	55.99	56.95
Region (Scale Thickness in mils)													
1	9.01	9.56	10.06	10.47	10.78	11.08	11.46	11.93	12.42	12.81	13.06	13.23	13.41
2	8.30	8.90	9.40	9.80	10.10	10.39	10.75	11.18	11.63	12.01	12.27	12.45	12.65
3	4.95	5.16	5.42	5.63	5.79	5.95	6.15	6.39	6.63	6.83	6.96	7.20	7.46
4	4.40	4.59	4.78	4.93	5.04	5.16	5.33	5.54	5.76	5.94	6.06	6.15	6.24
5	1.49	1.57	1.66	1.73	1.78	1.83	1.89	1.97	2.05	2.12	2.17	2.20	2.24
Region (Total Deposit Thickness in mils)*													
1	10.39	10.94	11.44	11.84	12.16	12.46	12.84	13.31	13.80	14.18	14.44	14.60	14.79
2	9.67	10.27	10.78	11.18	11.48	11.77	12.12	12.56	13.01	13.39	13.65	13.83	14.03
3	6.32	6.54	6.80	7.00	7.17	7.33	7.53	7.77	8.01	8.21	8.34	8.58	8.84
4	5.78	5.97	6.15	6.30	6.42	6.53	6.71	6.92	7.14	7.32	7.44	7.52	7.62
5	2.86	2.95	3.03	3.10	3.16	3.20	3.27	3.35	3.43	3.50	3.55	3.58	3.62
Region (Final Fuel Cladding Temp in deg. F)													
1	188.50	190.00	191.46	192.66	193.61	194.55	195.74	197.21	198.76	200.05	200.91	201.51	202.18
2	186.71	188.18	189.56	190.69	191.57	192.43	193.52	194.86	196.27	197.46	198.28	198.86	199.52
3	178.26	178.92	179.61	180.18	180.63	181.07	181.62	182.30	183.01	183.59	183.99	184.43	184.92
4	176.64	177.20	177.75	178.20	178.56	178.91	179.38	179.95	180.54	181.04	181.38	181.62	181.89
5	170.03	170.25	170.46	170.63	170.76	170.89	171.05	171.25	171.45	171.62	171.74	171.82	171.91
Region: Boiling in node at end of computer run?													
1	N	N	N	N	N	N	N	N	N	N	N	N	N
2	N	N	N	N	N	N	N	N	N	N	N	N	N
3	N	N	N	N	N	N	N	N	N	N	N	N	N
4	N	N	N	N	N	N	N	N	N	N	N	N	N
5	N	N	N	N	N	N	N	N	N	N	N	N	N

*** Scale Thickness + 1.38 mils (Average Initial Cladding Oxide/Crud Thickness)**

Table F.4-9 EPRDM Output For Core Elevations 40-52

Elevation	40	41	42	43	44	45	46	47	48	49	50	51	52
Region (Scale Thickness in microns)													
1	346.67	352.99	357.43	357.96	353.56	344.23	329.26	307.73	276.00	225.75	146.33	72.09	13.34
2	328.52	336.51	342.18	342.83	337.26	325.55	309.07	288.30	258.70	207.05	137.39	66.70	12.70
3	198.08	206.92	213.11	213.84	207.73	194.68	175.57	164.59	148.27	124.44	94.04	41.51	8.43
4	162.17	166.42	169.63	170.03	166.83	160.67	152.77	142.87	128.94	110.75	70.68	35.07	7.42
5	58.34	60.02	61.30	61.48	60.20	57.78	54.70	50.90	45.50	36.93	25.58	13.30	3.31
Region (Scale Thickness in mils)													
1	13.65	13.90	14.07	14.09	13.92	13.55	12.96	12.12	10.87	8.89	5.76	2.84	0.53
2	12.93	13.25	13.47	13.50	13.28	12.82	12.17	11.35	10.19	8.15	5.41	2.63	0.50
3	7.80	8.15	8.39	8.42	8.18	7.66	6.91	6.48	5.84	4.90	3.70	1.63	0.33
4	6.38	6.55	6.68	6.69	6.57	6.33	6.01	5.62	5.08	4.36	2.78	1.38	0.29
5	2.30	2.36	2.41	2.42	2.37	2.27	2.15	2.00	1.79	1.45	1.01	0.52	0.13
Region (Total Deposit Thickness in mils)*													
1	15.03	15.28	15.45	15.47	15.30	14.93	14.34	13.49	12.24	10.27	7.14	4.22	1.90
2	14.31	14.63	14.85	14.88	14.66	14.19	13.55	12.73	11.56	9.53	6.79	4.00	1.88
3	9.18	9.52	9.77	9.80	9.56	9.04	8.29	7.86	7.22	6.28	5.08	3.01	1.71
4	7.76	7.93	8.06	8.07	7.95	7.70	7.39	7.00	6.45	5.74	4.16	2.76	1.67
5	3.67	3.74	3.79	3.80	3.75	3.65	3.53	3.38	3.17	2.83	2.39	1.90	1.51
Region (Final Fuel Cladding Temp in deg. F)													
1	203.12	204.19	205.00	205.09	204.29	202.73	200.58	197.80	193.89	188.16	180.54	173.32	167.40
2	200.48	201.59	202.42	202.52	201.69	200.08	197.96	195.39	191.82	186.37	179.59	172.85	167.30
3	185.60	186.36	186.93	186.99	186.43	185.32	183.83	182.57	180.76	178.12	174.68	170.40	166.68
4	182.29	182.77	183.14	183.19	182.82	182.13	181.25	180.17	178.66	176.52	173.23	169.80	166.52
5	172.05	172.21	172.34	172.35	172.23	171.99	171.70	171.33	170.80	169.98	168.83	167.39	165.80
Region: Boiling in node at end of computer run?													
1	N	N	N	N	N	N	N	N	N	N	N	N	N
2	N	N	N	N	N	N	N	N	N	N	N	N	N
3	N	N	N	N	N	N	N	N	N	N	N	N	N
4	N	N	N	N	N	N	N	N	N	N	N	N	N
5	N	N	N	N	N	N	N	N	N	N	N	N	N
*** Scale Thickness + 1.38 mils (Average Initial Cladding Oxide/Crud Thickness)**													

F.4.6 Conclusion

The purpose of this analysis was to perform a conservative evaluation of the core chemical effects associated with the long term core cooling capability of the U.S. EPR design. This analysis considers the presence of fibrous, particulate and chemical debris in the recirculating fluid following a postulated design basis LOCA. This evaluation was performed based on conservative assumptions using the EPRDM to evaluate the final deposit thicknesses and peak cladding temperatures expected for a single postulated condition.

The results of this calculation show that the acceptance criteria were met for each location in the core throughout the accident. The EPRDM calculation with U.S. EPR-specific information calculated a peak cladding temperature of 375°F (refer to Table F.4-5 at 3.31 hours). From the total deposit thickness results presented in Table F.4-6 through Table F.4-9, the maximum total deposit thickness is 15.47mils, which is well below the maximum acceptable limit of 50 mils.

Therefore, the results of this calculation show that chemical precipitation and deposition will not prevent adequate removal of core decay heat and the long-term core cooling criterion of 10 CFR 50.46(b)(5) is met.

F.5 Testing Summary

F.5.1 Testing Purpose

U.S. EPR fuel assembly tests have been conducted to justify acceptance criteria for the amount of debris that can reach the RCS without impeding long-term core cooling flows to the core. These acceptance criteria are used in part to demonstrate adequate flow for long term decay heat removal. This appendix section summarizes and analyzes the results of these tests as they apply to the U.S. EPR design.

F.5.2 Testing Acceptance Criteria

Determining sufficient long-term core cooling is highly dependent on the break location and ECCS injection configuration that is postulated in the simulations. [

]

Table F.5-1 Maximum K/A^2 Summary

Break	Injection	Core Flow Direction	[ ]
Hot Leg	Cold Leg	Bottom to Top	
Cold Leg	Cold Leg	Bottom to Top	
Hot Leg	Hot Leg	Bottom to Top	
Cold Leg	Hot Leg	Top to Bottom	

F.5.3 Test Facility

AREVA NP contracted with Continuum Dynamics Incorporated (CDI), an engineering and testing firm in Ewing, NJ, to perform the fuel assembly tests on AREVA NP fuel. CDI designed and constructed a test loop to measure the pressure drop across a full area, partial height test fuel assembly with a FUELGUARD lower end fitting. The details of the test loop and fuel assembly are provided in the sections below.

F.5.3.1 *Test Loop*

The CDI test loop consists of a mixing tank, a submersible pump, piping to deliver flow to a clear test chamber, and piping to return the flow to the mixing tank. The test chamber consists of a core support plate (located approximately 12 inches above the bottom of the chamber), a 52 inch tall 17x17 fuel assembly that includes a lower end fitting (LEF), four spacer grids, simulated fuel rods, control rod guide tubes, and an instrument tube.

During CLI tests, flow enters from the bottom of the chamber as shown in Figure F.5-1, passes through the fuel assembly, and exits out of the top of the chamber. An inverted right circular cone directs flow along the bottom of the chamber to minimize settling of debris. A submersible pump pumps water and debris from the mixing tank through a flow meter and flow control valve and into the test chamber. The flow rate is manually controlled by adjusting the pump bypass flow valve and flow control valve. The mixing tank allows debris to be added to the system and is well agitated by the pump bypass flow and a motor driven agitator to minimize settling and agglomeration. A cooling coil is used to control water temperature.

During HLI tests, the flow is reversed in the test chamber so that it enters from the top and exits the bottom as shown in Figure F.5-2. The enclosure around the fuel assembly was fabricated from transparent PVC. Support ribs spaced approximately every four inches limit the deflection of the enclosure to maintain the gap space between the fuel assembly and the test facility walls at the fuel bundle pitch used in the plant reactor core. The enclosure is flanged at two locations to allow the fuel assembly to be removed. An upper test chamber was installed for HLI tests to facilitate flow distribution across the upper core plate. Pressure taps were installed below the fuel assembly, above the assembly, and between each support grid to allow differential pressure (dP) measurements across the full assembly and any grid or combination of grids to be measured. The pressure taps were installed on the walls two to three inches below the spacer grids and centered between fuel rods. Each pressure tap had a valve installed on it to facilitate switching dP measurements.

Figure F.5-1 Cold Leg Injection Flow Path

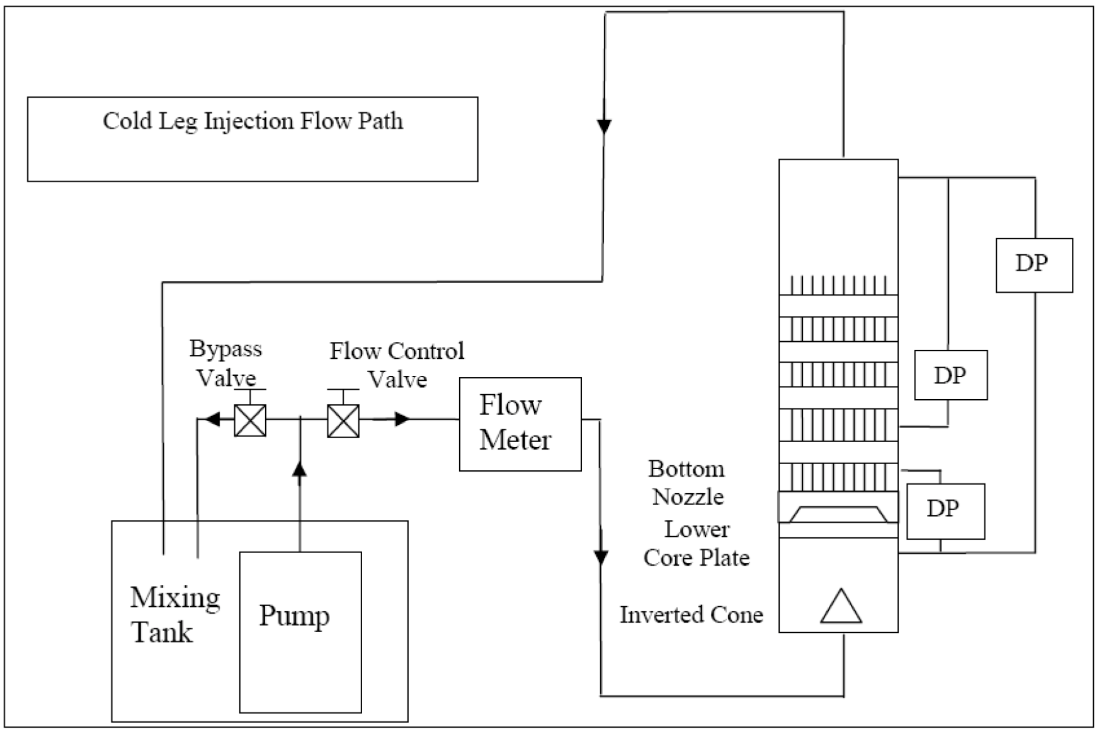

Figure F.5-2 Hot Leg Injection Flow Path

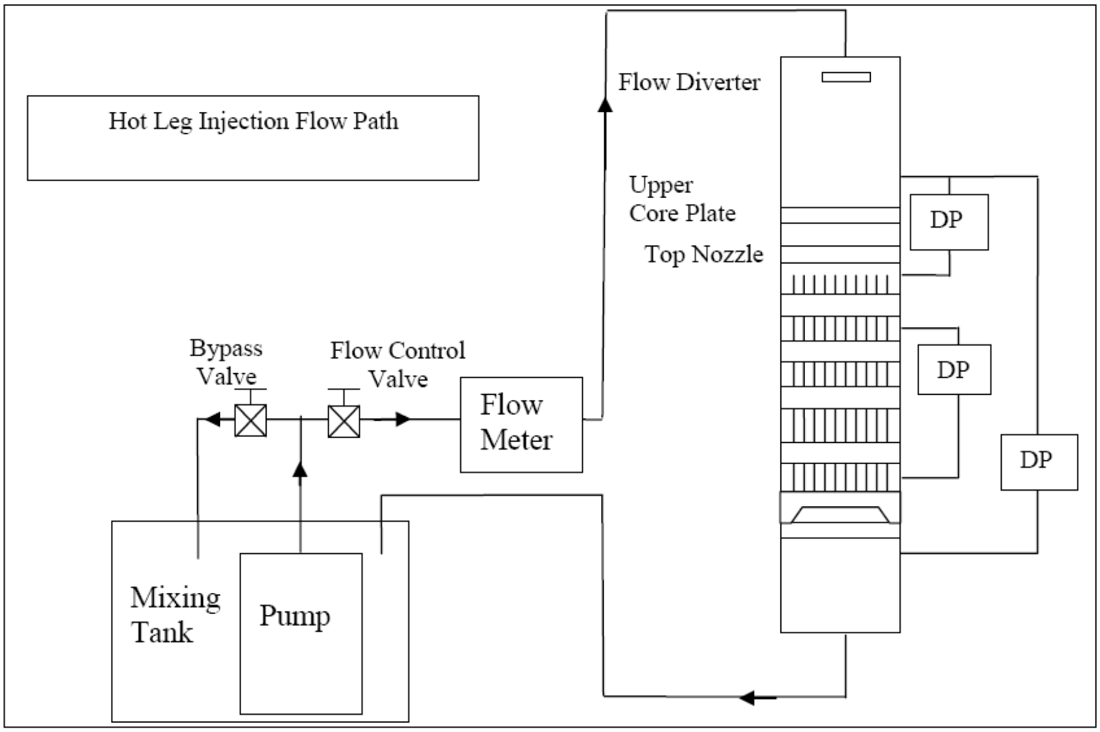

F.5.3.2 *The Simulated Lower Core Plate*

The simulated lower core plate represents a section of a typical operating plant core support plate. **[**

]

[

]

Figure F.5-3 Simulated Lower Core Plate

F.5.3.3 *Fuel Assembly*

This section contains a description of the four- and seven-grid fuel assemblies used in the testing. The four grid fuel assembly provided by AREVA NP contains a 17x17 array of fuel rods including 24 guide tubes and a center instrument tube (See Figure F.5-4). These tubes were plugged at both the top and bottom so that no flow could pass through them. Some small holes in the bottom of the tubes were not plugged. However, they were filled with liquid prior to beginning the test; no significant amount of debris entered them during the test. The guide tubes extended approximately [ ] above the top of the lower end fitting and were approximately [ ] in diameter. There are 264 simulated fuel rods supplied with the assembly with a diameter of approximately [ ] and a length of [ ] depending on type. These fuel rods were installed by sliding them through all of the grids until they were in the desired position. For CLI tests, the fuel rods were located [ ] above the LEF. For HLI tests, the fuel rods were located [ ] below the upper end fitting (UEF). The fuel assembly was fastened to the lower end fitting by screws in the 24 guide tubes. These screws also served to plug the guide tubes on the lower end.

Figure F.5-4 AREVA NP Four Grid Test Fuel Assembly

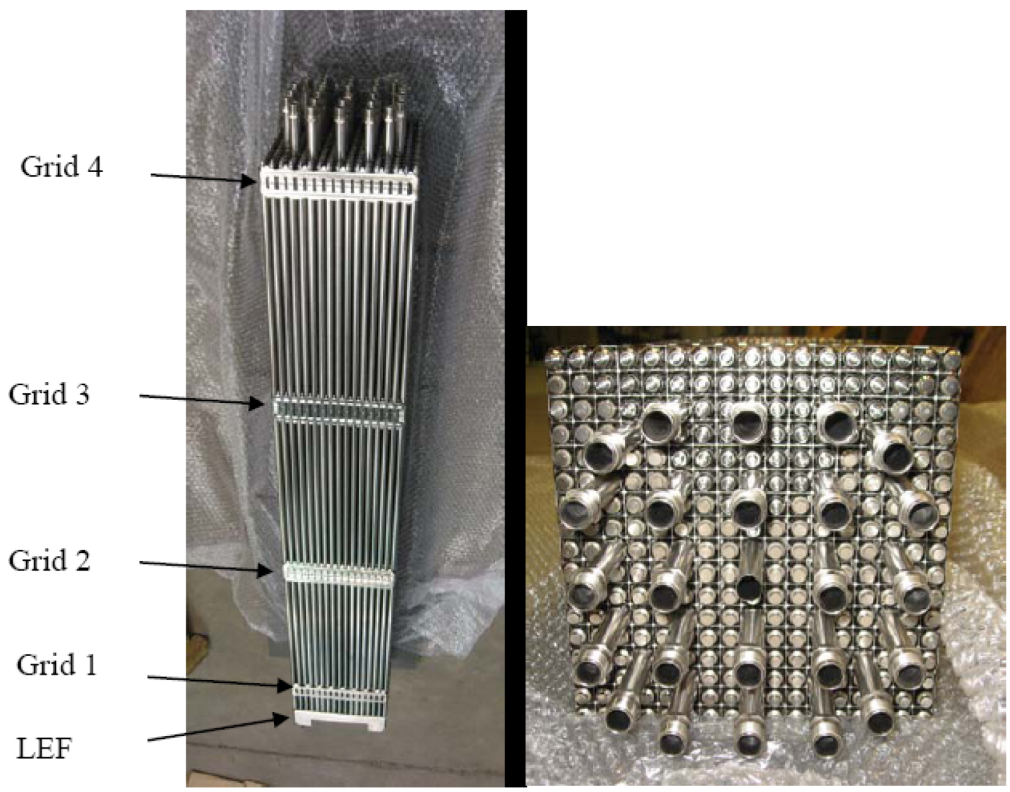

Figure F.5-5 AREVA NP Seven Grid Test Fuel Assembly

Figure F.5-6 Representation of Grid Type Tested

Figure F.5-7 Representation of Grid Type Tested

Figure F.5-8 Representation of HTP Grids

[ ]

F.5.4 Tests

Over the course of 2009-2011, AREVA NP performed fuel assembly tests to support resolution of GSI-191. These tests were conducted specifically with AREVA NP fuel and were performed to support [ ] the U.S. EPR design. The test procedure for all of tests was the same and is described in Section F.5.4.1.3. The debris types and size distribution were also the same and are discussed in Section F.5.4.2. The overall results matrix is identified in Table F.5-27.

F.5.4.1 *Test Procedure Summary*

The overall test plan was developed by CDI. The objective of the tests is to define the maximum mass of each debris type that can be tolerated in the RCS and core before core cooling is potentially compromised.

Previous fuel assembly testing experience indicated that the particulates and chemical precipitates are small debris types that readily pass through the debris filters or fuel assemblies. The addition of fiber to the mix can have a strong influence on the pressure drop, because fiber is more readily trapped by the fuel assembly grids, thereby forming a debris bed that could potentially capture the smaller debris types. Based on this knowledge, the order of debris addition is particulate first, fiber second, and chemical precipitates last. This is done to conservatively maximize the pressure drop of the debris bed by minimizing the porosity of the debris bed as it forms. Particulate debris does not catch in the core unless the debris is large enough to plug the opening. Fibrous debris, however, could snag on the leading edges of spacer grids or filters and begin to build a bed across the smaller portions of the openings (e.g., from the corners).

Fiber by itself is fairly porous, even with very small fibers. If particulates are present, they can fill the interstitial gaps among the fibers and decrease the porosity of the debris bed and increase the pressure drop. Having all of the particulates available in the test loop from the start of the test ensures that the openings in the fiber bed can be filled as the bed forms. [

]

The chemical precipitates are added after the particulates and fiber because they do not form until well into the transient. They are expected to form a layer on top of the established debris bed and could possibly compress the bed, further increasing the pressure drop of the bed. U.S. EPR testing has indicated that the amount of chemical precipitates have a limited effect on the overall pressure drop through the debris bed.

[

]

F.5.4.1.1 General Test Conditions

The following conditions were present during each of the tests:

- Tap water was used in the test.
- The tap water was filtered with a GE string wound sediment filter model FXUSC.
- The water temperature remained at 70°F ± 10°F and was cooled by a copper cooling coil to maintain within the temperature range.
- If the measured pressure drop across the entire assembly reached 14 psid during a test, then the flow rate was reduced so that the pressure drop remained below 14psid.
- Debris in the mixing tank was kept in suspension by agitation.
- Mixing tank agitation was provided by return flow from the test loop, bypass flow from the pump, and by a mechanical variable-speed mixer.
- Head Loss stabilization is defined as Head Loss ≤ 2 percent change over the previous 2 turnover times.
- At the conclusion of each test, the mixing tank was inspected for evidence of debris settling. No debris settling was found.

F.5.4.1.2 Pre-Test Procedures

The following steps were taken before the start of each test:

- The water temperature was adjusted to 70°F ± 10°F.
- Initial pH was measured and adjusted if it fell outside the range of 6.5-9.0.
- Debris quantities were weighed.
- The chemical surrogate was tested for settling.

F.5.4.1.3 Test Procedure

The following procedure was used in all tests. The number of particulate, fiber, chemical (PFC) batches, size of PFC batches, flow configuration, and turnover times varied among the tests. See Table F.5-3 for a summary of specific test inputs.

1. The dry debris was soaked (with water from the mixing tank) and mixed in preparation for addition to the mixing tank.
2. The particulate was added to the mixing tank first.
3. After 5 turnover times, the first batch of fiber was added.
4. At least two turnover times were allowed in between each fiber addition.
5. After all of the fiber had been added and the head loss had stabilized, the first batch of chemical surrogate was added to the mixing tank.
6. At least two turnover times were allowed between each chemical addition.

F.5.4.2 *Debris*

All of the debris was soaked in water and mixed prior to adding to the mixing tank. Water from the mixing tank was used to wet the debris. The mixing tank was agitated by the pump bypass flow and motor driven agitator to minimize settling and agglomeration. These steps mitigate the possibility of debris settling in the mixing tank, residing in the tank liquid volume, or remaining floating on the liquid surface in the mixing tank. The following is a summary of the debris (i.e., particulate, fiber, chemical) used in the tests.

F.5.4.2.1 Particulate

Tests were conducted with various particulate loads from **[ ]** (see Table F.5-3). The particulate debris was represented by silicon carbide with an average diameter of 8.64 μm in diameter. The size distribution of the test particulate was verified in each test to be consistent with the size distribution that provides for a conservative head loss in a fiber bed. Because of the small size of the particles and the test loop design, agitation, and flow rates, the particulate settling is minimized.

F.5.4.2.2 Fiber

Fibrous debris in the tests was represented by Nukon low density fiberglass. The fiber was prepared by taking shredded fiber, adding it to water, and processing it in a blender. It was then dried and analyzed microscopically to ensure the size distribution was met. The analysis consisted of distributing a small sample of the prepared fiber on a microscope slide and photographing a random region where individual fibers could be resolved. Fibers were manually classified into three length bins (<0.5mm, ≥0.5mm and <1mm, ≥1mm) and percentages based on count were calculated. Table F.5-2 shows the target fiber size distribution. This distribution matches the industry reported average strainer bypass distribution. For all tests, the fiber met the length distribution requirements.

Table F.5-2 Target Fiber Size Distribution

F.5.4.2.3 Chemical Surrogate AlOOH

Following the LOCA, the chemistry of the fluid in the IRWST and the core could produce chemical precipitates, which could affect the pressure drop in a debris bed. Studies were completed to identify the specific compounds and bounding quantities of materials that may precipitate within the U.S. EPR IRWST following a LOCA. These studies report that, at 720 hours (30 days), the predicted precipitates include sodium aluminum silicate, calcium phosphate, and aluminum hydroxide (Appendix D). Sodium aluminum silicate is a hazardous material and not used for testing. Tests with sodium aluminum silicate surrogate show that it is not quite as efficient as aluminum hydroxide in increasing head loss. Since aluminum precipitates as aluminum oxyhydroxide (AlOOH) at higher temperatures, the testing used AlOOH as the chemical surrogate, which is effective in increasing the head loss across a fiber bed.

F.5.4.3 *Debris Suspension*

Debris in the mixing tank is kept in suspension by agitation. The mixing tank agitation is provided by return flow from the test loop, bypass flow from the pump, and by a mechanical variable speed mixer. This mixing prevents debris from settling, floating, and remaining in the mixing tank during a test. Prior to introduction, the chemical surrogate is mixed with an agitator for at least an hour. It must then meet a settling test criteria of >60 percent turbid volume after a one hour settling test. The constant agitation and settling test requirement ensure the chemicals are adequately mixed. The fibrous and particulate debris are manually shaken with water from the mixing tank prior to introduction to ensure they are adequately mixed. During introduction, the debris is slowly and carefully poured into the mixing tank to ensure no air is entrained into the debris or test loop. At the conclusion of each test, the mixing tank was inspected for evidence of debris settling. Previous testing has shown that the agitation described is sufficient to keep debris in suspension before and during testing and to prevent settling or floating.

F.5.4.4 *Test Inputs*

Table F.5-3 contains the inputs for the 21 specific tests used to support the U.S. EPR design.

Table F.5-3 Test Inputs

F.5.5 Test Results

The results of the testing performed at CDI to support the U.S. EPR design are presented below.

F.5.5.1 *Hot Leg Break / Cold Leg Injection Test Results*

F.5.5.1.1 Test 3-FG-FPC

Figure F.5-9 Test 3-FG-FPC Head Loss, Flow Rate, and Temperature

Table F.5-4 Test 3-FG-FPC Results Summary

[

]

F.5.5.1.2 Test 4-FG-FPC

[

]

Figure F.5-10 Test 4-FG-FPC Head Loss, Flow Rate, and Temperature

Table F.5-5 Test 4-FG-FPC Results Summary

[

]

F.5.5.1.3 Test 5-FG-FPC

Figure F.5-11 Test 5-FG-FPC Head Loss, Flow Rate, and Temperature

Table F.5-6 Test 5-FG-FPC Results Summary

[

]

F.5.5.1.4 Test 6-FG-FPC

Figure F.5-12 Test 6-FG-FPC Head Loss, Flow Rate, and Temperature

Table F.5-7 Test 6-FG-FPC Results Summary

[

]

F.5.5.1.5 Test 12-FG-FPC

[

]

Figure F.5-13 Test 12-FG-FPC Head Loss, Flow Rate, and Temperature

Table F.5-8 Test 12-FG-FPC Results Summary

[

]

F.5.5.1.6 Test 13-FG-FPC

[

]

Figure F.5-14 Test 13-FG-FPC Head Loss, Flow Rate, and Temperature

Table F.5-9 Test 13-FG-FPC Results Summary

[

]

F.5.5.1.7 Test 0-FG-CLI-FPC

[

]

Figure F.5-15 Test 0-FG-CLI-FPC Head Loss, Flow Rate, and Temperature

Table F.5-10 Test 0-FG-HL-FPC Results Summary

[

]

Note: All of the following tests used a test assembly representative of the U.S. EPR fuel assembly.

F.5.5.1.8 Test 1-FG-CLI-FPC

[

]

Figure F.5-16 Test 1-FG-CLI-FPC Head Loss, Flow Rate, and Temperature

Table F.5-11 Test 1-FG-CLI-FPC Results Summary

[

]

F.5.5.1.9 Test 1-FG-CLI-FPC-2, Reversed Flow

Figure F.5-17 Test 1-FG-CLI-FPC-2 Head Loss, Flow Rate, and Temperature

Table F.5-12 Test 1-FG-CLI-FPC-2 Results Summary

[

]

F.5.5.1.10 Test 4-FG-CLI-FPC, Reversed Flow

[

]

F.5.5.1.11 Ability of Reversed Flow to Disrupt Debris Bed

Figure F.5-18 Test 4-FG-CLI-FPC Head Loss, Flow Rate, and Temperature

Table F.5-13 Test 4-FG-CLI-FPC Results Summary

[

]

F.5.5.1.12 Test 8-FG-CLI-FPC

Figure F.5-19 Test 8-FG-CLI-FPC Head Loss, Flow Rate, and Temperature

Table F.5-14 Test 8-FG-CLI-FPC Results Summary

[

]

F.5.5.1.13 Test 12-FG-CLI-FPC

Figure F.5-20 Test 12-FG-CLI-FPC Head Loss, Flow Rate, and Temperature

Table F.5-15 Test 12-FG-CLI-FPC Results Summary

[

]

F.5.5.2 *Cold Leg Break / Cold Leg Injection Test Results*

These tests were also performed with a test assembly representative to the U.S. EPR fuel assembly.

F.5.5.2.1 Test 7-FG-CLI-FPC

[

]

Figure F.5-21 Test 7-FG-CLI-FPC Head Loss, Flow Rate, and Temperature

Table F.5-16 Test 7-FG-CLI-FPC Results Summary

[

]

F.5.5.2.2 Test 11-FG-CLI-FPC

Figure F.5-22 Test 11-FG-CLI-FPC Head Loss, Flow Rate, and Temperature

Table F.5-17 11-FG-CLI-FPC Results Summary

[

]

F.5.5.3 *Cold Leg Break / Hot Leg Injection Test Results*

These tests were also performed with a test assembly representative to the U.S. EPR fuel assembly.

F.5.5.3.1 Test 0a-FG-HLI-FPC

[

]

Figure F.5-23 Test 0a-FG-HLI-FPC Head Loss, Flow Rate, and Temperature

Table F.5-18 Test 0a-FG-HLI-FPC Results Summary

[

]

F.5.5.3.2 Test 2-FG-HLI-FPC

Figure F.5-24 Test 2-FG-HLI-FPC Head Loss, Flow Rate, and Temperature

Table F.5-19 Test 2-FG-HLI-FPC Results Summary

[

]

F.5.5.3.3 Test 3-FG-HLI-FPC, Simulated Boiling

[

]

Figure F.5-25 Test 3-FG-HLI-FPC Head Loss, Flow Rate, and Temperature

Table F.5-20 Test 3-FG-HLI-FPC Results Summary

F.5.5.3.4 Test 5-FG-HLI-FPC, Simulated Boiling

Figure F.5-26 Test 5-FG-HLI-FPC Head Loss, Flow Rate, and Temperature

Table F.5-21 Test 5-FG-HLI-FPC Results Summary

F.5.5.3.5 Test 6-FG-HLI-FPC, Simulated Boiling

Figure F.5-27 Test 6-FG-HLI-FPC Head Loss, Flow Rate, and Temperature

Table F.5-22 Test 6-FG-HLI-FPC Results Summary

F.5.5.3.6 Test 9-FG-HLI-FPC

Figure F.5-28 Test 9-FG-HLI-FPC Head Loss, Flow Rate, and Temperature

Table F.5-23 Test 9-FG-HLI-FPC Results Summary

[

]

F.5.5.3.7 Test 13-FG-HLI-FPC

[

]

Figure F.5-29 Test 13-FG-HLI-FPC Head Loss, Flow Rate, and Temperature

Table F.5-24 Test 13-FG-HLI-FPC Results Summary

[

]

Table F.5-25 Final Head Loss per Assembly Grid (4 Grid Tests)

[

]

Note (1): The pressure exceeded the instrument's upper limit.

Grid 1 is the bottom grid and Grid 4 is the top grid.

Table F.5-26 Final Head Loss per Assembly Grid (7 Grid Tests)

[ ]

Table F.5-27 GSI-191 Test Results

Notes:

F.5.6 Discussion of Test Results

The following sections summarize the test results presented in Section F.5.5.

F.5.6.1 *Tests at Fiber Amount Expected for U.S. EPR Plant*

The expected fiber amount for a U.S. EPR design is [ ]. There are nine tests summarized in this report that were conducted with [ ] fiber: seven CLI tests and two HLI tests. All of these tests passed their [ ] acceptance criteria with sufficient margin as described in each test description in Section F.5.5. They also all reached head loss stabilization without throttling the flow rate down to maintain the facility pressure limit.

F.5.6.1.1 Cold Leg Injection Tests

[ ]

F.5.6.1.2 Hot Leg Injection Tests

[ ]

F.5.6.2 *Sensitivity of Results to Fiber Amount*

Seven tests were conducted with [ ] of fiber; [ ] what is expected for the U.S. EPR design. Of the seven tests, three were CLI tests, four were HLI tests.

F.5.6.2.1 Cold Leg Injection Tests

[ ]

F.5.6.2.2 Hot Leg Injection Tests

[ ]

F.5.6.3 *Sensitivity of Results to Flow Rate*

While the test results were the most sensitive to fiber amount, the results were also sensitive to flow rate.

F.5.6.3.1 Cold Leg Injection Tests

[ ]

[ ]

F.5.6.3.2 Hot Leg Injection Tests

During the CLB/HLI tests, distributed debris beds were observed during all tests except one. That was the only test performed at the low flow of [ ] with [ ] of fiber. All other [ ] HLI tests were run at the expected CLB/HLI 136 gpm, created distributed debris beds across the assembly, and met the acceptance criteria with margin.

F.5.6.4 *Sensitivity of Results to the Number of Spacer Grids*

[ ]

F.5.6.5 *Sensitivity of Results to Alternate Grid Designs*

[

]

Figure F.5-30 Intermediate Spacer Grid Configuration

F.5.6.5.1 Debris Accumulation

F.5.6.6 *Sensitivity of Results to p:f Ratio*

[ ]

F.5.6.7 *Summary and Conclusion*

Testing showed that a transitional region exists where test results may vary between acceptable and unacceptable. This region includes tests performed at [ ] , where fiber bed resistance and final flow rate varied between acceptable and unacceptable values. To move away from this transition region, the latent fiber source term was re-evaluated. Discussions with operating plants supported a reduction from 22.5 lbs of latent fiber to 10.2 lbs of latent fiber. Accounting for strainer efficiency yields a fiber loading of [ ] This amount was then tested and consistent acceptable results were obtained over nine tests. The conclusion was reached that the fiber loading was sufficiently below the transition region. This was based on high margins to the acceptance criteria, maintenance of initial flow rate, and reduced differential pressures.

F.6 Summary and Conclusion

Analyses and testing were performed to evaluate the effect of debris and chemical products on core cooling for the U.S. EPR design when the ECCS is actuated. The objective of the program was to demonstrate sufficient LTCC to comply with the requirements of 10 CFR 50.46 (b)(5), considering debris and chemical products that might be transported to the reactor vessel and core by coolant recirculating from the IRWST. The debris composition includes particulate and fiber debris, as well as post-accident chemical products. This evaluation considered the design of the U.S. EPR plant, the design of the open-lattice fuel, the design and tested performance of the strainer baskets and sump screens, the tested performance of materials inside containment, and the tested performance of fuel assemblies in the presence of debris. Specific areas addressed in this evaluation include:

- Collection of debris on fuel assembly bottom nozzle or intermediate spacer grids,
- Production and deposition of chemical precipitants and debris on the fuel rod cladding.

To address the collection of debris in the fuel assembly bottom nozzle or at the spacer grids, fuel assembly testing was performed. The purpose of this testing was to quantify the mass of debris that can be deposited at the core entrance or spacer grids and not impede long-term core cooling flows to the core. This report provides the inputs and boundary conditions, the success criteria, and the testing results.

An evaluation of the deposition of chemical precipitates and debris on the fuel rods was performed by applying U.S. EPR-specific design parameters to the U.S. EPR LOCA Deposition Analysis Model (EPRDM). This calculation provides a conservative evaluation of (1) deposition thicknesses on fuel rod surfaces due to chemical and debris deposition and (2) to determine the cladding temperatures under the buildup for up to 30 days following a LOCA. The results of this calculation demonstrate that long-term core cooling is maintained for each location in the core throughout the accident.

F.6.1 References

1. NRC GL 2004-02, "Potential Impact of Debris Blockage on Emergency Recirculation During Design Basis Accidents at Pressurized Water Reactors," September 13, 2004 (ML042360586).

2. AREVA NP Topical Report BAW-10192P-A, Rev. 2, "BWNT LOCA – BWNT Loss-of-Coolant Accident Evaluation Model for Once-Through Steam Generator Plants."

3. AREVA NP Topical Report BAW-10168P-A, Rev. 2, "RSG LOCA – BWNT Loss-of-Coolant Accident Evaluation Model for Recirculating Steam Generator Plants."

4. AREVA NP Topical Report BAW-10155A, "FOAM2 – Computer Program to Calculate Core Swell Level and Mass Flow Rate During Small Break LOCA," October 1987.

5. Palazov, Vesselin V., "Scaling Approach for Turbulent Mixing During Rapid Boron Dilution Transients in Pressurized Water Reactors," Master of Science Thesis from University of Maryland, 1998.

6. Crane Technical Paper No. 410, "Flow of Fluids Through Valves, Fittings, and Pipe," 1988.

7. WCAP-16793-NP, Rev. 1, "Evaluation of Long-Term Cooling Considering Particulate, Fibrous and Chemical Debris in the Recirculating Fluid," April 2009.

8. B. B. Banh, K. E. Kasza, and W. J. Shack, "Technical Letter Report on Follow-on Studies in Chemical Effects head-Loss Research; Studies on WCAP Surrogates and Sodium Tetraborate Solutions," Argonne National Laboratory, NRC Contract N6100.

9. A. Helalizadeh, H. Muller-Steinhagen, M. Jamialahmadi, “Crystallization Fouling of Mixed Salts During Convective Heat Transfer and Sub-Cooled Flow Boiling Conditions,” 2003 ECI Conference on Heat Exchanger Fouling and Cleaning: Fundamentals and Applications, Paper 6, Santa Fe, New Mexico.

10. NEI 04-07, “Pressurized Water Reactor Sump Performance Evaluation Methodology,” Volumes 1 (Methodology) and 2 (Safety Evaluation), December 2004.

11. V.N. Slesarenko, V.G. Dobrzansky, V.V. Slesarenko, “The account of heat exchange features when modelling scale formation at distillation plants,” Desalination 152 (2002) 229–236, April 2002.

12. Fahmi Brahim, Wolfgang Augustin, Matthias Bohnet, “Numerical simulation of the fouling process,” International Journal of Thermal Sciences 42 (2003) 323-334.

13. AREVA NP Topical Report ANP-10278P, Rev. 1, “U.S. EPR Realistic Large Break Loss of Coolant Accident, January 2010.”

14. ASTM STP754-EB, “Zirconium in the Nuclear Industry,” American Society for Testing and Materials, January 1982.

15. Paul Cohen, “Water Coolant Technology of Power Reactors,” Gordon and Breach Science Publishers, New York, NY, p. 25-26, 1969.

16. Hans Muller-Steinhagen, “Heat Exchanger Fouling- Mitigation and Cleaning Technologies,” (Institution of Chemical Engineers, Rugby, UK, 2000) p. 4.

17. AREVA NP Technical Report ANP-10299P, Rev. 1, “Applicability of AREVA NP Containment Response Evaluation Methodology to the U.S. EPR™ for Large Break LOCA Analysis.”

18. U.S. Nuclear Regulatory Commission, “Standard Review Plan,” NUREG-0800, most recent revision.

19. AREVA NP Technical Report ANP-10288P, Rev. 1, “U.S. EPR Post-LOCA Boron Precipitation and Boron Dilution.”

Appendix G
Ex-Vessel Downstream Effects Evaluation

G.1 Introduction

This appendix documents the ex-vessel downstream effects evaluation for the U.S. EPR emergency core cooling system (ECCS) to verify that this system and its components function as designed under post-LOCA conditions. This evaluation verifies that inadequate core or containment cooling will not occur because of debris blockage at flow restrictions, plugging or excessive wear of close-tolerance subcomponents in pumps, valves, and other components in the ECCS flow path. This evaluation uses the guidance of NRC Generic Letter GL 2004-02 for ex-vessel downstream evaluation.

G.1.1 Safety Injection Function

Each ECCS train delivers borated water to the RCS by one of three systems that share common piping and valves:

- MHSI.
- LHSI.
- Accumulator injection systems.

The MHSI and LHSI systems share an isolable suction line from the IRWST, and a three-way valve connects the IRWST to either the MHSI or LHSI pump suctions. The injection pumps draw water from the IRWST for their emergency function. The discharge lines for the MHSI, LHSI, and accumulator injection systems branch together to a single injection nozzle on the associated RCS cold leg. The MHSI and the accumulators inject directly into the cold legs. The LHSI pumps inject through the LHSI heat exchangers to the cold legs. In the long-term cooling following a LOCA, the LHSI discharge can be switched to the RCS hot legs to prevent boron precipitation and mitigate steaming from the break.

G.2 Assumptions and Design Information

G.2.1 Accident Scenarios

ECCS actuation provides protection for different postulated transients, accidents, and anticipated operational occurrences. This evaluation addresses accident scenarios with the potential for debris transportation to the IRWST that could get to the ECCS sump strainers and potentially affect ECCS operation. These accidents are the following:

- Small break LOCA (SBLOCA)
- Large break LOCA (LBLOCA)

This evaluation addresses ECCS operation during long-term decay heat removal from the RCS and mitigation of boric acid precipitation.

G.2.1.1 *SBLOCA*

The most limiting SBLOCA is a break with a cross-sectional area of up to approximately 0.5 ft^2 in the cold leg between the ECCS injection location and the RPV, with coincident loss of offsite power (LOOP). This event may not immediately challenge the ECCS if the CVCS compensates for the reactor coolant loss. The loss of primary coolant eventually results in a decrease in primary system pressure and pressurizer level. The ECCS actuates on low pressurizer pressure and automatically starts the MHSI and LHSI pumps. During partial cooldown, the RCS pressure decreases sufficiently to allow MHSI injection into the cold legs. The LHSI pumps actuate and re-circulate, through their specific tangential minimum flow line, into the IRWST, where they take suction.

In contrast to an LBLOCA, the stages of the SBLOCA (such as partial cooldown, controlled state and safe shutdown state) prior to long-term decay heat removal occur over a longer period. The duration of each stage depends on the break size and the performance of the ECCS.

For this evaluation, the SBLOCA is bounded by the LBLOCA, recirculation, and post-LOCA, long-term cooling. The ECCS flows and debris generated during an SBLOCA will be smaller than during an LBLOCA. The SBLOCA is bounded by the conditions of the LBLOCA regarding the evaluation of downstream components.

G.2.1.2 *LBLOCA*

For the LBLOCA, the break is assumed to open instantaneously and results in a large loss of reactor coolant inventory, and high temperature and pressure inside the containment. This LBLOCA, also called the double-ended break, evolves in three phases:

- The blowdown until accumulator injection.
- Refill of the RPV lower plenum by the ECCS.
- Re-flooding of the core by the accumulators first, and then by the MHSI and LHSI pumps until a complete quenching of the core is obtained.

To reach the safe shutdown state, the LHSI cold leg injection is switched to LHSI hot leg injection (required for cold leg breaks) to prevent boron precipitation inside the core and excessive boron dilution inside the IRWST. The break flow is compensated by the ECCS. The ECCS aids in containment heat removal.

The MHSI pumps maintain cold leg injection.

G.2.2 Mission Time

"Mission time" is defined as the amount of time that a given component is required to fulfill its safety function in a post-LOCA accident condition. Defining a mission time for this evaluation establishes a duration for which wear or debris-induced failure of a component will not have an adverse impact on ECCS operation. For this evaluation, the mission time for ECCS components following LBLOCA is 30 days of continuous operation.

G.2.3 Components of Interest

Table G.2-1 lists the ECCS/RHRS/IRWST components in the downstream effects evaluation. These components are in the ECCS flow path during SBLOCA and LBLOCA operations.

Table G.2-1 Components in the ECCS Flow Path during an LBLOCA

Components	Description
PUMPS	
LHSI Pump (30JND10/20/30/40 AP001)	**Type**: Centrifugal **Arrangement**: Horizontal **Flow Rate**: ~441.6 lbm/s (maximum)
MHSI Pump (30JNG10/20/30/40 AP001)	**Type**: Centrifugal **Arrangement**: Horizontal **Flow Rate**: ~152.6 lbm/s (maximum)
HEAT EXCHANGERS	
LHSI Heat Exchanger (30JNG10/20/30/40 AC001)	**Type**: Shell and Tube, U-Tube, Horizontally Mounted **Number of Shell in Series**: 1 **Number of Tube Passes**: 2 **Tube Material**; Austenitic Steel **Flow rate**: ~392.4 lbm/s (during LBLOCA LHSI Injection)
VALVES AND ORIFICES	
Motor Operated Valves:	
30JNG10/20/30/40 AA102	**Function**: LHSI Heat Exchanger Control Valve **Size**: 8 inches **Type**: Globe Valve
30JNG10/20/30/40 AA104	**Function**: LHSI Throttle Control Valve **Size**: 8 inches **Type**: Globe Valve
30JNG10/20/30/40 AA060	**Function**: LHSI Discharge Valve **Size**: 8 inches **Type**: Globe Valve
30JNG10/20/30/40 AA061	**Function**: LHSI Discharge Valve **Size**: 4 inches **Type**: Globe Valve

Components	Description
30JNA10/20/30/40 AA002	**Function**: Hot Leg (RCPB) Isolation Valve **Size**: 10 inches **Type**: Globe Valve
30JNG10/20/30/40 AA001	**Function**: LHSI Pump Suction from IRWST Isolation Valve **Size**: 14 inches **Type**: Gate Valve
30JNG12/22/32/42 AA001	**Function**: LHSI Hot Leg Injection Isolation Valve **Size**: 8 inches **Type**: Globe Valve
30JNK10/20/30/40 AA001	**Function**: IRWST 3-Way Isolation Valve **Size**: Inlet – 16 inches; MHSI Outlet – 10 inches; LHSI Outlet – 14 inches **Type**: 3-Way Globe Valve
30JND10/20/30/40 AA002	**Function**: MHSI Pump Discharge Valve **Size**: 6 inches **Type**: Globe Valve
30JND10/20/30/40 AA004	**Function**: MHSI Small Miniflow Line Isolation Valve **Size**: 2 inches **Type**: Globe Valve
30JNG10/20/30/40 AA004	**Function**: LHSI Tangential Miniflow Line Check Valve **Size**: 4 inches **Type**: Lift Check with Electric Motor
30JNA10/20/30/40 AA001	**Function**: Hot Leg (RCPB) Isolation Valve **Size**: 10 inches **Type**: Gate Valve
Manual Valves:	
30JND10/20/30/40 AA001	**Function**: MHSI Suction Isolation Valve **Size**: 10 inches **Type**: Globe Valve
30JND10/20/30/40 AA003	**Function**: MHSI 2nd RCPB Isolation Valve **Size**: 6 inches **Type**: Globe/Check Valve
30JNG10/20/30/40 AA006	**Function**: LHSI 2nd RCPB Isolation Valve **Size**: Inlet – 8 inches ; Outlet – 10 inches **Type**: Globe/Check Valve

Components	Description
Check valves:	
30JND10/20/30/40 AA007	**Function**: MHSI Check Valve **Size**: 6 inches **Type**: Swing Check Valve
30JNG12/22/32/42 AA002	**Function**: LHSI Hot Leg Injection Check Valve **Size**: 8 inches **Type**: Swing Check Valve
30JNG10/20/30/40 AA009	**Function**: LHSI Check Valve **Size**: 8 inches **Type**: Swing Check Valve
30JNG10/20/30/40 AA011	**Function**: LHSI Check Valve **Size**: 8 inches **Type**: Swing Check Valve
30JNG13/23/33/43 AA005	**Function**: Cold Leg Check Valve **Size**: 12 inches **Type**: Swing Check Valve
30JNK10/20/30/40 AA010	**Function**: MHSI Check Valve **Size**: 4 inches **Type**: Swing Check Valve
Orifices:	
30JND10/20/30/40 BP003	**Function**: MHSI Discharge Orifice **Size**: 6 inches
30JND10/20/30/40 BP002	**Function**: MHSI Miniflow Orifice **Size**: 2 inches
30JNG12/22/32/42 BP001	**Function**: LHSI Hot Leg Injection/Suction Orifice **Size**: 8 inches
30JNG10/20/30/40 BP001	**Function**: LHSI Tangential Miniflow Orifice **Size**: 4 inches
30JNG10/20/30/40 BP061	**Function**: LHSI Outside Containment Bypass Line Orifice **Size**: 4 inches

G.2.4 Post-LOCA Fluid Constituents

Debris in the post-LOCA fluid consist of latent debris (particulate and fiber), coating particles (i.e., epoxy, inorganic zinc, and unqualified), insulation materials, and miscellaneous debris. Miscellaneous debris includes materials placed inside containment for an operational, maintenance, or engineering purpose. Materials include tape, tags, stickers, adhesive labels used for component identification, fire barrier materials, and other materials (e.g., rope, fire hoses, ventilation filters, plastic sheeting).

Debris sizes are classified as particulates, small fines, and large pieces. The size range for each size category given in Table G.2-2 is established based on the following:

1. This evaluation conservatively assumes that 100 percent of the particulates will bypass the ECCS strainers. Therefore, it is reasonable to assert that the size of the particulate debris is less than (or equal to) the mesh size of the ECCS strainers, 0.08 inches.
2. Small fines are defined as debris materials that are less than 4 inches by 4 inches in size (based on guidance from NEI 04-07 Volume 1, Section 3.6.3).
3. Large pieces are defined as debris materials that are greater than 4 inches in size (based on guidance from NEI 04-07 Volume 1, Section 3.6.3).

Table G.2-2 Size Range of Debris Materials

Debris Size Category	Size Range
Particulates	0 – 0.08 inches
Small Fines	< 4 inches
Large Pieces	> 4 inches

The total amount of debris generated during a LBLOCA is estimated in Appendix C and summarized in Table G.2-3. The amount of reflective metallic insulation (RMI) listed in Table G.2-3 is based on a size distribution of 75 percent of small fines and 25 percent for large pieces (Appendix C).

Table G.2-3 Total Quantity of Debris Generated during an LBLOCA

Debris Source	Particulate	Small Fines	Large Pieces	Totals
Reflective Metal Insulation (RMI) (ft^2)	0	1589.27	529.76	2119.03
Microtherm (ft^3)	1.00	0	0	1.00
Qualified Epoxy Coatings (lbm)	126.30	0	0	126.30
Qualified IOZ Coatings (lbm)	958.70	0	0	958.70
Unqualified Coatings (lbm)	250.00	0	0	250.00
Latent Debris (lbm) Particulates – Dirt and Dust Small fines - Fibers	139.80* 127.50**	10.20* 22.50**	0	150.00
Miscellaneous (ft^2)	0	0	100.00	100.00

* Latent debris quantities used for downstream effects testing (based on weight percentage of fiber and particulate components in latent debris samples from four nuclear power plants analyzed in NUREG/CR 6877). Debris quantity is conservative with respect to amount of dust and dirt particulates.

** Latent debris quantities used for strainer testing (based on NRC recommended values of 85% particulate and 15% fiber). Debris quantity is conservative with respect to the amount of fiber.

The amount of debris that passes through the sump screen depends on the size of the sump screen hole, ratio of open to closed area of the screen, the fluid approach velocity to the screen, and the screen geometry. This evaluation assumes that LBLOCA debris materials that are less than or equal to the mesh size of the sump screen (0.08 in × 0.08 in) will bypass the sump strainer. As a result, the ECCS will ingest 100 percent of the microtherm and coating particulates.

Miscellaneous debris materials are large pieces with a debris size range that is significantly greater than the mesh size of the sump screen. As a result, the ECCS will not ingest miscellaneous debris materials.

Bypass testing of the latent debris yielded a fiber bypass percentage of less than 70 percent (see Appendix E, Section E.7.3). This evaluation uses bounding bypass percentages of 100 percent for latent particulates (i.e., dust and dirt) and 70 percent for latent fiber.

Results of the NRC debris generation test documented in NUREG/CR-6808 show that RMI debris size distribution ranges from 0.25 inches to 6 inches. Transport testing performed by AREVA demonstrated that RMI debris pieces will sink in the retaining basket (See Appendix E, Section E.7.1). In the unlikely event that RMI debris bypasses the retaining baskets, RMI debris will not bypass the sump screens and enter the ECCS because the size of the RMI debris is greater then the mesh size of the sump screen. As a result, this evaluation assumes no RMI bypasses through the sump screen.

G.2.5 ECCS Flow Rate and Flow Velocity

To evaluate debris settlement and component wear during LBLOCA, this evaluation conservatively assumes ECCS flow rates ranging from shutoff head conditions to run-out conditions.

The LHSI and MHSI pumps provide minimum flow rates of 72.8 lbm/s (≈525 gpm) and 22.9 lbm/s (≈165 gpm), respectively, to provide pump operation at shutoff head conditions. These minimum flow rates are assumed for evaluating debris settlement in the ECCS.

The debris settlement evaluation (Section G.3.3.1) compares the ECCS fluid velocities with the terminal settling velocities of the debris source materials listed in Table G.2-4. The velocity of the debris in the post-LOCA fluid is equal to the velocity of the fluid. If the ECCS fluid velocity is greater than the terminal settling velocity of the debris, the debris will not settle.

The minimum flow rate of the LHSI and MHSI pumps at shutoff head conditions will be verified during component procurement.

The ECCS is designed to limit maximum flow rates to 441.6 lbm/s (3220 gpm) and 152.6 lbm/s (1110 gpm) for the LHSI and MHSI pumps, respectively. Flow rates of 3520 gpm for the LHSI pumps and 1320 gpm for the MHSI pumps are conservatively assumed for component wear evaluation. The component wear rate evaluation is detailed in Section G.3.1.

Table G.2-4 Terminal Settling Velocity of Debris Source Materials

Debris Source Material	Terminal Settling Velocity (ft/sec)	Reference/Comments
Microtherm	N/A	Microtherm, a microporous insulation material similar to calcium silicate, is expected to dissolve in the post-LOCA fluid (NUREG/CR-6772).
Qualified Epoxy Coatings	0.15	NEI 04-07 (page 4-34, epoxy).
Qualified IOZ Coatings	0.000674	NEI 04-07 (page 4-34, inorganic zinc).
Unqualified Coatings	0.15	Estimated to the settling velocity of epoxy coatings.
Latent Debris	0.008	The densities of loose fiber and latent particulates are comparable (NEI 04-07). Therefore, the settling velocity of the latent debris is estimated to the settling velocity of loose fiber.

G.2.6 Summary of Assumptions and Conservatisms

Assumptions and conservatisms used in this evaluation are summarized as follows:

1. 100 percent of all particulates (i.e., microtherm, coating debris, latent particulates) and 70 percent of latent fiber are assumed to pass through the strainers and enter into the ECCS. RMI debris generated during an LBLOCA will be stopped by the retention basket.
2. The minimum LHSI and MHSI pump flow rates of 72.8 lbm/s (~525 gpm) and 22.9 lbm/s (~165 gpm), respectively, are assumed for the evaluation of debris settlement in the ECCS.

3. LHSI and MHSI pump flow rates of 3520 gpm and 1320 gpm, respectively, are assumed for component wear evaluation.

Table G.2-5 lists the amount of debris in the post-LOCA fluid (downstream of the sump screen) that will be used for confirmatory tests. The amount of debris in the ECCS during post-LOCA operation is based on Assumption #1. The amount of latent debris in Table G.2-5 is conservatively based on the maximum amount of latent particulates and 70 percent of the maximum amount of fiber listed in Table G.2-3.

The size range of the debris materials is based on (i) the assumption that 100 percent of particulates will bypass the ECCS strainers, and (ii) guidance from NEI 04-07 Volume 2 Appendix V. The concentration of the post-LOCA fluid constituents is conservatively estimated based on the assumption that the IRWST contains 400,000 gallons of water during post-LOCA operation, which is less than the minimum IRWST water volume of 500,342 gallons. Estimating the debris concentration at less than the expected IRWST volume yields a more concentrated debris-laden fluid for confirmatory tests, and produces conservative test results.

Table G.2-5 Post-LOCA Fluid Constituents Downstream of ECCS Screen

Debris	Amount	Concentration (ppm)	Density (lb/ft^3)	Size Range (inches)	% by Mass
Microtherm	1.00 ft^3	3.6	12	0 – 0.08	100
Qualified Epoxy Coatings	126.30 lbm	38.4	94	0 – 0.08	100
Qualified IOZ Coatings	958.70 lbm	291	457	0 – 0.08	100
Unqualified Coatings	250.00 lbm	76	94	0 – 0.08	100
Latent Particulates	139.80 lbm	42.5	169		
Fine Sand				< 0.003	37.4
Medium Sand				0.003 – 0.02	35.3
Coarse Sand				0.02 – 0.08	27.3
Latent Fiber	15.75 lbm[b]	4.8	2.4[a]	< 4	100

a. As-fabricated density

b. Fiber amount is conservative

G.3 ECCS Component Evaluations

This section evaluates the ECCS pumps, heat exchangers, valves, instrument tubes, and piping regarding wear, blockage, and fouling (heat exchanger).

G.3.1 LHSI and MHSI Pump Evaluation

The LHSI and MHSI pumps are horizontally mounted, centrifugal pumps with single mechanical seals. The pumps are sized in safety injection mode to provide nominal flow rates.

Generally, particulates tend to accumulate and potentially affect flow through close clearances. The LHSI and MHSI pumps will be designed with increased clearances to support successful post-LOCA operations.

The LHSI and MHSI pumps and associated mechanical seals will be qualified to operate with the post-LOCA fluids for at least 30 days, using the qualification guidance of QME-1-2007 endorsed by RG1.100 Revision 3. As part of the qualification process, the pump vendor, at a minimum, will fulfill the following pump criteria:

1. Provide tests and/or analyses to confirm that the opening sizes and internal running clearances of the LHSI and MHSI pumps yield acceptable operation in post-LOCA fluids for at least 30 days. Also, provide a list of the opening sizes and internal running clearances in the qualification documentation.
2. Provide hydraulic performance test results and/or analyses to confirm that the LHSI and MHSI pumps can provide the required safety injection flow for at least 30 days of ECCS post-LOCA operation.
3. Provide tests and/or analyses to confirm that the wear rates of the LHSI and MHSI pump wetted surface materials (e.g., wear rings, pump internals, bearing, casing) provide acceptable operation in the post-LOCA fluids for at least 30 days.

Also, provide a list of the wetted pump surfaces materials, hardness of each material, and verification of acceptable wear rates in the qualification documentation.

4. Provide mechanical performance (i.e., pump vibration, rotor dynamics, bearing load) test results and/or analyses to confirm that there will be no adverse changes in system vibration response or rotor dynamics performance during ECCS operation for at least 30 days. Also, provide relevant test results and/or analyses to confirm that any increases in internal bypass flow caused by impeller or casing wear will not decrease the performance of the pumps or cause accelerated internal wear for at least 30 days of post-LOCA operation.

5. Provide mechanical seal assembly performance test results and/or analyses to confirm that ECCS operation with post-LOCA fluids will not impair seal performance, or cause seal failure, or significantly degrade seal leakage during the 30 day post-LOCA mission time.

6. Provide test and/or analysis to confirm:

   - that the cyclone separator or any filtering device designed to protect the mechanical seal, if applicable, is not susceptible to clogging or impairment by fiber or other particulates;

   - that there is no adverse impact on pump performance or reliability,

   for at least 30 days of operation with post-LOCA fluids. If the cyclone separator or any filtering device could be impaired within 30 days of post-LOCA operation, the test results and/or analysis will show that the absence of a cyclone separator or any filtering device yields acceptable seal performance.

7. The vendor will also identify any additional potential pump malfunctions, per QME-1-2007 Section QP-7200.

8. The vendor will verify that the LHSI and MHSI pumps provide minimum flow rates of 72.8 lbm/s and 22.9 lbm/s, respectively, at shutoff head conditions.

9. The vendor will verify that LHSI and MHSI pumps provide flow rates at run-out conditions of less than 3520 gpm and 1320 gpm, respectively.

G.3.2 LHSI Heat Exchanger Evaluation

The LHSI heat exchangers are evaluated for potential susceptibility to tube plugging, fouling, and abrasive wear.

G.3.2.1 Heat Exchanger Tube Plugging

Post-LOCA debris will not plug the heat exchanger tubes if the tube inside diameter is greater than the expected particle size (based on the opening size of the sump screen). In addition, debris will not settle in the heat exchanger tubes if the fluid velocity in the tubes is greater than the terminal settling velocity of the debris (Table G.2-4).

The vendor will provide data to confirm that post-LOCA debris will not plug the heat exchanger tubes during the 30 day mission time. In addition, the vendor will perform one of the following:

- Provide test and/or analyses to confirm that the debris settlement will not occur in the heat exchanger tubes and/or affect the performance of the heat exchanger (due to fouling by post-LOCA debris) for the 30 day mission time.
- Evaluate heat exchanger debris settlement, if the fluid velocity is less than the settling velocity, and provide results to confirm that the heat transfer performance of the heat exchanger will not be adversely affected over the 30 day mission time.

G.3.2.2 Heat Exchanger Performance and Wear

The LHSI heat exchangers are specified and designed with conservative fouling factors to maximize heat transfer efficiency and performance. The post-LOCA fluid could potentially cause particulate fouling of the heat exchanger tubes if the fluid velocity is less than the terminal settling velocity of the debris. However, fouling is considered a long-term phenomenon. In addition, the heat load of the LHSI heat exchangers decreases over the 30 day mission time.

Based on the conservative fouling factors, decrease in heat load over the 30 day mission time, and vendor confirmation that no plugging or settling of debris will occur in the tubes, the heat removal performance of the heat exchanger will not be degraded over the 30 day mission time.

The vendor will also provide test and/or analysis to confirm that the heat exchanger tube material will not degrade significantly (i.e., “eroded” tube thickness > minimum tube thickness required to retain pressure) in post-LOCA fluid over the 30 day mission time.

G.3.3 Evaluation of Valves, Orifices, Pipes and Instrument Tubing

G.3.3.1 *Blockage and Debris Settling Evaluation for Valves, Orifices, Pipes and Instrument Tubing*

Fluid velocity decreases with increase in pipe diameter. Therefore, the lowest velocity in the ECCS will occur in the region with the largest pipe diameter/flow area.

The suction lines of the LHSI and MHSI pumps are the largest lines in the ECCS.

The LHSI pump suction line is a 14-inch Schedule 30 stainless steel pipe (inside diameter = 13.25 inches). The velocity in this line at the minimum flow rate is 1.23 ft/s. This velocity is greater than the terminal settling velocities of the post-LOCA debris materials (Table G.2-4). Therefore, settling will not occur in the LHSI flow path to the RCS.

The MHSI pump suction line is a 10-inch Schedule 40S stainless steel pipe (inside diameter = 10.02 inches). The velocity in this line at the minimum flow rate is 0.68 ft/s. This velocity is greater than the terminal settling velocities of the post-LOCA debris materials (Table G.2-4). Therefore, settling will not occur in the MHSI flow path to the RCS.

An analysis will be performed to confirm that post-LOCA debris will not clog the ECCS instrument lines during post-LOCA operation for at least 30 days.

G.3.3.2 *Wear Rate Evaluation for Valves, Orifices and Pipes*

Erosive wear is caused by particles that impinge on a component surface and remove material from the surface because of momentum effects. The wear rate of a material depends on the debris type, debris concentration, material hardness, flow velocity, and valve position.

Flow rates of 3520 (490 lbm/s) and 1320 gpm (184 lbm/s) for LHSI and MHSI, respectively, are conservatively assumed for the wear rate evaluation of the components listed in Table G.2-1.

The vendor will qualify the ECCS valves to operate with the post-LOCA fluids for at least 30 days, using the qualification guidance of QME-1-2007 endorsed by RG1.100 Revision 3. As part of the qualification process, the vendor will provide data and/or analyses to support acceptable wear rates during operation in post-LOCA fluids (Table G.2-5) at the associated flow velocities listed in Table G.3-1.

Vendor(s) will also provide tests and/or analyses to support acceptable wear rates of pipes and orifices. In addition, an analysis will be provided to confirm that the overall system resistance/pressure drop across the ECCS is consistent with the safety analysis results for the 30 day mission time.

The ECCS design flow rates listed in Table G.3-1 include the maximum flow rate of the LHSI pump, MHSI pump, and the sum of the LHSI and MHSI flows based on system configuration. For conservatism, vendors will perform component wear evaluations at the assumed flow rates/velocities.

Table G.3-1 Flow Velocities for Component Wear Evaluation

Components	Inside Diameter (inches)	Designed ECCS Flow (lbm/s)	Assumed Flow Rate (lbm/s)	Assumed Velocity (ft/s)
Piping				
14” LHSI Pump Suction Line (SS Schedule 30)	13.25	441.6	490	8.27
8” LHSI Pump and Heat Exchanger Discharge (SS Schedule 80S)	7.625	441.6	490	24.73
10” MHSI Pump Suction Line (SS Schedule 40S)	10.02	152.6	184	5.37
6” MHSI Discharge Line (SS Schedule 40S)	6.065	152.6	184	14.66
10” RCS Cold Leg Discharge (SS Schedule 160)	8.5	< 594.2	674	27.37
8” Hot Leg Injection/Suction Line (SS Schedule 80S)	7.625	< 441.6	490	24.73
Orifice				
4” Orifice on LHSI valve/line bypass	-	< 441.6	490	-
8” Orifice on line between cold leg injection and hot leg injection/suction	-	< 441.6	490	-
6” Orifice on MHSI pump discharge line	-	152.6	184	-
2” Orifice on MHSI Miniflow Orifice	-	-	50	-

G.4 Conclusions

Vendor testing and/or analyses of the components identified in Section G.3 should show that the system as procured will meet the design requirements assumed in the design bases analyses. Meeting these requirements provides assurance that system components are not blocked by debris, or degraded to an extent that they cannot perform their safety function.